เบนซิเลชันของแอโรแมติกและเททระไฮโดรไพรานิเลชันของแอลกอฮอล์และฟีนอลโดยใช้อะลูมิเนียมพิลลาร์มอนต์มอริลโลไนต์อิมแพรกเนตด้วยนีโอดีเมียมคลอไรด์

นางสาวณัฐธิดา มณีจันทรา

วิทยานิพนธ์นี้เป็นส่วนหนึ่งของการศึกษาตามหลักสูตรปริญญาวิทยาศาสตรมหาบัณฑิต
สาขาวิชาปิโตรเคมีและวิทยาศาสตร์พอลิเมอร์
คณะวิทยาศาสตร์ จุฬาลงกรณ์มหาวิทยาลัย
ปีการศึกษา 2557

BENZYLATION OF AROMATICS AND TETRAHYDROPYRANYLATION OF ALCOHOLS AND PHENOLS USING $NdCl_3$ IMPREGNATED ALUMINUIM PILLARED MONTMORILLONIITE

Miss Natthida Maneechandra

A Thesis Submitted in Partial Fulfillment of the Requirements
for the Degree of Master of Science Program in Petrochemistry and Polymer Science
Faculty of Science
Chulalongkorn University
Academic Year 2014

Thesis Title	BENZYLATION OF AROMATICS AND TETRAHYDROPYRANYLATION OF ALCOHOLS AND PHENOLS USING $NdCl_3$ IMPREGNATED ALUMINUIM PILLARED MONTMORILLONIITE
By	Miss Natthida Maneechandra
Field of Study	Petrochemistry and Polymer Science
Thesis Advisor	Assistant Professor Warinthorn Chavasiri, Ph.D.

Accepted by the Faculty of Science, Chulalongkorn University in Partial Fulfillment of the Requirements for the Master's Degree

....Dean of the Faculty of Science
(Professor Supot Hannongbua, Dr.rer.nat.)

THESIS COMMITTEE

....Chairman
(Professor Pattarapan Prasassarakich, Ph.D.)
....Thesis Advisor
(Assistant Professor Warinthorn Chavasiri, Ph.D.)
....Examiner
(Associate Professor Nuanphun Chantarasiri, Ph.D.)
....External Examiner
(Assistant Professor Jinda Yeyongchaiwat, Ph.D.)

ณัฐธิดา มณีจันทรา : เบนซิเลชันของแอโรแมติกและเททระไฮโดรไพรานิเลชันของแอลกอฮอล์และฟีนอลโดยใช้อะลูมิเนียมพิลลาร์มอนต์มอริลโลไนต์อิมแพรกเนตด้วยนีโอดีเมียมคลอไรด์ (BENZYLATION OF AROMATICS AND TETRAHYDROPYRANYLATION OF ALCOHOLS AND PHENOLS USING $NdCl_3$ IMPREGNATED ALUMINUIM PILLARED MONTMORILLONIITE) อ.ที่ปรึกษาวิทยานิพนธ์หลัก: ผศ. ดร. วรินทร ชวศิริ, 120 หน้า.

ได้สังเคราะห์ตัวเร่งปฏิกิริยาอะลูมิเนียมพิลลาร์มอนต์มอริลโลไนต์ที่อิมแพรกเนตด้วยนีโอดีเมียมคลอไรด์ 2 เปอร์เซ็นต์ (2%$NdCl_3$/Al-PLM) และพิสูจน์เอกลักษณ์ด้วยเทคนิคการเลี้ยวเบนของรังสีเอ็กซ์ เทคนิคการดูดซับ-การคายแก๊สไนโตรเจน และเทคนิคฟลูเรียร์ทรานส์ฟอร์มอินฟราเรดสเปคโทรมิเตอร์ ได้ใช้ตัวเร่งปฏิกิริยาชนิดนี้สำหรับปฏิกิริยาเบนซิเลชันของแอโรแมติกและเททระไฮโดรไพรานิเลชันของเบนซิลแอลกอฮอล์ พบว่าให้ผลผลิตสูงและเลือกจำเพาะต่อการเกิดการแทนที่ตำแหน่งเดียวสำหรับ ซี-เบนซิเลชันภายใต้ภาวะที่เหมาะสมในปฏิกิริยาเบนซิเลชันสามารถนำกลับมาใช้ซ้ำได้ 5 ครั้งโดยให้ปริมาณผลิตภัณฑ์ในระดับดี และได้ใช้ตัวเร่งปฏิกิริยาชนิดนี้ในปฏิกิริยาเททระไฮโดรไพรานิเลชันของเบนซิลแอลกอฮอล์พบว่าให้ปริมาณผลิตภัณฑ์ในระดับดีมากภายใต้ภาวะที่เหมาะสม การฟื้นฟูตัวเร่งปฏิกิริยาก่อนการใช้ซ้ำผ่านการเผาที่อุณหภูมิ 450 เป็นเวลา 4 ชั่วโมง และแบบไม่ผ่านการเผาได้นำมาเปรียบเทียบประสิทธิภาพ พบว่าตัวเร่งปฏิกิริยาแบบผ่านการเผาที่อุณหภูมิ 450 เป็นเวลา 4 ชั่วโมงช่วยกำจัดถ่านและนำกลับมาใช้ซ้ำได้ 5 ครั้งโดยให้ปริมาณผลิตภัณฑ์ในเกณฑ์ดี

สาขาวิชา ปิโตรเคมีและวิทยาศาสตร์พอลิเมอร์ ลายมือชื่อนิสิต ....
ปีการศึกษา 2557 ลายมือชื่อ อ.ที่ปรึกษาหลัก ....

5571973123 : MAJOR PETROCHEMISTRY AND POLYMER SCIENCE

KEYWORDS: 2% NEODYMIUM CHLORIDE IMPREGNATED ON ALUMINIUM OXIDE PILLARED MONTMORILLONITE CLAY / TETRAHYDROPYRANYLATION OF BENZYL ALCOHOL / REUSABILIITY / BENZYLATION OF AROMATICS

NATTHIDA MANEECHANDRA: BENZYLATION OF AROMATICS AND TETRAHYDROPYRANYLATION OF ALCOHOLS AND PHENOLS USING $NdCl_3$ IMPREGNATED ALUMINUIM PILLARED MONTMORILLONIITE. ADVISOR: ASST. PROF. WARINTHORN CHAVASIRI, Ph.D., 120 pp.

A 2% neodymium chloride impregnated on aluminium oxide pillared montmorillonite clay catalyst (2%$NdCl_3$/Al-PLM) was synthesized and characterized by XRD, N_2 adsorption-desorption and FT-IR. The benzylation of aromatics and tetrahydropyranylation of benzyl alcohol over 2%$NdCl_3$/Al-PLM were investigated. In term of benzylation of aromatics, the high selectivity for mono-substitution of *C*-benzylated products under the optimized conditions was presented. Nonetheless, it could be reused for 5 times without losing catalytic activity. In addition, tetrahydropyranylation of benzyl alcohol was proceeded in the presence of this catalyst to furnish the corresponding product with an excellent yield. It was regenerated by two different methods, re-calcination at 450 °C for 4 h as compared with not re-calcination for activation of spent catalyst. Burning off coke by re-calcination showed superior performance which retained its activity for 5 cycle runs in tetrahydropyranylation of benzyl alcohol.

Field of Study:	Petrochemistry and Polymer Science	Student's Signature Advisor's Signature	....
Academic Year:	2014		

ACKNOWLEDGEMENTS

I would like to express my gratitude to my supervisor Assistant Professor Dr. Warinthorn Chavasiri for the useful comments, remarks and engagement through the learning process of this master thesis. I have learnt many things since I became his student. I am also grateful to Dr.Veerachai Pongkittipan and Dr.Piyarat Trikittiwong for spending time read and providing useful suggestions about this thesis.

During the period of three years, many colleagues are helpful to color my life. I have to acknowledge all my colleagues in NPRU units for their assistances in many aspects that I cannot list them all because of limited space.

Last but not the least important, I owe more than thanks to my family members which includes my parents, my aunt and my elder sister, for their financial support, love, assistance, understanding and encouragement throughout my life. Without their support, it is impossible for me to achieve the goal.

CONTENTS

Page

Page

Page

CONTENTS OF FIGURES

CONTENTS OF SCHEMES

CONTENTS OF EQUATIONS

CONTENTS OF TABLES

LIST OF ABBREVIATIONS

BJH	Barrett Joyner and Halenda
BET	Brunauer-Emmett-Teller
J	coupling constant (NMR)
δ	chemical shift
°C	degree Celsius
$CDCl_3$	deuterated chloroform
d	doublet
g	grams (s)
mg	milligram (s)
Hz	hertz
h	hour (s)
MB	mass balance
mL	milliliter (s)
mmol	millimole (s)
min	miniute (s)
M	molar
m	multiplet (NMR)
NaOH	sodium hydroxide
Å	Angstrom unit
CEC	Cation Exchange Capacity
Q	quartet (NMR)
RT	room temperature
s	singlet (NMR)
t	triplet (NMR)
XRD	X-ray diffraction
IR	Fourier transform infared spectroscopy
NMR	Nuclear magnetic resonance spectrometer

CHAPTER I
INTRODUCTION

1.1 Introduction to clay

Clay minerals occurred abundantly in nature could be classified as phyllosilcated or layered silicate. They possessed various properties for catalytic applications owing to their high surface area, adsorption, ion-exchange and acidity. They contain both Brönsted and Lewis acid. Because of these advantages, the development of clay has been an interest for many years as an efficient heterogeneous catalyst in organic reactions [1].

1.2 The structure of clay mineral

Clay mineral possesses a layered structure. It is composed of two basic building blocks: tetrahedral and octahedral sheets which are held together by sharing apical oxygen atoms [2].

1.2.1 Tetrahedral sheet

Tetrahedral sheets are constituted from individual tetrahedron units. They are arranged in a hexagonal pattern with the three basal oxygen atoms linked to other tetrahedral and the remaining apical oxygen atom pointing up or down. In typical, tetrahedron contains Si^{4+}, Al^{3+} and Fe^{3+}. A single tetrahedral silica and a sheet structure of silica tetrahedral arranged in a hexagonal network were shown in Figure 1.1.

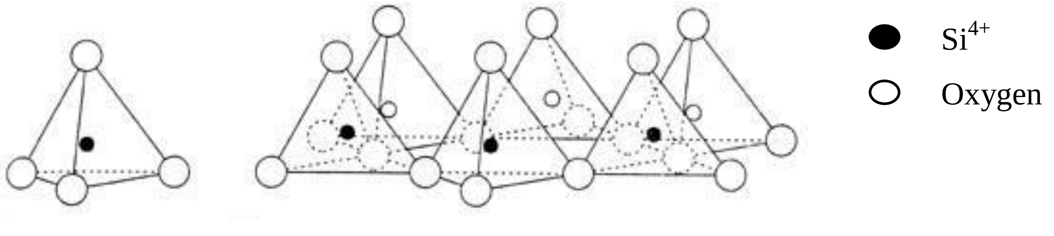

Figure 1.1 A single tetrahedral silica (a), and a sheet structure of silica tetrahedral arranged in a hexagonal network (b) [5]

1.2.2 Octahedral sheet

Octahedral sheets are composed of individual octahedron units. Each octahedron unit contains cation coordinated by six oxygen atoms which linked to neighboring octahedral by sharing edges. Octahedral cations are usually Al^{3+}, Fe^{3+}, Mg^{2+} and Fe^{2+}. These octahedrons are also arranged in a hexagonal pattern which demonstrated in Figure 1.2.

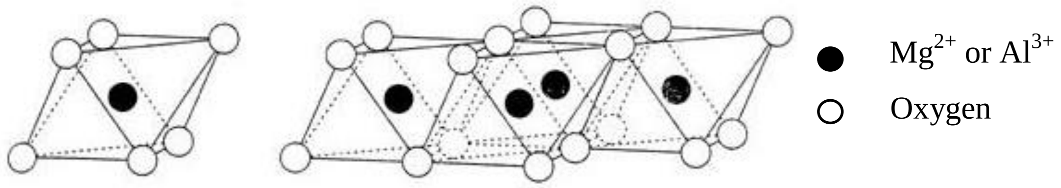

Figure 1.2 A single octahedral unit (a) and a sheet structure of octahedral unit arranged in a hexagonal network (b) [5]

1.3 Smectite clay

Smectite is an important mineral because of the high surface area and adsorptive property of water molecules in the interlayer sites. Smectite clay has three layers, based on two silica tetrahedral ($Mg_6Si_8O_{20}(OH)_4$) and one alumina octahedral ($Al_4Si_8O_{20}(OH)_4$) sheets in the layer structure. This combination makes a tetrahedron-octahedron-tetrahedron (T:O:T) like a sandwich when the interlayer site is hydrated. Substitution of cation (for example, Al^{3+} for Si^{4+} in tetrahedral sheets and Mg^{2+} for Al^{3+} in octahedral sheets) either in tetrahedral or octahedral sheet results in the formation of negative charge in the layers. The excess negative charge is balanced by monovalent cations between the interlayer of clay with hydrated exchangeable cations [3]. The structure of smectite is shown in Figure 1.3.

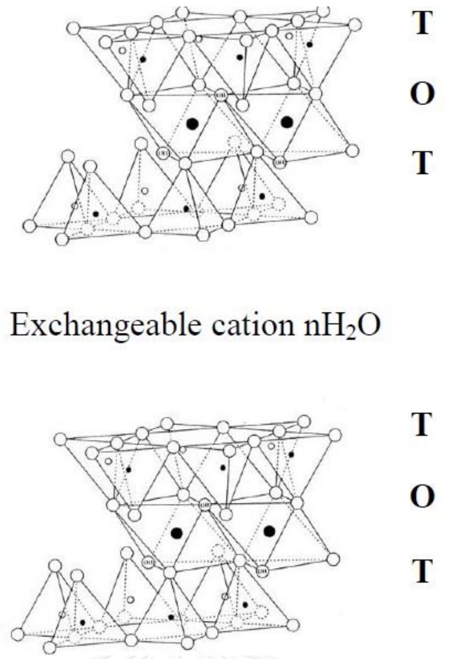

Figure 1.3 Structure of smectite clay [5]

1.3.1 Montmorillonite

Montmorillonite is the most frequently used for modification clay in catalytic application because the cation-exchange capacity is high [4]. It is purified from bentonite, which is the member of smectite group by the eradication of quartz and other impurities by fractionated sedimentation. Its ideal formula was shown as $(Si_8)(Al_{4-X}Mg_X)O_{20}(OH)_4A_x\cdot nH_2O$ (where A is a monovalent or divalent cation), which Mg/Al in the octahedral sheet [5].

1.4 Properties of clay

1.4.1 Ion exchange

Exchangeable cations in the lattice could occur in clay by two processes: (i) the isomorphous substitution of cations in the lactice by valent ions, such as the substitution of Al^{3+} for Si^{4+} in the tetrahedral layer, Mg^{2+} for Al^{3+} in the octahedral layer, and (ii) crystal defects. From those reasons, clay layers have an overall negative charge which is balanced by cations between the layers. These balance cations can be readily replaced by other cations in aqueous solution. It elaborated that the capability in replaceable of exchangeable cations depends on its size and charge. The smaller size and higher charge give higher power in replacement. The following series are presented as follows in Figure 1.4.

$$\mathbf{M^+ \ll M^{2+} \ll H_2O^+ \approx K^+ \approx NH_4^+ < M^{3+} < M^{4+}}$$

$$\xrightarrow{\hspace{12em}}$$

increasing exchange power
(decreasing ease of exchange)

Figure 1.4 The exchange properties of cations with clays [5]

The concentration of exchangeable cations (CEC) is determined in milliequivalents per 100 g of dried clay. Smectite clay is noted because of the highest concentration of interlayer cations (70-120 mequiv/100 g). It is noticeable that structural defects at layer edges give high amount of CEC and a small amount of anion exchange capacity [1].

1.4.2 Swelling

Many clay minerals adsorb water between their layers which move the layers apart and cause the clay swelling. The released energy from attractive forces must high enough to overwhelm hydrogen bondings between the adjacent layers. In T:O:T clay minerals (smectite clay), the ability to swell depends on the solvation of interlayer cation and layer charge. In T:O:T smectite clay with the low layer charge has very low concentration of interlayer cations. It does not swell readily. At the other extreme, those clay minerals with very high layer charges have strong electrostatic forces holding alternate anionic layers and the interlayer cations together, thus prevent swelling. Those with univalent interlayer cations swell most readily. Those with divalent, trivalent and polyvalent cations, swelling decrease accordingly. The extent of swelling can be observed by measuring interlayer separation using XRD [1].

1.4.3 Acidity of clays

Some of the polarizing cations (*e.g.* Al^{3+}) which are located at the interlayerlead to the strong Brönsted acid. The higher the electronegativity of cations, the stronger are the acidic sites created. The terminal hydroxyl groups and the bridging oxygen atoms can generate Brönsted acid [1]. Introduction the coordination of an organic compound into the cations between clays will cause Lewis acid [5]. In addition, weaker Brönsted and Lewis acid can generate from layer surface and edge defects in clay [1]. Because of the acidity of clay, it is widely used as heterogeneous catalyst in acid organic reactions [1].

1.4.4 Intercalation

Intercalation is the insertion of organic compounds, metal complexes and metal cations into the interlayer space of clay which layered structure of clay is not destroyed by using ion exchange properties. The intercalation can be observed by XRD pattern, resulting in the expanded d-basal spacing [1].

1.4.5 Pillaring

Pillaring is an intercalation process that uses to convert the layered clay (2d structure) to highly porous (3d structure) by exchanging the prior interlayer cations with a variety of inorganic polyoxocations. Upon calcination, polyoxocation species are transformed into metal oxide pillars with the preservation of clay structure. Those pillaring species connected permanently to silicate sheet, resulted in the pillared clay. The advantages of pillared clay are large surface area and high acidic which utilize for the application as catalyst and adsorbent in organic reactions [6]. Diagram for the preparation of pillared clay compound (cross section) is shown in Figure 1.5.

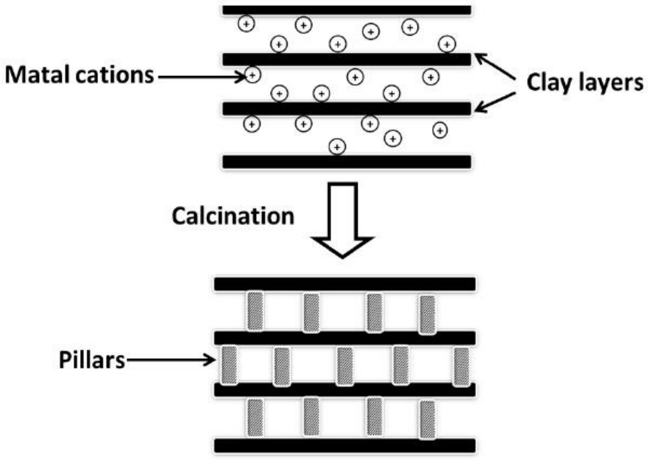

Figure 1.5 Diagram for pillared clay compound (cross section) [5]

1.4.6 Impregnation

Transition metal and metal chloride are active components for which pillared clay serves as the supported material to improve its quality. Generally, the support material was contacted with a solution of those compounds which are held on to the support *via* heat treatment [7]. Diagram for the preparation of impregnated pillared clay compound (cross section) was shown in Figure 1.6.

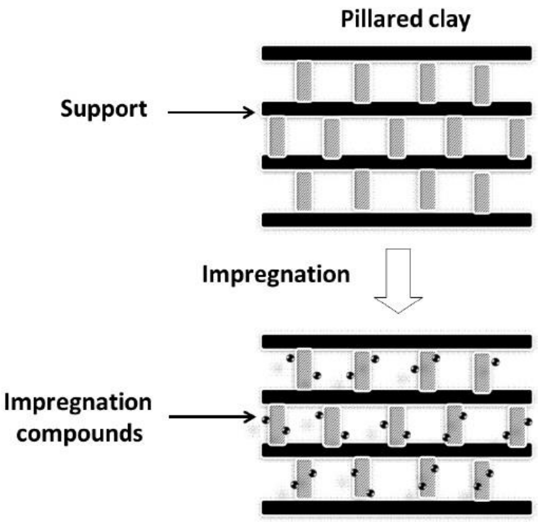

Figure 1.6 Diagram for the impregnated pillared clay compound (cross section) [5]

1.5 Characterization of clays and clay catalysts

1.5.1 Powder X-ray diffraction (XRD)

X-ray diffraction (XRD) is a technique for identification the transformation of solid material. It can provide the information on unit cell dimension. Its principle was a collimated beam of monochromatic X-rays strike onto the thin layer of surface sample affected to the diffracted X-ray to specific angle. Figure 1.7 demonstrates a monochromatic beam of X-ray on the crystal surface at angel ϴ. The scattered intensity can be measured as a function of scattering angle 2ϴ. The intensity of detected X-rays is plotted as a function of angle, resulted in the X-ray diffraction pattern which is characteristic for the sample material [5].

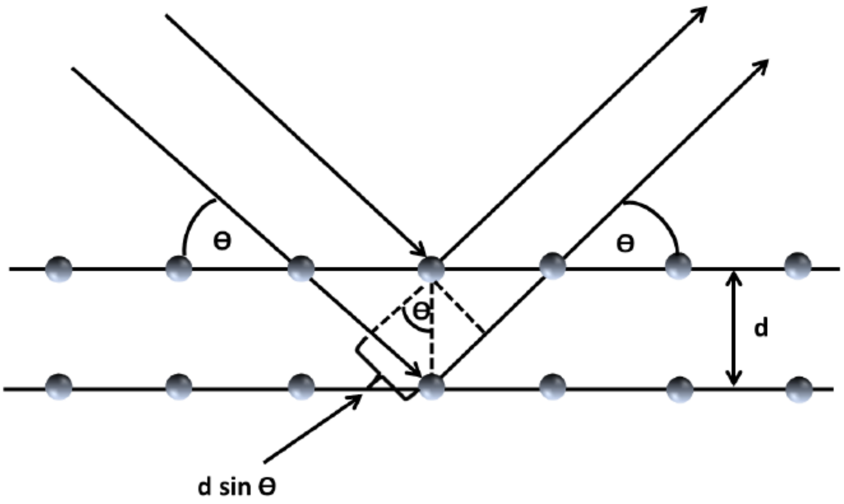

Figure 1.7 Diffraction of X-ray by regular planes of atoms [5]

Bragg's law is the equation which is relevant to the wavelength of the incident X-rays, angle of incidence and spacing between the crystal lattice planes of atom.

Equation 1.1 Bragg's law equation [5]

$$n\lambda = 2d\sin\theta$$

where n = an integer of the diffracted beam

λ = wavelength

d = a distance between adjacent planes of atoms (d-spacing)

θ = an angle between the incidence beam and the scattering planes

1.5.2 Nitrogen adsorption-desorption isotherm

Nitrogen adsorption-desorption isotherm is usually used for surface area and pore size determination in mesoporous material. Adsorption of gas by a porous material is described by an adsorption isotherm, the amount of adsorbed gas on the material at a constant temperature as a function of pressure. The process of adsorption is usually studied through graphs which known as an adsorption isotherm. It is the graph between the amounts of gas adsorbate adsorbed on the surface of adsorbent and pressure at constant temperature. The IUPAC classifications of six types of adsorption isotherm are shown schematically in Figure 1.8 [5].

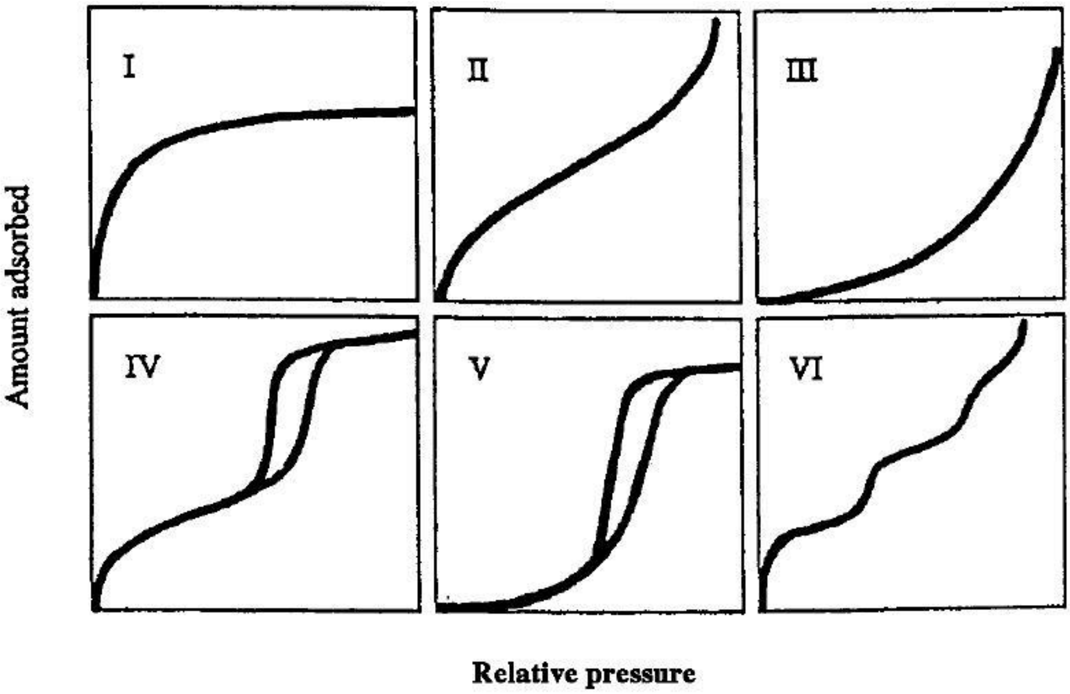

Figure 1.8 The types of adsorption isotherms [5]

An adsorption isotherm is obtained by measuring the amount of gas adsorbed across a wide range of relative pressures at a constant temperature (typically liquid N_2, 77K). Conversely, a desorption isotherm is achieved by measuring gas removed as pressure is reduced. It could be implied that, the strength of the interaction between the sample surface and gas adsorbed can differentiate the feather of sample. Adsorption isotherm could be classified in 6 types which demonstrated in table 1.1.

Table 1.1 Features of adsorption isotherms [5]

Type	Features	Porosity
	Interaction between sample surface and gas adsorbate	
I	Relatively strong	Micropore
II	Relatively strong	Nonporous

III	Weak	Nonporous
IV	Relatively strong	Mesopore
V	Weak	Mesopore
		Micropore
VI	Relatively strong Sample surface has an even distribution of energy	Nonporous

The method of Barrett Joyner and Halenda (BJH) is a procedure for calculating pore size distributions from experimental isotherms using the Kelvin model of pore filling. It applies to the mesopore. The Kelvin equation provides a correlation between pore diameter and pore condensation pressure. This method is based on the assumption that the initial relative pressure is close to unity, all pores are filled with liquid. The Kelvin equation provides a correlation between pore diameter and pore condensation pressure [8].

Equation 1.2 The Kelvin equation provides a correlation between pore diameter and pore condensation pressure [8]

$$ln\frac{P}{P_0} = \frac{-2\gamma V_l}{r_p RT}$$

Where γ = surface tension of liquid nitrogen

V_l = liquid molar volume

r_p = pore radius

R = universal gas constant

T = temperature

P = the equilibrium pressure

P_0 = the saturation pressure

Pore types are classified as shown in Table 1.2.

Table 1.2 IUPAC classification of pores [8]

Type	**Pore diameter (Å)**
Micropore	Up to 20
Mesopore	20 to 500
Macropore	500 or up

The multilayer Brunauer, Emmett and Teller (BET) method is commonly used to measure total surface area. The specific surface area of clay is determined by physical adsorption gas and calculated the amount of adsorbate gas corresponding to a monomolecular layer on the surface.

Equation 1.3 BET method for surface area calculation [5]

$$\frac{1}{W[(P_0/P)-1]} = \frac{1}{W_m C} + \frac{C-1}{W_m C}\left(\frac{P}{P_0}\right)$$

Where W = weight of nitrogen adsorbed at a given P/P_0

W_m = weight of gas to give monolayer coverage

C = a constant that is related to the heat of adsorbtion

P = the equilibrium pressure

P_0 = the saturation pressure

The quantity of nitrogen adsorbed in the monolayer was calculated by the slope and intercept from linear relationship between $1/W[(P_0/P)-1]$ and P/P_0. The intercept was taken as zero or a small positive value for a single point method. The slope of BET plot resulted in the surface area measurement [5].

1.5.3 Determination of Brönsted and Lewis acid

There are several methods to determine the surface acidity site of clay such as Hammett indicator, *n*-butylamine back titration, NH_3-TPD and FT-IR. FT-IR is an available technique in many laboratories and reliable method for surface clay characterization, including acidity determination. Its procedure for acid detection needs time less. The IR absorption spectra are obtained from these popular following sample preparations; self-supporting films, alkali-halide disk, attenuated total reflection FTIR (ATR-FTIR). However, the sample preparation for observation of acid sites by using self-supporting films and alkali-halide disk has drawback. Polyethylene sheet and KBr are required for self-supporting films and alkali-halide disk detection, respectively whereas ATR-FTIR needs none. Hence, the most suitable and simplistic in sample preparation is ATR-FTIR which clay sample could be easily located onto the diamond crystal for data acquisition.

Acid sites are examined from the IR spectrum at 1400-1700 cm^{-1} region of pyridine adsorbed on clay surface. Physisorbed pyridine was assigned to these following bands; hydrogen-bonded pyridine at ~1440 and 1590 cm^{-1}; Lewis acid-bound pyridine at ~1445, 1490 and 1590 cm^{-1} and Brönsted acid-bound pyridinium cation to ~1550 and 1640 cm^{-1}. Brönsted and Lewis sites can be distinguished from the characteristic center sites at 1550 and 1445 cm^{-1}, respectively [9]. The Brönsted acid-bound pyridinium cation and Lewis acid-bound pyridine was illustrated in Figure 1.9.

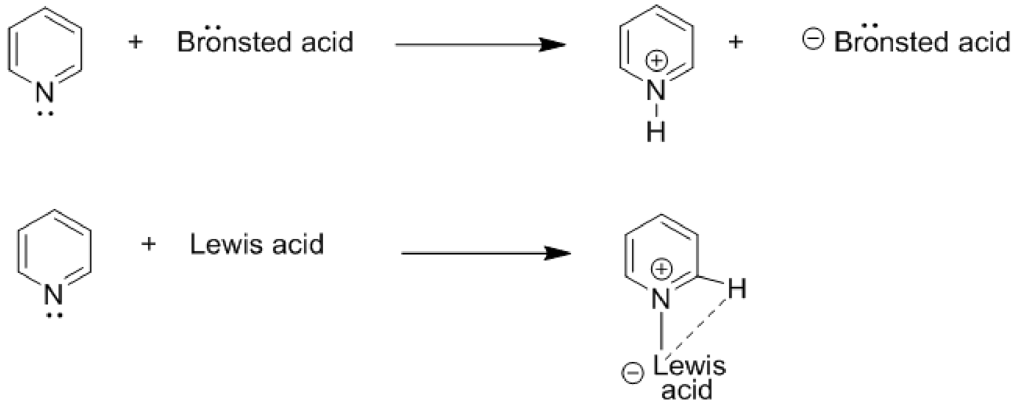

Figure 1.9 Brönsted acid-bound pyridinium cation and Lewis acid-bound pyridine [9].

1.6 The importance of benzylated aromatics from benzylation of aromatics

Friedel-Crafts benzylation of aromatics is an important synthesis for wide variety benzylated products. They are key intermediates for the production in pharmaceutical and chemical industries [10-12]. For examples, diphenylmethane and its derivatives (doxylamine, diphenhydramine and orphenadrine) are classified as antihistaminics drugs. They are commonly used to cure colds, asthma and other allergic deseases [13]. In chemical laboratory, they are precursor to synthesize benzophenone. In polymer industries, they are monomer for the production of polycarbonate resin and platisizer. In textile industries, they are solvent for dyes and thermal stability additive for polyester. In jet fuel industries, they are used to improve the stability of lubricants [14]. In fragrance industries, they are used to enhance the scent of soap [14]. For agricultural industries, they are catalysts for the production of pesticides and insecticides [15].

1.7 Literature reviews of the catalysis for the benzylation of aromatics

The general catalyst which plays a role in Friedel-Crafts benzylation reaction is Lewis acid. Conventionally, these benzylations were carried out industrially by dangerous homogeneous acid catalysts such as $AlCl_3$, BF_3, H_2SO_4, HF, HNO_3, *etc*. They generated high volume of waste materials. Moreover, they also posed several problems such as corrosion, toxicity, difficulty in separation, disposal, and reusability of the catalysts [21-26].

1.7.1 Benzylation of aromatics using homogeneous catalysts

Homogeneous catalysts are dissolved in reaction mixtures, hence all catalyst sites are available for the reactions. Many researches have reported various homogeneous catalysts utilizing for Friedel-Crafts benzylation for decades [16].

In 2005, Yi and Cai studied catalysis performance of rare earth(III) perfluorooctanesulfonates ($RE(OSO_2C_8F_{17})_3$) in benzylation of aromatics with benzyl alcohol in fluorous solvents. Benzylation of anisole and benzyl alcohol was used as template compounds. $Yb(OSO_2C_8F_{17})_3$ was found to catalyze the reaction of anisole with benzyl alcohol in perfluorodecalin ($C_{10}F_{18}$) with excellent yield (96%). Moreover, the fluorous phase containing only catalyst could be reused with a little decrease in activity.

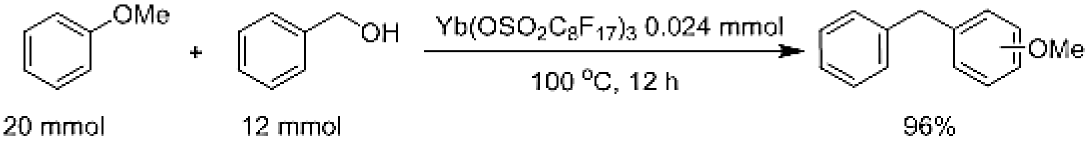

For further exploration, the reactions of benzyl alcohol with various aromatics were tested. Electron donating groups (fluorobenzene, ethylbenzene and toluene) gave good yields (80%) of target products. On the other hand, benzene and chlorobenzene gave lower yields. Since there is no electron donating group substitution on the benzene ring and chlorobenzene was an electron withdrawing group, respectively [16].

In 2008, Wang and his colleagues studied the effect of transition metal catalyst such as $ZnCl_3$, $FeCl_3$, $InCl_3$ *etc.* on benzylation of arenes and thiophenes with benzyl methyl ether. The results showed good reactivity (72-90%) in the benzylation of arenes and thiophenes with benzyl methyl ether *via* $FeCl_3$ catalyzation.

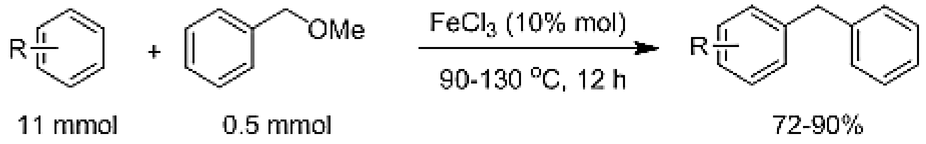

Different benzyl methyl ethers were chosen to react with benzene. The reactivity of those benzyl methyl ethers were in range of 27-90% due to the nature of benzylating agent [17].

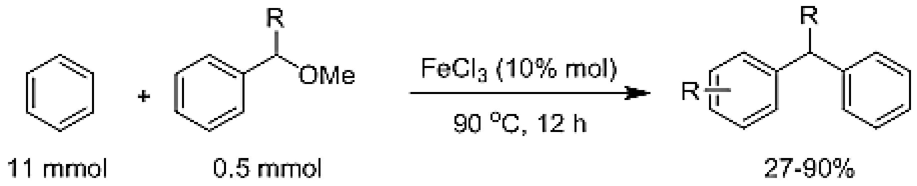

In 2011, Sakai and his colleagues were interested in $InBr_3$ catalyzation in the Friedel-Crafts benzylation. Carboxylic acid was first used as a benzylating agent in the presence of 5 mol% $InBr_3$ in anisole. Benzyl anisole was obtained in good yield (85%).

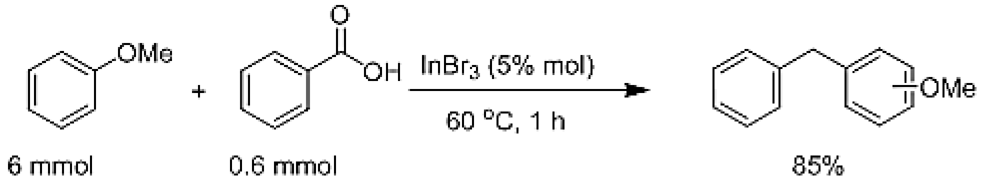

In addition, the yield of target molecules were good in case of electron donating groups. However, these optimum conditions could not apply for bromo- and cyanobenzenes because they were electron withdrawing groups.

Then, they tried to compare the efficiency of benzyl alcohol and benzyl silyl ether in presence of 5 mol% $InBr_3$ in anisole. The results indicated that benzyl silyl ether was more efficient benzylating agent than benzyl alcohol under these conditions [18].

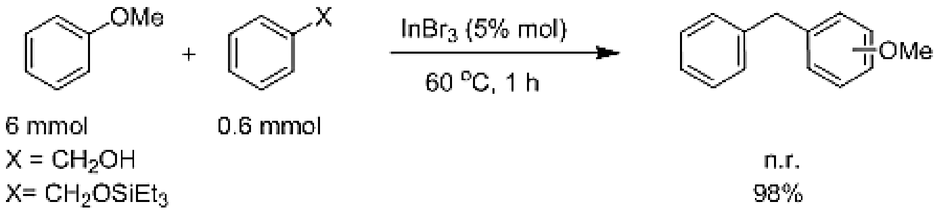

In 2012, Smutek and his colleagues interested in dilute acids to promote the alkylation of phenols with benzyl alcohol. Benzyl phenol was obtained in good yield (78%) under these conditions.

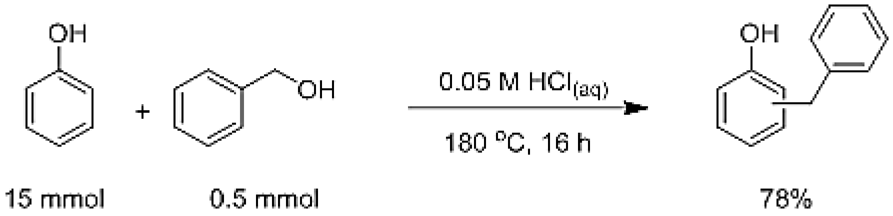

Then, they studied alkylation of phenols with different alcohols and found that only strong activated alcohols such as benzyl alcohol, sec-phenethyl alcohol and 4-hydroxybenzyl alcohol yielded high amounts of the alkylation product (68-93%). Among those alkylating agents, benzyl alcohol was the best which could alkylated with catechol and *p*-Cresol in good yields [19].

In 2015, Huang and his colleagues used boron trifluoride diethyl etherate ($BF_3.OEt_2$) as a promoter in benzylation of toluene with benzyl chloride. The optimum conditions were observed in the presence of 1.5 equivalents $BF_3.OEt_2$ and 0.4 equivalent of water.

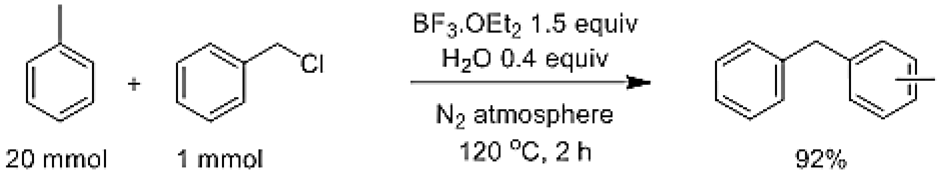

Then, benzylating agents (benzyl donor) reacted with aromatics were investigated underwent these optimal conditions. Only electron-donating groups gave good yields in range 67-98% [20].

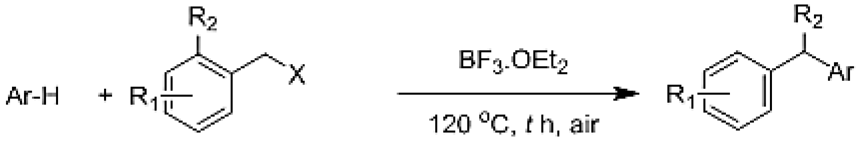

However, the preparation of some homogeneous catalysts is complicated. They are not stable at high temperature or difficult to separate from the reaction. Guideline to solve these problems has been considered as a heterogeneous catalyst, which is simplistic in preparation and recycle [21].

1.7.2 Benzylation of aromatics with heterogeneous catalyst

The interest in green chemical catalyst promotes the development of heterogeneous catalysis. The establishment of heterogeneous catalysis by supporting Lewis acid on mesoporous, zeolite and clay was easy. Moreover, the ease of separation and reusability were clearly demonstrated in advantages [21].

In 2000, Narayanan and Deshpenda synthesized Ce exchange and aluminium pillared clay in order to catalyze benzylation of toluene with benzyl alcohol. This catalyst was characterized by XRD and nitrogen adsorption desorption, respectively. After modified clay by Ce exchange and aluminium pillaring, this catalyst affected good creation of benzyl toluene [22].

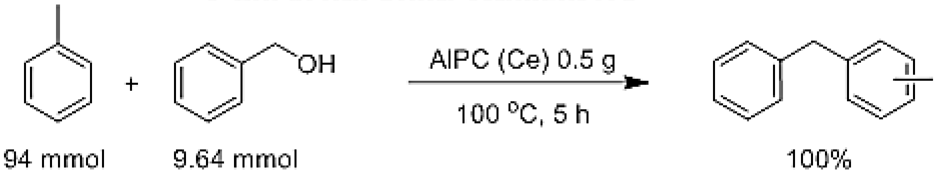

In 2003, Shrigadi and his colleagues synthesized iron oxide impregnated on K10 (K10-Fe_2O_3) to catalyze Friedel–Crafts benzylation of different arenes with benzyl chloride. Its transformation was detected by XRD and its acidity was checked by FT-IR. The reaction underwent at 80 °C within 5-10 min to give 100% conversion of benzyl chloride with arenes (benzene, toluene, ethyl benzene, cumene, propyl benzene, anisole, phenetole and chlorobenzene). This catalyst could be reused for 5 times [23].

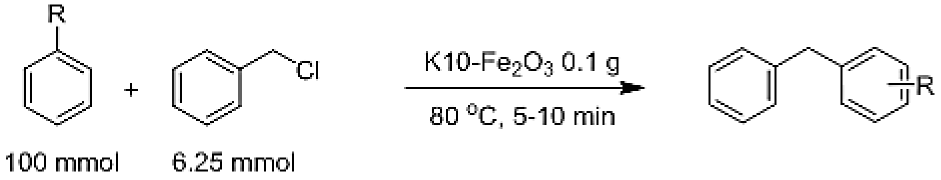

In 2007, Bachari and Cherifi synthesized tin containing mesoporous material (Sn-HMS-40) in order to catalyze Friedel-Crafts benzylation of benzene with benzyl chloride. This catalyst was characterized by XRD, nitrogen adsorption desorption, XPS, UV-Vis and FT-IR. The presence of tin(IV) was detected by XPS, UV-Vis and FT-IR. After used Sn-HMS-40 in benzylation of benzyl chloride and benzene, 75.3% yield of diphenylmethane in fresh use of this catalyst was acheived. This catalyst could be reused twice with appreciable yield of diphenylmethane 70% [24].

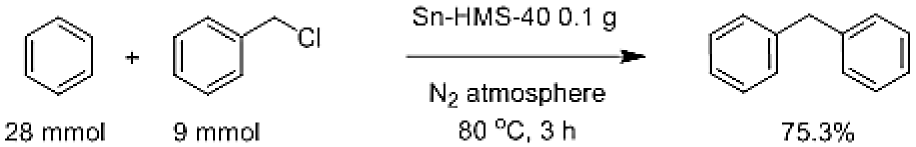

In 2013, Li and her colleagues prepared iron containing HMCM-68 zeolite by impregnation $FeCl_3$ on HMCM-68. It was characterized by XRD, nitrogen adsorption, UV-vis and NH_3-TPD. The presence of iron on zeolite surface could be detected by UV-Vis. The amount of acid in this catalyst was determined by NH_3-TPD. It was noticeable that this catalyst was Lewis acid in benzylation of toluene with benzyl chloride yielding quantitative yield of benzyl toluene. Nonetheless, it could be reused twice without losing catalytic activity [25].

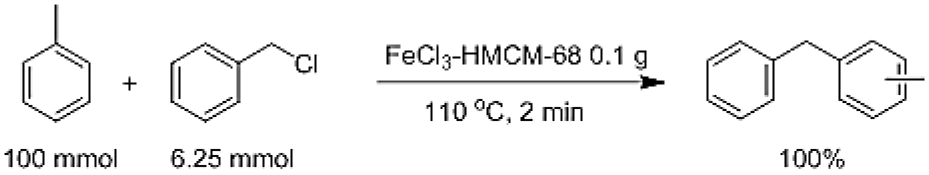

In 2014, Cuong and his colleagues synthesized nanoporous α-Fe_2O_3 nanoparticle as catalyst with an average of size 100 nm. It was observed by XRD, FT-IR and nitrogen adsorption whereas its morphology was observed by SEM and TEM. The prepared catalyst was employed in Friedel-Crafts benzylation of aromatics and benzyl chloride. Different arenes including benzene, toluene and *p*-Xylene, were investigated to produce monobenzylated products in range 98-100% yield [26].

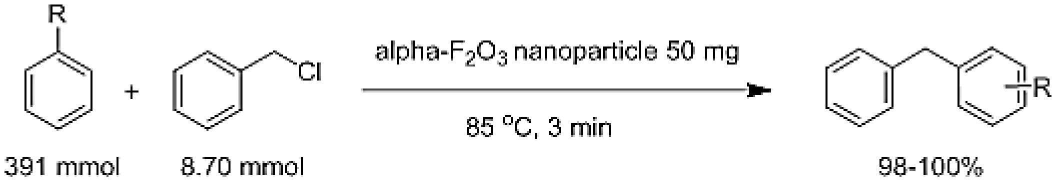

1.8 The important of tetrahydropyranyl ether

The tetrahydropyranyl group is a versatile protecting group for alcohols and phenols owing to its stability under strongly alkaline conditions, Grignard and alkyllithium reagents, reduction with inorganic hydrides, and alkylating and acylating agents. A hydroxyl group is a derivative lacking active hydrogen in those reactions. Since an important method that is applicable to protect hydroxyl group is to form tetrahydropyranyl ether (THP group). 3,4-Dihydro-2H-pyran (DHP) has been widely utilized as a protective group of hydroxyl compounds requiring protic or lewis acid as a typical promoters for tetrahydropyranylation reaction [27].

1.9 Literature reviews of the catalyst for tetrahydropyaranylation reaction

Tetrahydropyranylation of alcohols and phenols can be accomplished by using a variety of lewis acid. For years, there is still a need to develop lewis acid either homogeneous or heterogeneous catalysts for simpler and milder methods for protection the hydroxyl groups.

1.9.1 Tetrahydropyranylation of alcohols and phenols using homogeneous catalyst

Homogeneous catalysts are dissolved in reaction mixtures, hence all catalyst sites are available for the reactions. Many researches have reported various homogeneous catalysts utilizing for tetrahydropyranylation reaction.

In 2004, Wang and his co-workers used $PdCl_2(CH_3CN)_2$ as a lewis acid in tetrahydropyranylation of alcohols and phenol. The investigation of reaction conditions for the protection of alcohols with 3,4-dihydro-2H-pyran (DHP) using palladium catalyst in anhydrous THF at room temperature. The categories of primary alcohols afforded the corresponding THP-protected alcohols in 72-90% yields. Notably, secondary alcohol, tertiary alcohol and phenols gave poor yields or did not react under the same conditions [28].

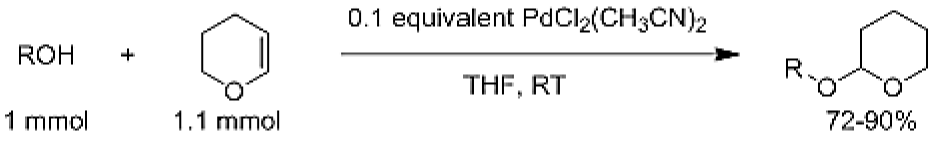

In the same year, Khan and his co-workers used cupric sulfate pentahydrate as a catalyst in tetrahydropyranylation of alcohols and phenols in acetonitrile at room temperature. The desired THP-protected alcohols could be achieved in primary alcohols, secondary alcohols and phenols in excellent yields (70-92%) [29].

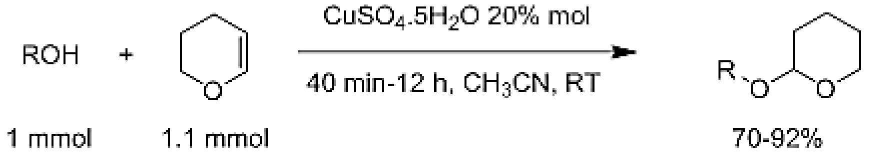

In 2007, Wang and his co-workers used coppermethane sulfonate-acetic acid in tetrahydropyranylation of alcohols and phenols. The results indicated that primary, secondary, tertiary and cyclic saturated alcohol reacted well to afford the corresponding THP-protected alcohols. The catalytic activity of short linear chain alcohols is higher than long or branched chain alcohols. Moreover, protection of phenolic hydroxy group was also achieved in the presence of this catalytic system [30].

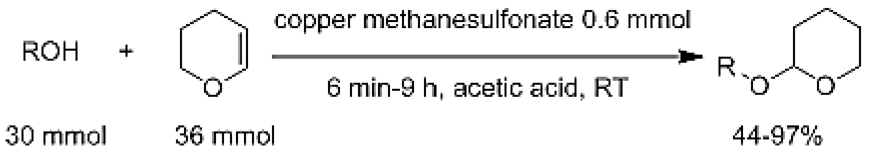

In 2011, Bodipati and his co-workers used trifluoro acetic acid (TFA) catalyzed tetrahydropyranylation of alcohols and phenols at ambient temperature. From the results, various primary, secondary alcohols and phenols were transformed easily into the corresponding products with appreciable yields (78-96%) [31].

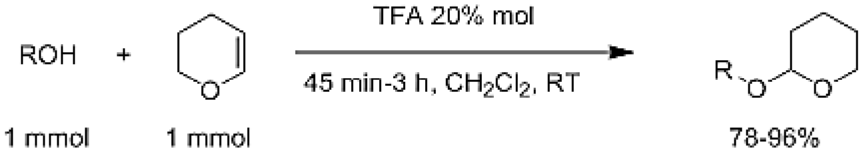

In 2014, they further investigated new catalytic system 3,5-dinitrobenzoic acid for tetrahydropyranylation of alcohols and phenols. Various primary, secondary alcohols and phenol derivatives gave appreciable yields of target products (80-97%) [32].

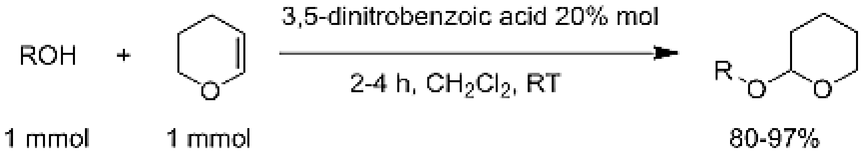

Although homogeneous catalytic system gave good yields of desired THP-protected alcohols products but some of those catalysts are corrosive and not eco-friendly. Therefore the heterogeneous catalysts are the alternative choices to solve these problems. Many researchers have developed the new catalytic heterogeneous catalysts for tetrahydropyranylation for years.

1.9.2 Tetrahydropyranylation of alcohols and phenols using heterogeneous catalyst

A remarkable advance in heterogeneous catalysts used for tetrahydropyranylation of alcohols and phenols has been reported. The development of zeolite, activated carbon and metal transition could enhance the acidity property for catalytic system. In addition, some of these catalysts could be recovered and reused for several times [33-37].

In 1997, Ballini and his colleagues used HSZ zeolite in tetrahydropyranylation of alcohols and phenols as a catalyst. The alcohols and phenols with electron donating and withdrawing groups were investigated. Their products were obtained in good yields (60-100%) [33].

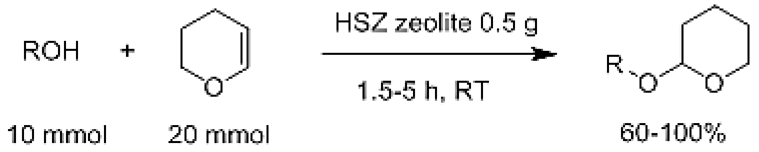

In 2008, Yang and his colleagues used activated carbon to synthesized THP ether products in tetrahydropyranylation of alcohols and phenols. Types of alcohols (primary, secondary and tertiary), phenol and *o*-Cresol were observed. They obtained the desired products with very good yields (88-95%) [34].

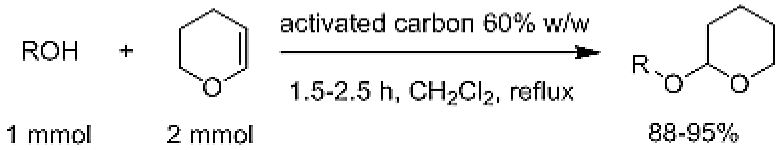

In 2010, Narender and her colleagues used Molybdenum supported on zeolite in acetic acid to catalyze tetrahydropyranylation. This method was applied to a variety of alcohols, phenols and naphthols. A wide range of alcohols, including primary, secondary, benzylic, heterocyclic and allylic alcohols as well as phenols and 2-naphthol underwent tetrahydropyranylation in moderate to excellent yields (45-95%). Moreover this catalyst could be reused for three times without losing the activity [35].

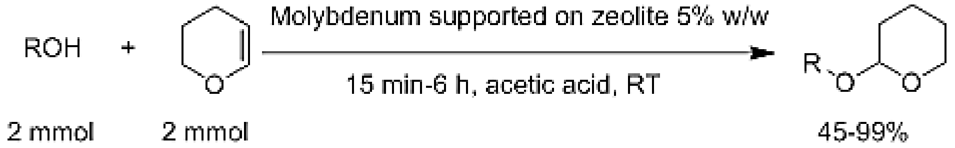

In 2011, Moghadam and his co-workers synthesized polystyrene-bound tin(IV) porphyrin for tetrahydropyranylation of alcohols and phenols. It was characterized by FT-IR and UV-Vis spectroscopic method. This catalytic system was active in the tetrahydropyranylation of alcohols (primary, secondary and tertiary) and also phenols with good yields (93-97%) within short reaction time (3-6 min) at RT. However, electron withdrawing group 4-nitrobenzyl alcohol and 4-nitrophenol gave only 62% yields of desired products. In addition, this catalyst could be reused for six times without losing activity in tetrahydropyranylation of 4-chlorobenzyl alcohol [36].

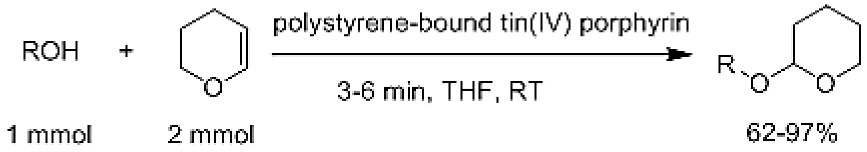

In 2011, Taghavi and his colleagues synthesized vanadium porphyrin tetraphenylporphyrinatovanadium(IV) trifluoromethanesulfonate [$V^{IV}(TPP)(OTf)_2$] as a catalyst for tetrahydropyranylation of alcohols and phenols. This catalyst was characterized by FT-IR. The results indicated that alcohol (primary, secondary, tertiary) and phenol derivatives in excellent yields (85-100%) within short reaction time (3-8 min) at RT. Moreover, this catalyst could be reused for five times in tetrahydropyranaylation of benzyl alcohol with no decrease in catalytic activity [37].

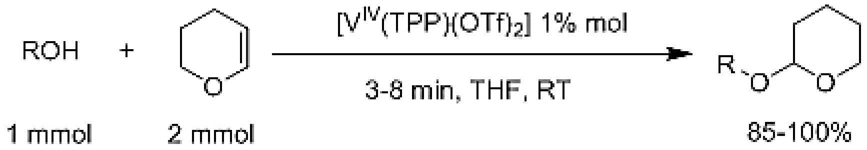

1.10 Literature review on clay catalyst

Clay catalyst has received much attention because of its advantages such as the environmental friendliness and the applicability in the desired catalytic conditions. Several methods using clay catalysts have been developed such as cation-exchange, pillaring and impregnation. However, the activity of these clay catalysts depended on the nature of the metal cation in acid treated clays. Organic modification clay catalysts were used in various reactions [6, 38].

1.10.1 Cleavage of aziridinine with alcohol

Ring opening of *N*–tosyl aziridinines with alcohol was reported in the presence of montmorillonite KSF acid clay at RT in CH_2Cl_2. Aryl-*N*-tosyl aziridinines reacting with alcohols gave predominantly the ring opened product **1** with a trace amount of **2**. On the contrary, the ring opened product **2** was predominant in case of alkyl-*N*-tosyl aziridinines. β-aminoethers were obtained in 90% yield.

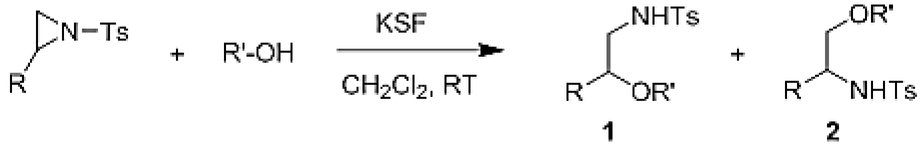

R = aryl, hexyl; R' = allyl, benzyl, propagyl, alkyl

β-Aminoethers were obtained in high yield (80-90%) within 3-9 h when cycloalkyl-*N*-tosyl aziridinines were reacted with alcohols [39].

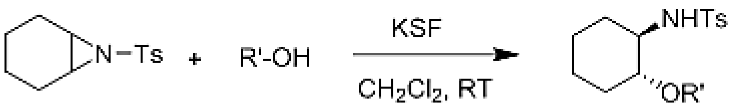

R' = allyl, benzyl, propagyl, alkyl

1.10.2 Coupling reaction

The protocol for three component-coupling reactions of aldehyde, amines and trimethylsilyl cyanide (TMSCN) to produce α-aminonitriles using montmorillonite KSF under mild conditions was investigated. A variety of aldehyde with a range of amines and TMSCN in the presence of montmorillonite KSF produced α-aminonitriles in 85-94% [40].

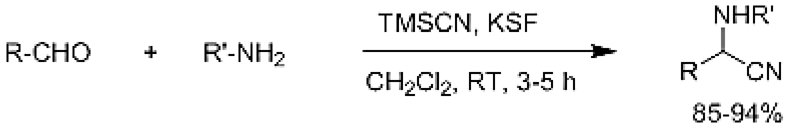

1.10.3 Cyclization

Synthesis of quinoline was accomplished *via* the cyclization reaction. The combination of K-10 catalyst and microwave irradiation method were utilized for the production of quinoline. The reaction could be accomplished at 90°C in a microwave irradiation within 6 min with 95%yield of quinoline. Several substituted cinnamaldehydes reacted with substituted anilines were observed followed those conditions which showed 60-95% yield [41].

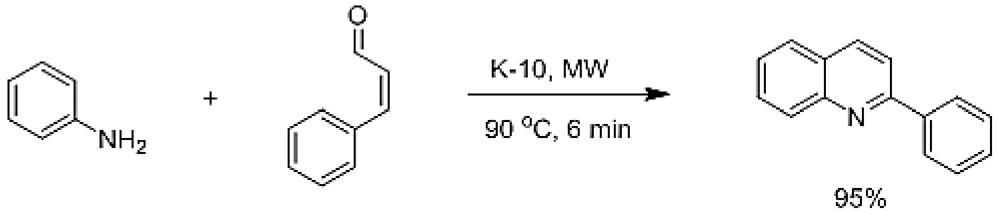

1.10.4 Acylation of aromatic ethers with acid anhydride

Acid mesoporous material, cation-exchanged K-10 montmorillonites (M^{n+}-mont, where $M^{n+} = Fe^{3+}$, Zn^{2+}, Cu^{2+}, Al^{3+} and Co^{2+}) were developed for acidity and investigated for its capability in acylation of aromatic ethers with acid anhydride. Acylation of 2-methoxynaphthalene, anisole and veratrole with acid anhydride were observed in the presence of cation-exchanged K-10 montmorillonite. Among these catalysts, Fe^{3+}-mont was the most appropriate catalyst for this reaction. Moreover, it could be reused for three times [42].

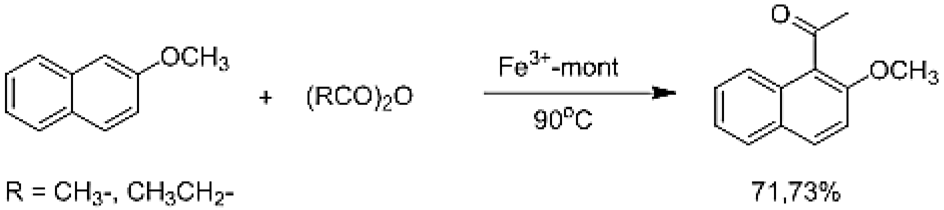

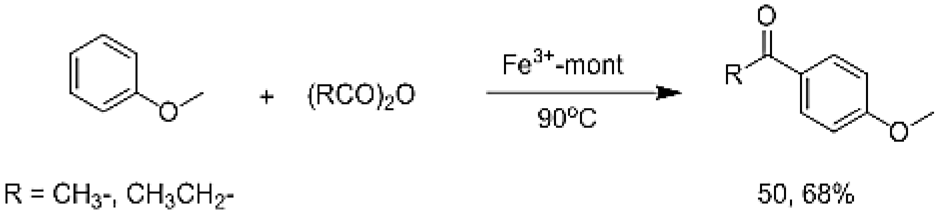

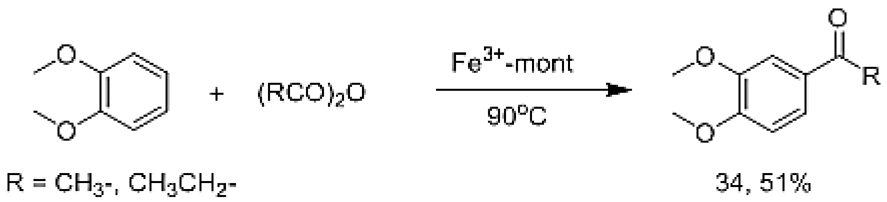

1.10.5 Epoxidation of cyclohexene

Cobalt salophen (*N*,*N′*-*bis*(salicylidene)-*o*-phenylenediamine) was immobilized into montmorillonite clay and acted as a catalyst for epoxidation of cyclohexene. This catalyst was characterized by AAS, FT-IR, UV–vis, XRD and

XPS. It exhibited high activity and epoxide selectivity for epoxidation of cyclohexene. Moreover, it could be reused for five times with an almost unchanged the efficiency of this catalyst [43].

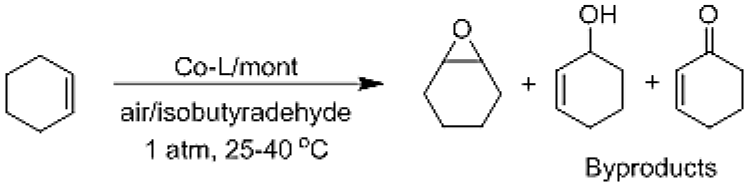

1.10.6 Esterification

Different cation-exchanged montmorillonite (M^{n+}-mont), where $M^{n+}=Al^{3+}$, Fe^{3+}, Cr^{3+}, Zn^{2+}, Ni^{2+} and Cu^{2+} were simply prepared for esterification catalysis. Their acidity tests were characterized by FT-IR, involving treatment pyridine adsorption. Trivalent cation-exchanged clay displayed both Brönsted and Lewis acid. On the other hand, divalent cation-exchanged clay showed predominantly Lewis acid. The esterification reaction of succinic acid with *iso*-butanol correlated with the presence of Brönsted sites. Among these catalysts, the production of esters was observed in the presence of Al^{3+}-mont (96%), Fe^{3+}-mont (74%) and Cr^{3+}-mont (51%) [44].

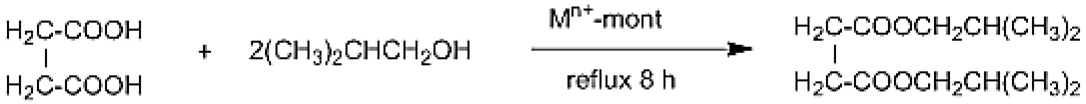

$$\begin{array}{c} H_2C\text{-}COOH \\ | \\ H_2C\text{-}COOH \end{array} + 2(CH_3)_2CHCH_2OH \xrightarrow[\text{reflux 8 h}]{M^{n+}\text{-mont}} \begin{array}{c} H_2C\text{-}COOCH_2CH(CH_3)_2 \\ | \\ H_2C\text{-}COOCH_2CH(CH_3)_2 \end{array}$$

1.10.7 Selective oxidation on H_2S

The catalytic performance of alumina-pillared clay (Al-PLC) and vanadia doped alumina-pillared clay (V/Al-PLC) in the selective oxidation of H_2S were investigated. Their characterizations were examined by XRD, nitrogen adsorption, XPS, ^{51}V NMR, H_2-TPR and NH_3-TPD. V/Al-PLC catalyst (96%) exhibited higher conversion of H_2S to sulfur than Al-PILC catalyst (90%) [45].

1.10.8 Hydrogenation of naphthalene

A variety of nickel supported clays was synthesized to catalyze naphthalene hydrogenation to tetralin and decalin. Nickel impregnated on montmorillonite

(Ni/MMT), nickel impregnated on cetyltrimethylammonium bromide-pillared montmorillonite (Ni/MMT-CTAB) and nickel impregnated on aluminium pillared montmorillonite (Ni/MMT-Al_2O_3) were synthesized and compared the catalytic activity. Ni/MMT-CTAB was found to be superior to the Ni/MMT and Ni/MMT-Al_2O_3 catalysts due to null of micropore in Ni/MMT-CTAB. Therefore, mass transfer of naphthalene and its hydrogenation bulky products (tetralin and decalin) were occurred easily [46].

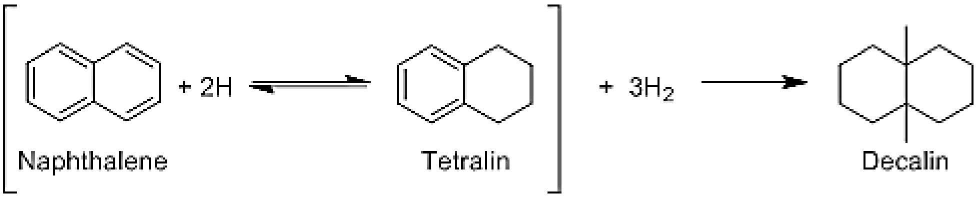

1.10.9 *O*-alkyaltion of phenol

In our research unit, $InCl_3$/Al-PLM was synthesized and characterized by XRD, nitrogen adsorption desorption, NH_3-TPD and ICP-OES to study the regeosilective for *O*-Alkylation of *p*-Cresol. The *O*-alkylated product (**1**) was occurred efficiently when applied only 5% mol $InCl_3$/Al-PLM under the optimized conditions. This protocol could be applied for other phenol alkylations in good yield (90-100%). In addition, this catalyst could be reused for 5 times without losing activity [5].

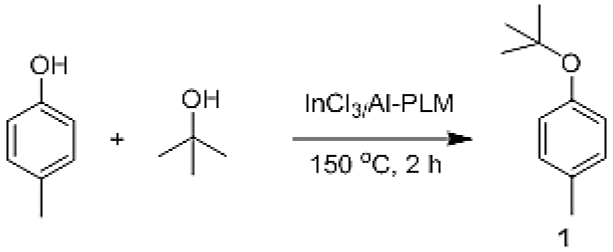

1.10.10 *C*-alkyltion of phenol

Recently, $NdCl_3$/Al-PLM was synthesized in our research unit and characterized by XRD, nitrogen adsorption desorption and NH_3-TPD. This catalyst was disclosed to regioselective *C*-alkyltion of *p*-Cresol with *tert*-butanol.

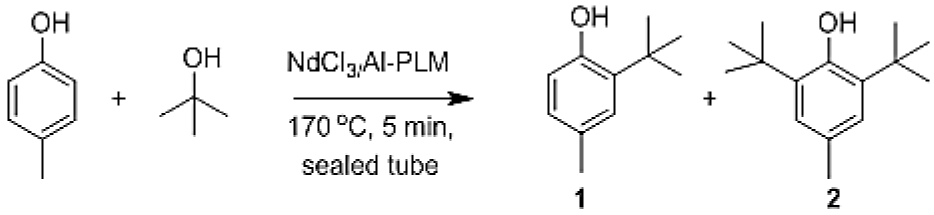

The *C*-alkylted products of *p*-Cresol was obtained in quantitative yield. With other alkylating agents and phenol derivatives, the *C*-alkylation products were produced in excellent yield (90-100%). Moreover, this catalyst could be reused for five times [47].

From those literature reviews on heterogeneous clay catalysts, the advantages of clay are an acid for reaction catalysis. Hence, modification of clay catalyst to improve its quality was the considerable objective for organic synthesis and industrial point of view. Although, the use of adjusted clays, $NdCl_3$/Al-PLM for acid catalyzed Friedel-Crafts alkylation of phenols was investigated, there is no report involving Friedel-Crafts benzylation of aromatics and tetrahydropyranylation of benzyl alcohols using this catalyst.

1.11 The goal of this research

The aim of this research could be summarized as follows:

1. To synthesize and characterize 2%$NdCl_3$/Al-PLM for Friedel-Crafts benzylation of aromatics and tetrahydropyranylation of benzyl alcohol.
2. To study the optimum conditions for *C*-benzylation of selected chemical models (toluene and benzyl alcohol) and apply for the other aromatics.
3. To study the optimum conditions for tetrahydropyranylation of benzyl alcohol
4. To study the use of regenerated 2%$NdCl_3$/Al-PLM in Friedel-Crafts benzylation of toluene and tetrahydropyranylation of benzyl alcohol reactions.

CHAPTER II
EXPERIMENTAL

2.1 Equipments and instrument

2.1.1 Centrifuge

The sediments of the purified and synthesized clays were collected by C2 series, Centurion Scientific centrifuge. Montmorillonite was purified by the eradication of quartz and other impurities, and the adjusted clay was collected by the removal of excess NaOH and $AlCl_3$ solution from the process.

2.1.2 Oven and furnace

Purified and synthesized clays were dried in a Memmert UM-500 oven at 100 °C for 24 h. The calcination of pillared and impregnated clays was conducted on a Cerbolite RHF 1600 muffle furnace in air. Pillaring was aimed to convert $AlCl_3$ in the interlayer of clays into aluminium oxide-pillared montmorillonite (Al-PLM) with the rate at 5°C/min and holding at 500°C for 1 h. Then, the impregnation of 2%$NdCl_3$ on Al-PLM (2%$NdCl_3$/Al-PLM) was heated with rate at 5°C/min and hold at 450°C for 4 h.

2.1.3 X-ray diffractrometer (XRD)

The XRD patterns and basal spacing of raw and modified clay catalysts were recognized by a Riguka, Dmax 2200/unimaplus XRD with a monochromate and Cu K radiation (40KV, 30 mA). The 2θ angel was ranged from 2 to 30° for bentonite. The scan speed and step were set at 3 degree/min and 0.02 degree, respectively. The scattering slit, divergent slit and receiving slit were fixed at 0.5 degree, 0.5 degree and 0.15 mm, respectively.

2.1.4 Nitrogen adsorption/desorption (BET and BJH method)

The Brunauer–Emmett–Teller (BET) specific surface areas and Barrett-Joyner-Halenda (BJH) pore diameter of raw and synthesized catalysts were measured by the Quantachrome Autosorp-1 nitrogen adsorptometer. The 0.04 g of clays was pretreated at 150°C for 2 h. After that the BET specific surface areas and BJH pore diameter were obtained from nitrogen adsorption at 77 K.

2.1.5 FT-IR Spectroscopy

The acidity of 2%$NdCl_3$/Al-PLM was measured by FTIR-Nicolet 6700 spectrometer which was equipped with a diamond crystal (refractive index n = 2.4). IR spectrum was recorded in transmittance as a function of wave number ranging from 1400 to 1700 cm^{-1}.

2.1.6 Nuclear magnetic resonance spectrometer (NMR)

The ^1H NMR spectra were obtained in $CDCl_3$ with teramethylsilane (TMS) as an internal reference on Varian proton nuclear magnetic resonance spectrometer, model Mercury plus 400 NMR spectrometer which operated at 399.84 MHz for ^1H nuclei. The chemical shifts (δ) are assigned by comparison with $CDCl_3$ solvent proton. The ^1H NMR of $CDCl_3$ was shown up at 7.26 ppm.

2.1.7 Chromatography

Thin layer chromatography (TLC) was carried on aluminium sheets percoated with silica gel (Merck's, kieselgel 60 PF254) in order to separate mixtures. Column chromatography was run on silica gel with pore size 60 Å (Merck grade 7734) in order to purify compounds. The gradient solvents of hexane, CH_2Cl_2 and EtOAc were used to isolate compounds.

2.2 Clays and chemicals

2.2.1 Bentonite

Raw bentonite was kindly supported by [a]Ceric international Co., Ltd. The compositions of bentonite are summarized in Table 2.1.

Table 2.1 [a]Bentonite compositions

	Bentonite (%)
SiO_2	63.60
Al_2O_3	17.60
K_2O	0.50
Fe_2O_3	3.10
CaO	3.00
Na_2O	3.40

2.2.2 Chemicals

The reagents for preparation of modified clay and catalytic study were purchased from Merck company (NaOH, benzene, nitrobenzene, biphenyl, benzyl chloride, toluene, 2-naphthol), Fluka company ($AlCl_3{\cdot}6H_2O$, *p*-cresol, benzyl ether, ethylbenzene, cyclododecane), Sigma-Aldrich (*tert*-butylbenzene, $NdCl_3.6H_2O$, 3,4-dihydro-*2H*-pyran), Carlo erba company (benzyl alcohol), BDH company (anisole) and Riedel-de Haën company (anhydrous $FeCl_3$). All solvents were distilled before use except for those which are reagent grade.

2.3 Homoionic clay

Homoionic clay was prepared by purification bentonite to get rid of quartz and then Na-ion exchange [5].

2.3.1 Purification of bentonite

Bentonite was purified by fractionated sedimentation. Bentonite 30 g was dispersed in deionized water 1 L under continually stirring for 3 h at RT. Then, quartz sediments were separated and discarded from the suspension of bentonite to obtain pure montmorillonite by centrifugation at 100°C for 48 h and was characterized with XRD measurement.

2.3.2 Na-ion exchange

Na-montmorillonite was prepared by cation exchange. Montmorillonite from previous step was suspended in 5 M NaOH with ratio of clay to NaOH solution 1 g: 50 mL for 24 h at RT and repeated this step for three times. The hydroxide ions and the excess sodium ions were removed from Na-montmorillonite using a dialysis membrane (Seamless Cellulose Tubing, small size 30 Wako chemical USA). The products were checked by universal indicator and confirmed by XRD measurement.

2.4 Synthesis of Al-pillared montmorillonite (Al-PLM)

Na-montmorillonite 10 g was dispersed in 500 mL of deionized water under continually stirring for 48 h at RT. The Al-pillaring agent was prepared, 0.2 M NaOH was added dropwise to 0.2 M $AlCl_3.6H_2O$ solution with the ratio of OH/Al 1.9 by using dropping funnel and stirred this mixture for 24 h at RT. Then the mixture of solution was added slowly to the clay suspension in previous step for 24 h at RT. The precipitates were collected by centrifugation at 4000 rpm for 10 min. Then, precipitates were cleaned by washed with deionized water to removed chloride ion and checked it with $AgSO_4$ solution. The intercalated product (Al-PLM) was dried at 100°C for 24 h and calcined at 500°C at the rate of 5°C/min for 1 h [5].

2.5 Synthesis of 2%neodymium (III) chloride impregnated on Al-pillared montmorillonite (2%$NdCl_3$/Al-PLM)

Al-PLM was impregnated using a solution of 2%$NdCl_3$ in amount of minimized EtOH. The slurry mixture was dried at 60°C and calcined at 450°C at the rate of 5°C/min for 4 h to obtain 2%$NdCl_3$/Al-PLM [5].

2.6 Determination of acidity.

Acidity of 2%$NdCl_3$/Al-PLM was determined by FT-IR Nicolet 6700 spectrometer of adsorbed pyridine. This catalyst was dried in hot air for 1 h at 100°C prior to pyridine treatment. 2%$NdCl_3$/Al-PLM 50 mg and pyridine 0.1 mL were poured into a sample cup. Then, the sample cup was kept in a hot air oven at 120°C for 1 h to remove physisorbed pyridine. After cooled down this catalyst, IR spectra of

2%$NdCl_3$/Al-PLM was recorded in transmittance as a function of wave number ranging from 1400 to 1700 cm^{-1}. Brönsted and Lewis acid sites can be distinguished from the IR spectrum of pyridine adsorbed on the clay surface. The relative concentration of Lewis and Brönsted sites $C_{L/B}$ can be calculated from the following equation 2.1 [9].

Equation 2.1 The relative concentration of Lewis and Brönsted sites [9]

$$C_{L/B} = \frac{A_{1445}\varepsilon_{1550}}{A_{1550}\varepsilon_{1445}}$$

Where $C_{L/B}$ is the relative concentration of Lewis and Brönsted sites. A_{1445} is the area of the IR band centered attributed to Lewis site, A_{1550} is the area of the IR band centered attributed to Brönsted site, and ε are the molar absorption coefficients for the corresponding bands at 1445 and 1550 cm^{-1}. Values of 1.28 and 1.13 cm μmol^{-1} have been reported for ε_{1445} and ε_{1550}, respectively.

2.7 Preparation of authentic samples

2.7.1 Preparation of authentic samples for benzylation of aromatics

In a sealed tube equipped with a magnetic stirring bar, benzyl chloride 3 mmol and anhydrous $FeCl_3$ 10% mol were mixed, then aromatics 6 mmol was added into the reaction mixture. The mixture was stirred at 170°C for 4 h. After the reaction was completed, the reaction mixture was extracted with EtOAc and DI water. The combined organic layer was collected and dried over anhydrous Na_2SO_4. The solution was evaporated to dryness. The mixture was purified by silica gel column using a gradient mixture of hexane, CH_2Cl_2 or EtOAc as an eluent to give the desired products. The structures of desired products were confirmed by ^1H NMR spectrum. The selected aromatics, toluene, ethylbenzene, anisole, *tert*-butylbenzene, *p*-cresol, *p*-xylene, benzene, biphenyl and 2-naphthol were carried out following this procedure.

Mixture of *o*-and *p*-benzyltoluene (1a and 1b) 260 mg (23.7%); colorless oil; R_f 0.43 (solvent system: hexane).

***o*-benzyltoluene (1a):** ^{1}H NMR (CDCl$_3$) δ (ppm): 7.31–7.25 (m, 5H$_\mathbf{a}$, Ar**H**), 7.16-7.11 (m, 4H$_\mathbf{c}$, Ar**H**), 4.01 (s, 2H$_\mathbf{d}$, C**H**$_\mathbf{2}$), 2.27 (s, 3H$_\mathbf{g}$, C**H**$_\mathbf{3}$).

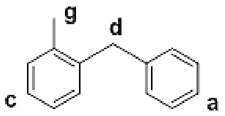

1a
ortho-benzyltoluene

***p*-benzyltoluene (1b)**: ^{1}H NMR (CDCl$_3$) δ (ppm): 7.22–7.18 (m, 5H$_\mathbf{b}$, Ar**H**), 7.16-7.11 (m, 4H$_\mathbf{c}$, Ar**H**), 3.97 (s, 2H$_\mathbf{e}$, C**H**$_\mathbf{2}$), 2.34 (s, 3H$_\mathbf{f}$, C**H**$_\mathbf{3}$).

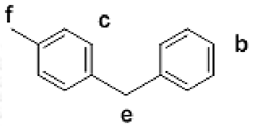

1b
para-benzyltoluene

Mixture of *o*-and *p*-benzylethylbenzene (2a and 2b) 263 mg (22.4 %); colorless oil; R$_f$ 0.49 (solvent system: hexane).

***o*-benzylethylbenzene (2a):** ^{1}H NMR (CDCl$_3$) δ (ppm): 7.32–7.27 (m, 5H$_\mathbf{a}$, Ar**H**), 7.17–7.08 (m, 4H$_\mathbf{c}$, Ar**H**), 4.05 (s, 2H$_\mathbf{d}$, C**H**$_\mathbf{2}$), 2.67-2.61 (q, J = 7.7 Hz, 2H$_\mathbf{f}$, C**H**$_\mathbf{2}$), 1.19-1.16 (t, J = 7.5 Hz, 3H$_\mathbf{h}$, C**H**$_\mathbf{3}$)

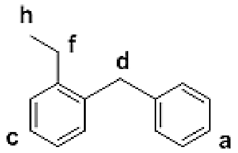

2a
ortho-benzylethylbenzene

***p*-benzylethylbenzene (2b)**: ^{1}H NMR (CDCl$_3$) δ (ppm): 7.24–7.19 (m, 5H$_\mathbf{b}$, Ar**H**), 7.17–7.08 (m, 4H$_\mathbf{c}$, Ar**H**), 3.98 (s, 2H$_\mathbf{e}$, C**H**$_\mathbf{2}$), 2.67-2.61 (q, J = 7.7 Hz, 2H$_\mathbf{f}$, C**H**$_\mathbf{2}$), 1.27-1.23 (t, J = 7.5 Hz, 3H$_\mathbf{g}$, C**H**$_\mathbf{3}$)

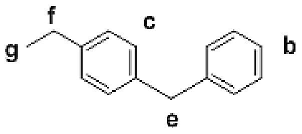

2b

para-benzylethylbenzene

Mixture of *o*-and *p*-benzyl-*tert*-butylbenzene (3a and 3b) 301 mg (22.4 %); colorless oil; R_f 0.49 (solvent system: hexane).

***o*-benzyl-*tert*-butylbenzene (3a):** ^{1}H NMR ($CDCl_3$) δ (ppm): 7.36–7.24 (m, 8H$_{\mathbf{a}}$, Ar**H**), 7.03–7.01 (d, *J* = 6.5 Hz, 1H$_{\mathbf{c}}$, Ar**H**), 4.03 (s, 2H$_{\mathbf{d}}$, C**H**$_{\mathbf{2}}$), 1.35 (s, 9H$_{\mathbf{f}}$, C**H**$_{\mathbf{3}}$)

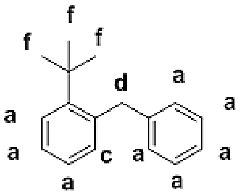

4a

ortho-benzyl-*tert*-butylbenzene

***p*-benzyl-*tert*-butylbenzene (3b):** ^{1}H NMR ($CDCl_3$) δ (ppm): 7.36–7.24 (m, 7H$_{\mathbf{a}}$, Ar**H**), 7.17–7.15 (d, *J* = 8.2 Hz, 2H$_{\mathbf{b}}$, Ar**H**), 4.00 (s, 2H$_{\mathbf{e}}$, C**H**$_{\mathbf{2}}$), 1.35 (s, 9H$_{\mathbf{f}}$, C**H**$_{\mathbf{3}}$)

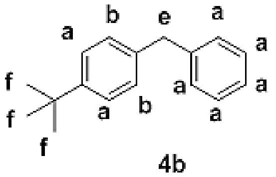

4b

para-benzyl-*tert*-butylbenzene

***o*-benzylanisole (4a),** 130 mg (21.9 %); colorless oil; R_f 0.38 in gradient of 10% EtOAc in hexane: ^{1}H NMR ($CDCl_3$) δ (ppm): 7.31–6.92 (m, 9H$_{\mathbf{a}}$, Ar**H**), 4.04 (s, 2H$_{\mathbf{b}}$, C**H**$_{\mathbf{2}}$), 3.84 (s, 3H$_{\mathbf{c}}$, C**H**$_{\mathbf{2}}$).

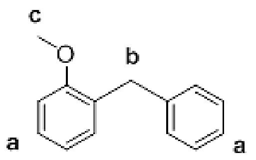

3a

ortho-benzylanisole

***p*-benzylanisole (4b)**: 130.1 mg (21.9 %); colorless oil; R_f 0.70 in gradient of 10% EtOAc in hexane: ^{1}H NMR ($CDCl_3$) δ (ppm): 7.35–6.93 (m, $9H_{\mathbf{a}}$, Ar**H**), 3.95 (s, $2H_{\mathbf{b}}$, C$\mathbf{H_2}$), 3.80 (s, $3H_{\mathbf{c}}$, C$\mathbf{H_2}$).

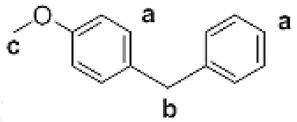

3b

para-benzylanisole

2-benzyl-4-methylphenol (5): 119 mg (20.0 %); colorless oil; R_f 0.51 (solvent system: 20% EtOAc in hexane); ^{1}H NMR ($CDCl_3$) δ (ppm): 7.28-6.63 (m, $8H_{\mathbf{a}}$, Ar**H**), 4.51 (s, $1H_{\mathbf{b}}$, O**H**), 3.93 (broad s, $2H_{\mathbf{c}}$, -C$\mathbf{H_2}$), 2.22 (s, $3H_{\mathbf{d}}$, C$\mathbf{H_3}$).

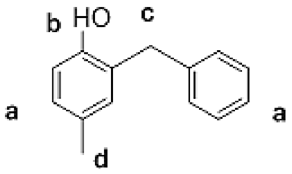

5

2-benzyl-4-methylphenol

2-benzyl-1,4-dimethylbenzene (6): 312 mg (53.0%); colorless oil; R_f 0.52 (solvent system: hexane); ^{1}H NMR ($CDCl_3$) δ (ppm): 7.32-6.97 (m, $8H_{\mathbf{a}}$, Ar**H**), 3.98 (s, $2H_{\mathbf{b}}$, C$\mathbf{H}_2$), 2.32 (s, $3H_{\mathbf{c}}$, -C$\mathbf{H_3}$), 2.23 (s, $3H_{\mathbf{d}}$, C$\mathbf{H_3}$).

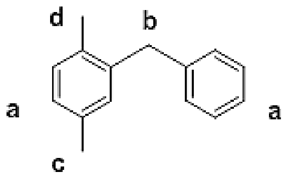

6

2-benzyl-1,4-dimethylbenzene

diphenylmethane (7a): 130 mg (25.8 %); colorless oil; R_f 0.51 (solvent system: 10% CH_2Cl_2 in hexane); ^1H NMR ($CDCl_3$) δ (ppm): 7.31–7.18 (m, 10$H_{\mathbf{a}}$, Ar**H**), 3.99 (s, 2$H_{\mathbf{b}}$, C$\mathbf{H_2}$).

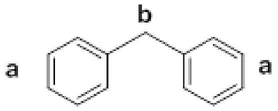

7a

diphenylmethane

1,2-dibenzylbenzene (7b): 99 mg (12.8 %); colorless oil; R_f 0.37 (solvent system: 10% CH_2Cl_2 in hexane); ^1H NMR ($CDCl_3$) δ (ppm): 7.29–7.07 (m, 14$H_{\mathbf{a}}$, Ar**H**), 3.96 (s, 4$H_{\mathbf{b}}$, C$\mathbf{H_2}$).

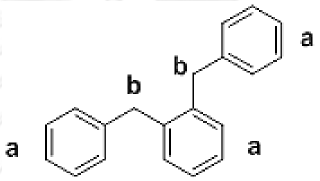

7b

1,2-dibenzylbenzene

1,4-dibenzylbenzene (7c): 107 mg (13.8%); colorless oil; R_f 0.46 (solvent system: 10% CH_2Cl_2 in hexane); ^1H NMR ($CDCl_3$) δ (ppm): 7.30–7.01 (m, 14$H_{\mathbf{a}}$, Ar**H**), 3.95 (s, 4$H_{\mathbf{b}}$, C$\mathbf{H_2}$).

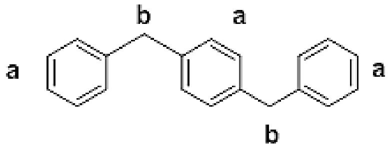

7c

1,4-dibenzylbenzene

***o*-benzylbiphenyl (8a):** 187 mg (25.2 %); white solid; R_f 0.25 (solvent system: 5% EtOAc in hexane); ^1H NMR ($CDCl_3$) δ (ppm): 7.39–6.99 (m, 14$H_{\mathbf{a}}$, Ar**H**), 3.97 (s, 2$H_{\mathbf{b}}$, C$\mathbf{H_2}$).

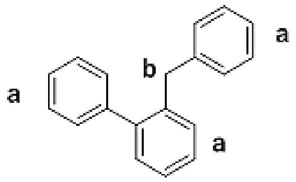

8a

ortho-benzylbiphenyl

***p*-benzylbiphenyl (8b):** 137 mg (18.7 %); white solid; R_f 0.64 (solvent system: 5% EtOAc in hexane); ^{1}H NMR ($CDCl_3$) δ (ppm): 7.57–7.21 (m, 14$H_\mathbf{a}$, Ar**H**), 4.02 (s, 2$H_\mathbf{b}$, C$\mathbf{H_2}$).

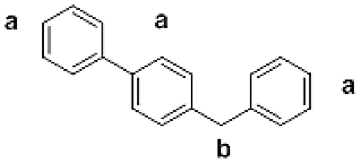

8b

para-benzylbiphenyl

1-benzyl-2-naphthol (9): 82 mg (11.7%); yellow oil; R_f 0.47 (solvent system: 70% CH_2Cl_2 in hexane); ^{1}H NMR ($CDCl_3$) δ (ppm): 7.80-6.97 (m, 11$H_\mathbf{a}$, Ar**H**), 4.33 (s, 2$H_\mathbf{b}$, C$\mathbf{H_2}$), 4.04 (s, 1$H_\mathbf{c}$, O**H**)

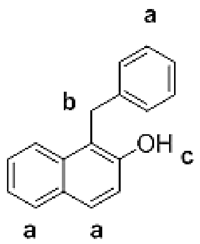

9

1-benzyl-2-naphthol

2.7.2 Preparation of authentic sample for 2-(benzyloxy)tetrahydro-2*H*-pyran in tetrahydropyranylation reaction

In a round bottomed flask with a magnetic stirring bar, benzyl alcohol 10.8 g (100 mmol) and $AlCl_3.6H_2O$ 4.8 g (20% mol) were mixed, then 3,4-dihydro-2*H*-pyran 9.2 g (110 mmol) was added into the reaction mixture. The mixture was stirred at 30°C (RT) for 24 h. After the reaction was completed, the reaction mixture was extracted with CH_2Cl_2 and DI water. The combined organic layer was collected and dried over anhydrous Na_2SO_4. The solution was evaporated to dryness. The product was purified by silica gel column using 10% EtOAc in hexane to give 2-(benzyloxy)tetrahydro-2*H*-pyran (**10**) which confirmed by ^{1}H NMR spectrum.

2-(benzyloxy)tetrahydro-2*H*-pyran (10): 14.4 g (75.0%); colorless liquid; R_f 0.48 (solvent system: 10% EtOAc in hexane); ^{1}H NMR ($CDCl_3$) δ (ppm): 7.36-7.28 (m, 5$H_{\mathbf{a}}$, Ar**H**), 4.81-4.78 (d, *J* = 12.0 Hz, 1$H_{\mathbf{b}}$, OC**H**$_2$), 4.72-4.71 (t, *J* = 3.42 Hz, 1$H_{\mathbf{c}}$, OC**H**O), 4.52-4.49 (d, *J* = 12.0 Hz, 1$H_{\mathbf{d}}$, OC**H**$_2$), 3.95-3.91 (m, 1$H_{\mathbf{e}}$, C**H**$_2$), 3.57-3.54 (m, 1$H_{\mathbf{f}}$, C**H**$_2$), 1.87-1.56 (m, 6$H_{\mathbf{g}}$, C**H**$_2$)

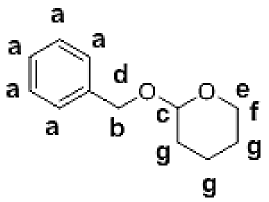

10

2-(benzyloxy)tetrahydro-2*H*-pyran

2.8 The effect of 2%$NdCl_3$/Al-PLM on benzylation of aromatics

2.8.1 Optimum conditions study on benzylation of aromatics reaction

2.8.1.1 General procedure

The benzylation of toluene with benzyl alcohol was performed as following. In a sealed tube with a magnetic stirring bar, catalyst 20 mg, benzyl alcohol 0.5 mmol and toluene 8 mmol were mixed together and stirred at 170°C for 1 h. The catalyst was filtered out, and washed with acetone several times before recycle process. The crude reaction mixture was quantified by ^{1}H NMR with an appropriate exact amount of internal standard (biphenyl) in comparison with authentic sample.

2.8.1.2 The effect of the amount of 2%$NdCl_3$/Al-PLM on benzylation of toluene

The benzylation of benzyl alcohol with toluene was performed according to the general procedure. In this part,various amount of 2%$NdCl_3$/Al-PLM: 0, 10, 20 and 50 mg were used in the reaction.

2.8.1.3 The effect of temperature on benzylation of toluene

Various temperatures: RT(30), 70, 120 and 170°C were used in benzylation of benzyl alcohol with toluene according to the general procedure. The aim is finding out the appropriate temperature providing high yield products.

2.8.1.4 Comparison the reaction system of benzylation of toluene.

The reaction system of benzylation of toluene with benzyl alcohol was compared the efficiency between pressured system and distillation technique. Pressured system, in a sealed tube with a magnetic stirring bar, catalyst 20 mg, benzyl alcohol 0.5 mmol and toluene 8 mmol were mixed together and stirred 170°C for 1 h. Another typical system, distillation technique (reflux), in a round bottom flask 25 mL with a magnetic stirring bar, catalyst 20 mg, benzyl alcohol 0.5 mmol and toluene 8 mmol were mixed together, stirred and refluxed in air at 170°C for 1 h.

2.8.1.5 The effect of reaction time on benzylation of toluene

Further study, the reaction time for benzylation of toluene with benzyl alcohol was investigated. In this part, various reaction time: 15, 30 and 60 min were carried out to ascertain high yield products.

2.8.1.6 The effect of molar ratio on benzylation of toluene

The appropriate molar ratio of aromatics to benzyl alcohol could prevent the production of benzyl ether. Thus, the series of molar ratio of toluene: benzyl alcohol as follows: 8:1, 8:0.5, 8:0.25 and 8:0.125 were studied to explore high yield products without benzyl ether.

2.8.1.7 The effect of benzylating agent on benzylation of toluene

According to general procedure, benzylation of toluene with benzyl alcohol was performed. The benzylating agent was switched to benzyl chloride and benzyl ether using the optimum conditions as follows: toluene (8 mmol), benzylating agent (0.5 mmol), sealed tube, 170°C, 1 h, 2%$NdCl_3$/Al-PLM (20 mg).

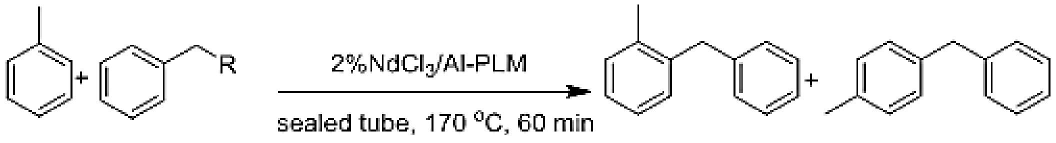

8 mmol 0.5 mmol 1a 1b

R = OH$^-$ (benzyl alcohol), Cl$^-$ (benzyl chloride), -OC_6H_5 (benzyl ether)

Scheme 2.1 Benzylation of toluene with different benzylating agents

2.8.2 Study on benzyltion of aromatics

According to the general procedure, in a sealed tube with a magnetic stirring bar, 2%$NdCl_3$/Al-PLM 20 mg, benzyl alcohol 0.5 mmol and aromatics (toluene, ethylbenzene, *tert*-butylbenzene, anisole, *p*-cresol, *p*-xylene, benzene, biphenyl, 2-naphthol and nitrobenzene) 8 mmol were mixed together and stirred at 170°C for 30 m. The crude reaction mixtures were quantified by ^1H NMR with an appropriate exact amount of internal standard (biphenyl and cyclododecane) in comparison with authentic samples.

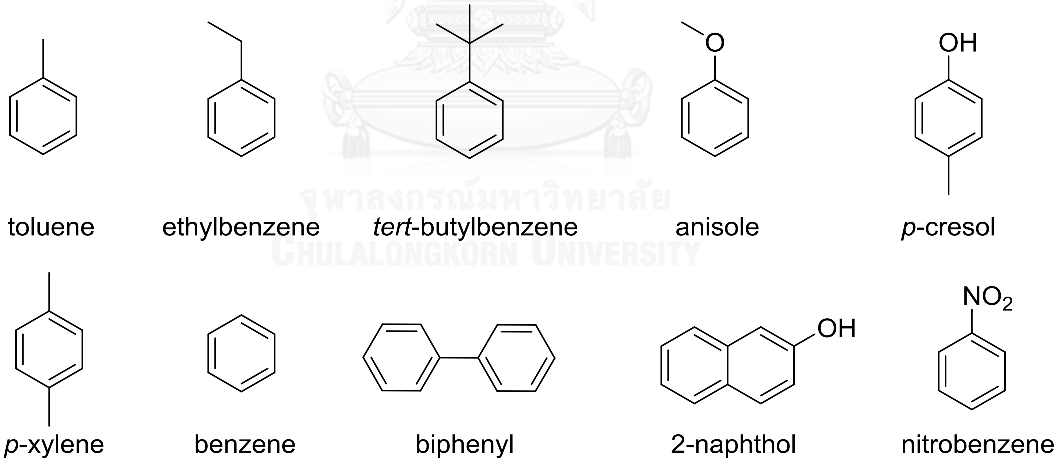

toluene ethylbenzene *tert*-butylbenzene anisole *p*-cresol

p-xylene benzene biphenyl 2-naphthol nitrobenzene

Figure 2.1 selected aromatics examined in benzylation using 2%$NdCl_3$/Al-PLM as a catalyst

2.9 The reusability of 2%$NdCl_3$/Al-PLM on benzylation of toluene with benzyl alcohol

2%$NdCl_3$/Al-PLM could be easily recovered by filtration. After washing with acetone several times, drying at 80°C in oven and calcination at 450°C at the rate of

5°C/min for 4 h, the regenerated 2%$NdCl_3$/Al-PLM was used in the next run for benzylation of toluene with benzyl alcohol.

2.10 The effects of 2%$NdCl_3$/Al-PLM on tetrahydropyranylayion of benzyl alcohol

2.10.1 Optimum conditions study on tetrahydropyranylayion of benzyl alcohol reaction

2.10.1.1 General procedure

The tetrahydropyranylation of benzyl alcohol was performed following this procedure. In a sealed tube with a magnetic stirring bar, catalyst 20 mg, benzyl alcohol 0.5 mmol and 3,4-dihydro-*2H*-pyran (DHP) 8 mmol were mixed together and stirred at 100°C for 1 h. The catalyst was filtered out, and washed with acetone several times before recycle process. The crude reaction mixture was quantified by ^1H NMR with an appropriate exact amount of internal standard (biphenyl) in comparison with authentic sample (**10**).

2.10.1.2 The effect of solvent on tetrahydropyranylation of benzyl alcohol

In a sealed tube with a magnetic stirring bar, catalyst 20 mg, benzyl alcohol 0.5 mmol, DHP 1 mmol and solvent 1 mL were mixed together and stirred at RT for 1 h. Various types of solvent such as ether, CH_2Cl_2, THF, MeCN, MeOH and none of solvent were chosen to study. The crude reaction mixture was filtered out and quantified by ^1H NMR.

2.10.1.3 The effect of temperature on tetrahydropyranylayion of benzyl alcohol

The exploration of temperature between 100 and 170 °C were investigated according to the general procedure. The aim is finding out the appropriate temperature providing high yield products.

2.10.1.4 The effect of 2%$NdCl_3$/Al-PLM amount on tetrahydropyranylayion of benzyl alcohol

The tetrahydropyranylation of benzyl alcohol was performed according to the general procedure. Various amounts of 2%$NdCl_3$/Al-PLM: 10, 20 mg and the absence of catalyst were used in the reaction.

2.10.1.5 The effect of reaction time on tetrahydropyranylayion of benzyl alcohol

The reaction time for tetrahydropyranylayion of benzyl alcohol was investigated. Various time: 15, 30 and 60 min were carried out to ascertain high yield products.

2.10.1.6 The effect of molar ratio on tetrahydropyranylayion of benzyl alcohol

The appropriate molar ratio of DHP: benzyl alcohol was investigated. The series of molar ratio of DHP: benzyl alcohol as follows: 8:0.5, 4:0.5, 2:0.5 and 1:0.5 were explored with the aim to get high yield products.

2.11 The reusability of 2%$NdCl_3$/Al-PLM on benzylation of toluene and tetrahydropyranylation of benzyl alcohol

The used 2%$NdCl_3$/Al-PLM catalysts from the reaction could be easily recovered by filtration, washing with acetone several times and drying at 100°C in oven. The catalysts were regenerated by two different modes: re-calcination (**A**) and not re-calcination (**B**) as shown in Figure 2.2 in order to compare the efficiency of catalysts under different methods before use in the next runs.

Treatment type A

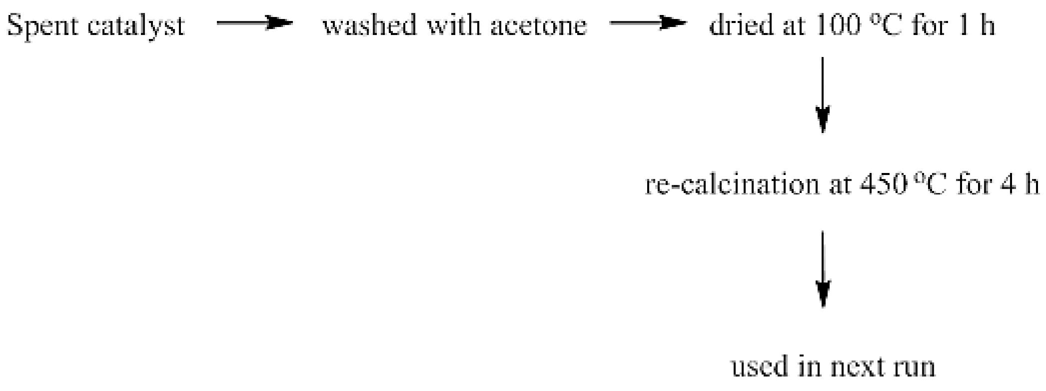

Treatment type B

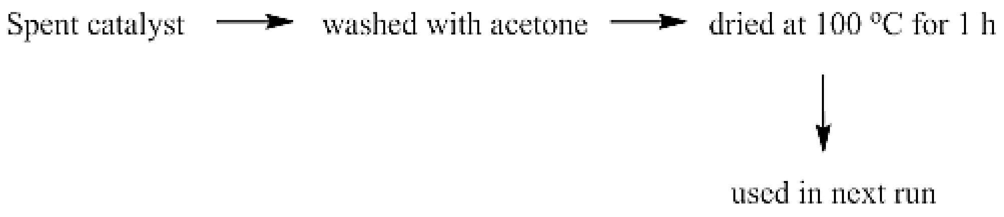

Figure 2.2 Two different methods for regenerating catalysts

CHAPTER III
RESULTS AND DISSCUSSION

3.1 Characterization of clay catalysts

This research focused on environmental friendly heterogeneous acid catalyst (2%$NdCl_3$/Al-PLM) which could catalyze benzylation of aromatics. Clay catalysts were characterized by XRD to observe the transformation and characteristic angles and d_{001}-basal spacings.

3.1.1 XRD patterns of clay catalysts

3.1.1.1 XRD patterns of bentonite and montmorillonite

Bentonite was classified as phyllosilicated-type clay consisting mostly montmorillonite and other impurities such as calcine, quartz, feldspars, crystobalite and humic acids. The amounts of those impurities were insignificant except for quartz. The presence of quartz in raw bentonite (Figure 3.1, **a**) could reduce the catalytic efficiency in organic reactions [1]. Hence, eradicating quartz by fractionated centrifugation is necessary for montmorillonite purification. After fractionated centrifugation, the characteristic peaks of quartz at 2θ of 22° and 24° were absence in montmorillonite purification XRD pattern (Figure 3.1, b). The pattern showed the characteristic peaks of montmorillonite **(a)** at 2θ of 8° and 19° which were related to the 001 and 100 planes of montmorillonite, respectively [3]. The 001 plane was used to monitor the intercalation of organic molecules. Its d_{001} basal spacing was 11.4 Å.

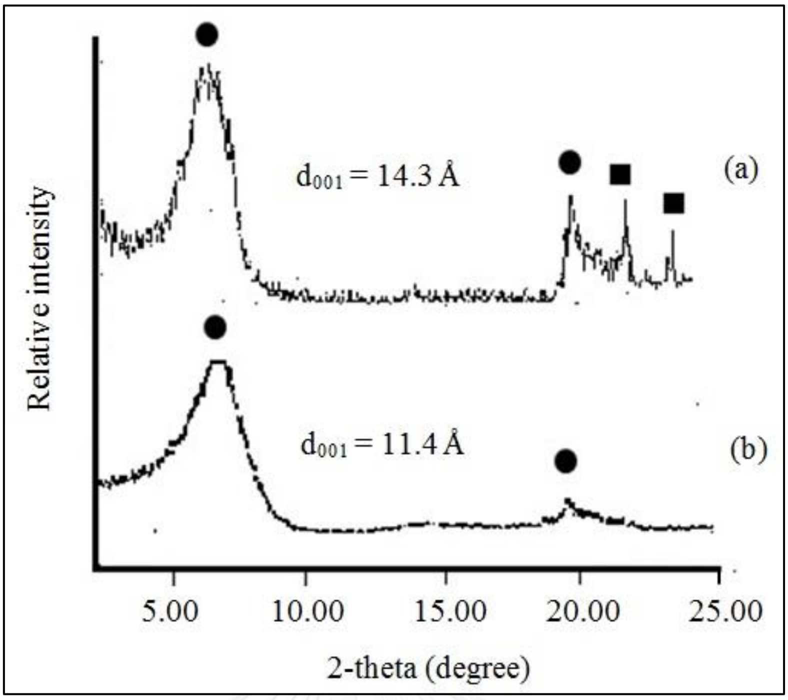

Figure 3.1 XRD patterns of raw material bentonite (**a**) and montmorillonite (**b**)

● represents the peaks of montmorillonite

■ represents impurity of quartz peaks

3.1.1.2 XRD patterns of montmorillonite and Na-montmorillonite

For the process of cleaning clay, montmorillonite was suspended in 5 M NaOH for three times and then excess sodium ions were removed by a dialysis membrane in order to discard minor mineral by ion exchange properties. The layer's structure of clays possessed a net negative charge which was balanced with interlayer Na^+. The XRD pattern of Na-montmorillonite (Figure 3.2, **b**) represented the characteristic peak of montmorillonite at 2θ of 7°. It was shifted to lower 2θ comparing with montmorillonite (2θ of 8°) (Figure 3.2, **a**), while d_{001} basal spacing of Na-montmorillonite (Figure 3.2, **b**) was increased from 11.4 to 12.5 Å. These could be rationalized that the intercalation of sodium ions for balancing charge expanded the interlayer spacing of the silicate gallery, leaded to a shift of the diffraction peak toward lower 2θ [9]. In addition, water molecule which solvated interlayer sodium ions caused the larger d-spacing of Na-montmorillonite.

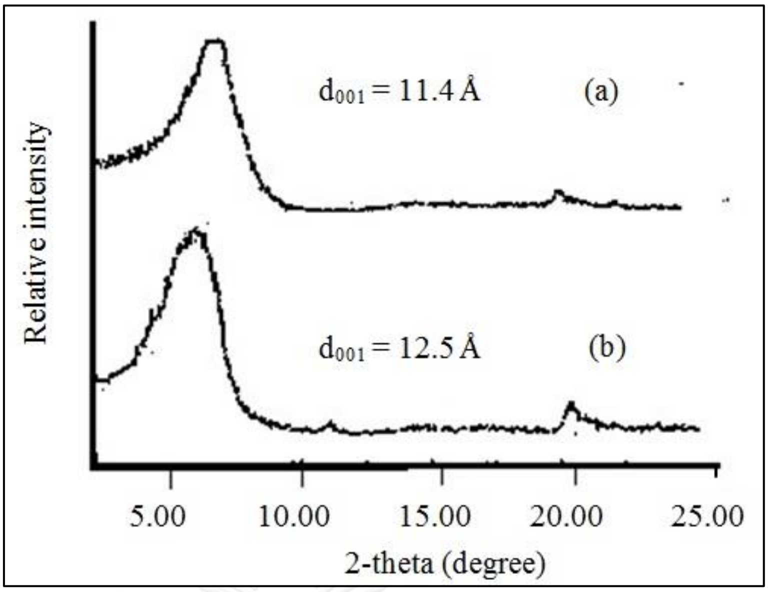

Figure 3.2 XRD patterns of montmorillonite (**a**) and Na-montmorillonite (**b**)

3.1.1.3 XRD patterns of Na-montmorillonite and Al-PLM

Aluminium pillaring was prepared by hydrolysis, adding 0.2 M NaOH to 0.2 M $AlCl_3$ with the ratio of OH/Al at 1.9 into Na-montmorillonite. The aluminium pillaring, polyoxocations $[Al_{13}O_4(OH)_{24}(H_2O)_{12}]^{7+}$ with Keggin structure and sodium ion were exchanged [5]. Then the synthesized clay was dried and converted to Al_2O_3 pillared montmorillonite (Al-PLM) during calcination process. The broad peak of Al-PLM at 2θ of 7° was larger than peak of Na-montmorillonite (Figure 3.3) because of the high calcination temperature. In addition, the pillaring of Al_2O_3 caused an increase in d-basal spacing from 12.5 to 13.2 Å which referred to a successful pillaring process of aluminium oxide species.

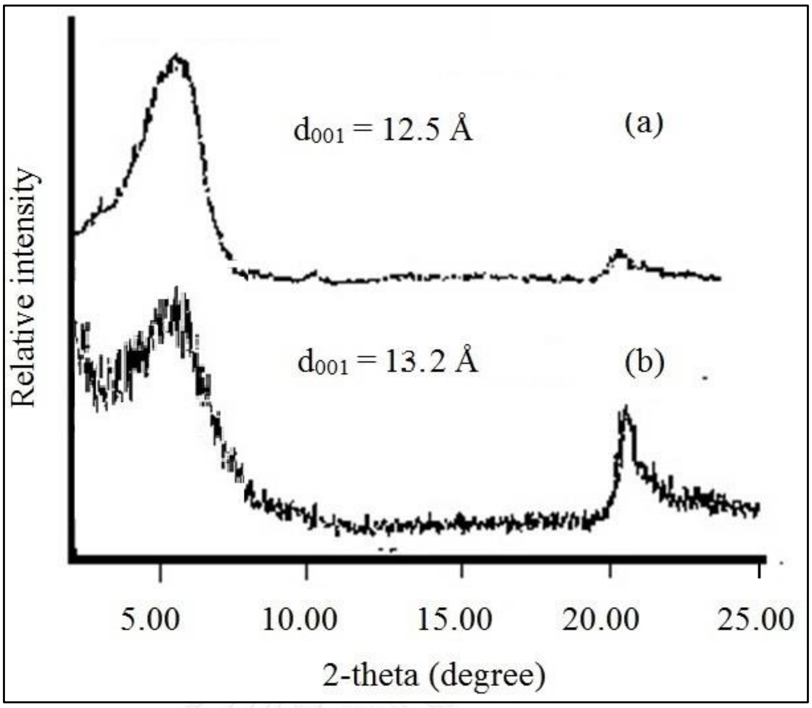

Figure 3.3 XRD patterns of Na-montmorillonite (**a**) and Al-PLM (**b**)

3.1.1.4 XRD patterns of Al-PLM and 2%$NdCl_3$/Al-PLM

2%$NdCl_3$/Al-PLM was prepared by impregnating 2%$NdCl_3$ in EtOH on Al-PLM *via* calcination at 450 °C for 4 h. The XRD pattern of 2%$NdCl_3$/Al-PLM (Figure 3.4) displayed the d_{001} basal spacing at 2θ of 7° and observed a large band by possibly derivetization from re-calcination process. The d_{001} value of the synthesized clay catalyst 2%$NdCl_3$/Al-PLM was 15.8 Å, indicating that the impregnation of $NdCl_3$ increased the disordering between the interlayer spacing of clay.

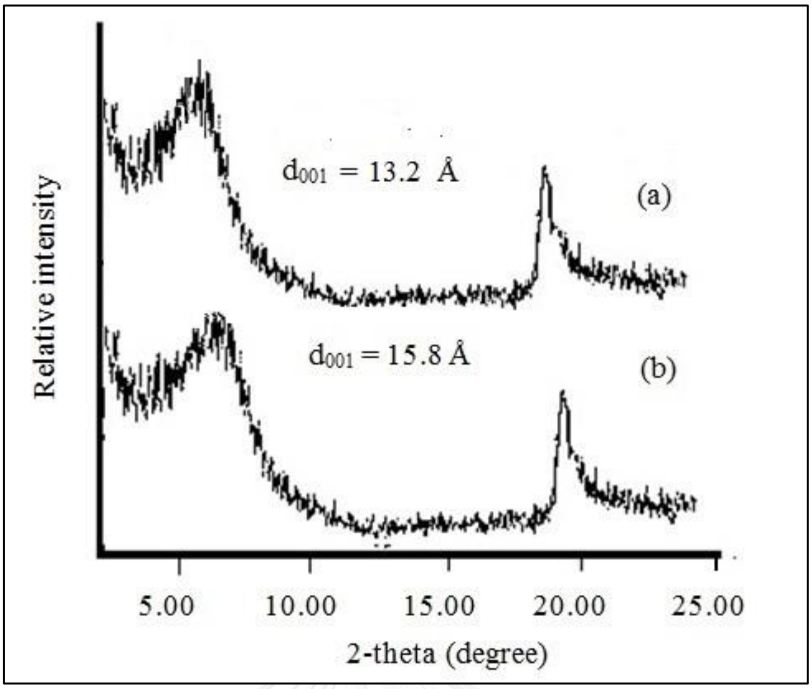

Figure 3.4 XRD patterns of Al-PLM (**a**) 2%$NdCl_3$/Al-PLM (**b**)

3.1.2 Surface area and pore size diameter

Brunauer–Emmett–Teller (BET) specific surface area and Barrett-Joyner-Halenda (BJH) pore size diameter were measured by nitrogen adsorption at 77 K. The results are shown in Table 3.1.

Table 3.1 BET specific surface area and BJH pore size diameter of clay catalysts

Entry	Type of clay catalyst	BET specific surface area (m^2/g)	Pore size diameter (Å)
1	montmorillonite	64.8	24.4
2	Na-montmorillonite	112.2	24.2
3	Al-PLM	126.0	24.2
4	2%$NdCl_3$/Al-PLM	66.4	32.8

The specific surface areas were measured using a Quantachrome Autosorp-1 nitrogen adsorptometer. The 0.04 g of clays was pretreated at 150°C for 2 h and then the BET specific surface areas were analyzed from nitrogen adsorption at 77 K. The total surface areas were evaluated by the Brunauer–Emmett–Teller (BET) method by the adsorption data of the isotherm. The N_2 adsorption/desorption isotherms of Al-PLM and 2%$NdCl_3$/Al-PLM presented the distorted reversible type IV isotherm. This was indicated that the pillars of Al_2O_3 converted clay-layered structure (2D structure) to mesoporous structure (3D structure) [48]. The BET surface areas of these catalysts were shown in Table 3.1. The BET surface area of Na-montmorillonite (112.2 m^2/g) was higher than montmorillonite (64.8 m^2/g) because of the intercalation of sodium ion. For clay catalyst development, the BET surface area of Al-PLM (126.0 m^2/g) was higher than montmorillonite and Na-montmorillonite after aluminuim pillaring due to the exchange between the layers of aluminum species and sodium ion. However, after the impregnation by 2%$NdCl_3$ on Al-PLM, Al-PLM still have surface area higher than 2%$NdCl_3$/Al-PLM (66.4 m^2/g), indicated that $NdCl_3$ blocked pore in catalyst site to decrease surface area [5]. For pore size diameter calculation, Barrett-Joyner-Halenda (BJH) method was used to determine the value of these mesoporous clay materials. Montmorillonite, Na-montmorillonite and Al-PLM exhibited the same pore size diameter (24.2-24.4 Å), whereas $NdCl_3$/Al-PLM showed larger pore size diameter (32.8 Å).

3.1.3 Surface acidity of 2%$NdCl_3$/Al-PLM

Physisorbed pyridine was assigned by ATR-IR as follows: Hydrogen bonded pyridine at 1440, 1577 cm^{-1} [HPy], Lewis acid-bound pyridine at ~1450, 1490, 1590 cm^{-1} [LPy] and the Brönsted acid-bound pyridinium cation at ~1540 and 1640 cm^{-1} [PyH or BPy] [9]. The observation of the peak was considered as the characteristics as Brönsted and Lewis acidity at 1540 and 1450 cm^{-1}, respectively [9]. The IR spectrum of 2%$NdCl_3$/Al-PLM showed two major transmittance bands at 1443 and 1491 cm^{-1}, respectively. For hydrogen bonded pyridine, the nitrogen lone pair electrons bonded with hydrogen (H-bond) of weakly acidic surface hydroxyl group [HPy] at 1440 cm^{-1}. For lewis acid, the pair electrons of nitrogen donated to the Lewis active site on surface catalyst [LPy] at 1450 and 1491 cm^{-1} [49]. These could be describes that the large band of 1443 cm^{-1} were presented because the band at 1440 (hydrogen-bonded pyridine) and 1450 (typical band of Lewis acid) cm^{-1} were overlapped at 1443 cm^{-1} [50]. If the Brönsted acidity of a surface hydroxyl group is sufficiently high, a proton can be extracted and formed with pyridinium ion formation [PyH or BPy]. However, the remarkable band of Brönsted acid at 1540 cm^{-1} was not detected. Indicating that, this catalyst had low concentration of Brönsted acid. Based on our knowledge, the nature of neodymium chloride (III) and aluminium oxide pillared montmorillonite were Lewis acid [48]. Due to the Lewis acid of this catalyst, its efficiency was studied in benzylation of aromatics and tetrahydropyranylation of benzyl alcohol. The assignment of moisture subtraction artefact was appeared at 1560 cm^{-1} [51].

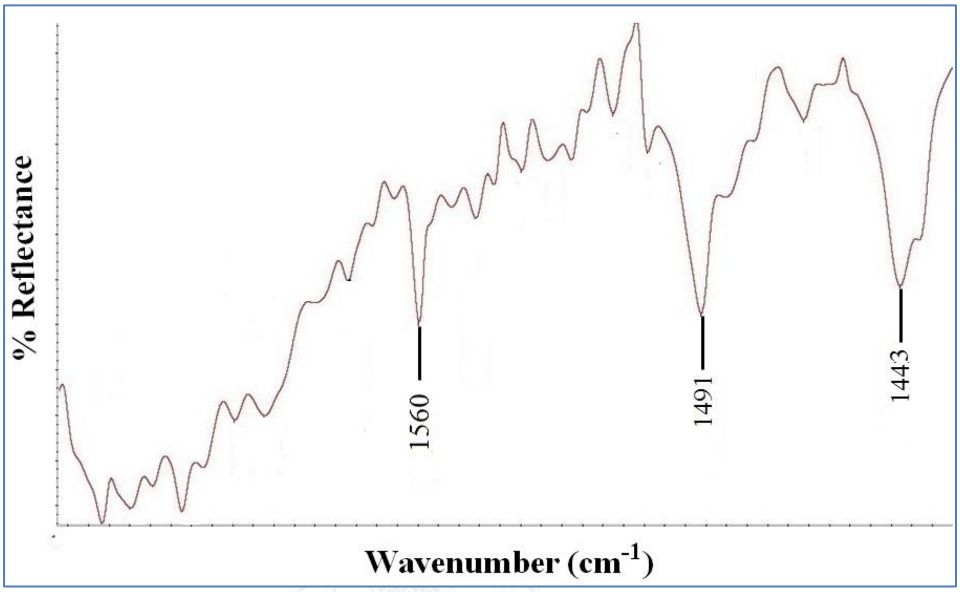

Figure 3.5 The ATR-FTIR spectrum of 2%$NdCl_3$/Al-PLM

3.2 Optimum conditions study on benzylation of toluene

Environmentally friendly heterogeneous acid catalyst, 2% $NdCl_3$/Al-PLM was utilized for benzylation of aromatics. The amount of catalyst, temperature, reaction time and molar ratio of substrate to benzylating agent were explored using toluene as a model and benzyl alcohol as a benzylating agent.

Benzylation of toluene with benzyl alcohol produced 3 major products: *o*- and *p*-benzyl toluenes (**1a** and **1b**, respectively) and benzyl ether (**1c**). The latter was formed by *O*-benzylation of benzyl alcohols, whereas **1a** and **1b** were produced from *C*-benzylation of toluene [52].

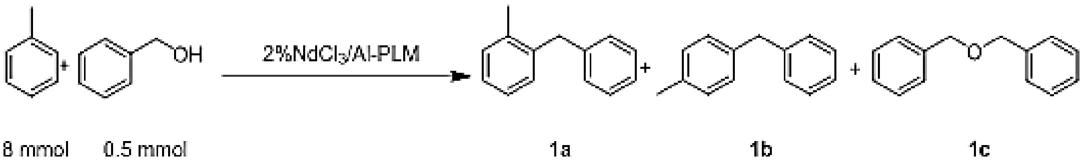

Scheme 3.1 Benzylation of toluene with benzyl alcohol by using 2%$NdCl_3$/Al-PLM as a catalyst

In reaction mixtures, the %recovery of benzyl alcohol and %yield of product **1c** were quantified by ^{1}H NMR with biphenyl as internal standard. The ^{1}H NMR spectra of benzyl alcohol and benzyl ether **(1c)** in the crude mixtures were compared with commercially available chemicals. The ^{1}H NMR spectrum of the reaction mixture of **1a** and **1b** was compared with the authentic samples in Figure 3.6. These products (**1a** and **1b**) were synthesized from benzylation of toluene and benzyl chloride using anhydrous $FeCl_3$ as a homogeneous catalyst. The mixtures of **1a** and **1b** were characterized by ^{1}H NMR.

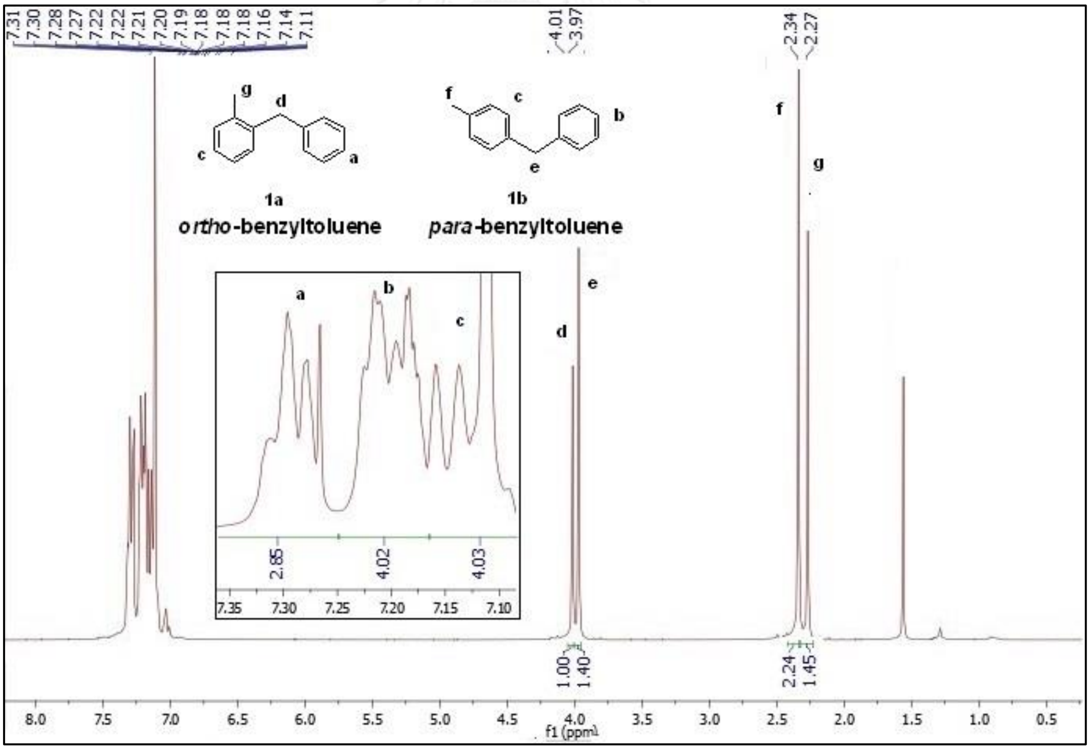

Figure 3.6 The ^{1}H NMR spectrum of authentic mixtures **1a** and **1b**

The benzyl protons of **1a** and **1b** revealed multiplet peaks at δ_H 7.31–7.25 (m, 5H_a) and 7.22–7.18 (m, 5H_b), respectively. Both toluene protons of **1a** and **1b** showed multiplet peaks at δ_H 7.16-7.11 (m, 4H$_c$, **1a** and **1b**). The methylene protons of **1a** and **1b** revealed singlet peaks at δ_H 4.01 (H$_d$) and 3.97 (H$_e$), respectively. The methyl protons of **1a** and **1b** revealed singlet peaks at δ_H 2.27 (H$_g$) and 2.34 (H$_f$), respectively. The ^{1}H NMR spectrum of authentic mixtures **1a** and **1b** were in good correlation with literature [18].

According to this developed analytical method, biphenyl as an internal standard was added to the complete reaction. A few drops of the reaction mixture were then taken and analyzed by ^{1}H NMR. From the calculation, the peak area of internal standard was compared with the area of the interested peak which can further calculate the percentage yields by the relative ratio of integration and number of proton shown in equation 3.1.

Equation 3.1 Calculation percentage yield of products by ^{1}H NMR

$$\%\ \text{yield A} = \frac{\text{mmol of biphenyl}}{\text{mmol of benzyl alcohol}} \times \frac{\text{a number of H of biphenyl}}{\text{Integration of biphenyl}} \times \frac{\text{Integration of A}}{\text{a number of H of A}} \times 100$$

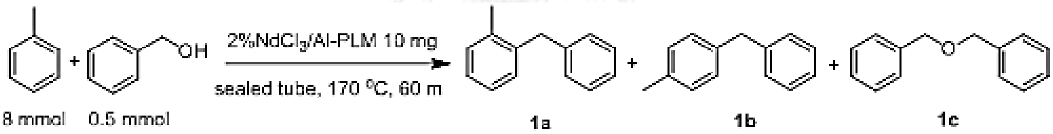

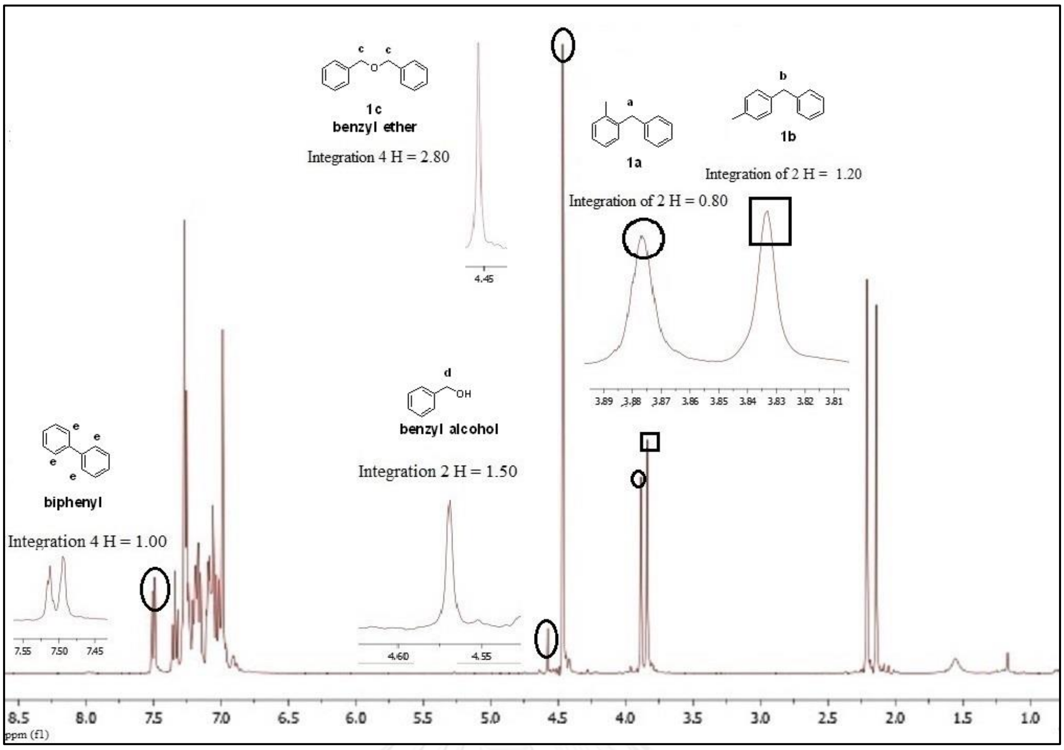

Figure 3.7 ^{1}H NMR spectrum of benzylation of toluene in the crude reaction mixture using biphenyl as an internal standard

The ^{1}H NMR spectrum presented in Figure 3.7 was obtained from the crude reaction mixture of benzyl alcohol reacted with toluene in the presence of 2%NdCl$_3$/Al-PLM 10 mg at 170^{o}C for 60 min. After the reaction finished, biphenyl (0.0487 mmol) was added as an internal standard for %recovery and yield calculation based on benzyl alcohol as a substrate.

$$\%\ \text{recovery} = \frac{0.0487\ \text{mmol of biphenyl}}{0.5\ \text{mmol of benzyl alcohol}} \text{ x } \frac{4\ \text{H}_e\ \text{of biphenyl}}{1} \text{ x } \frac{1.50}{2\ \text{H}_d} \text{ x } 100 = 29.2\%$$

$$\%\ \mathbf{1a} = \frac{0.0487\ \text{mmol of biphenyl}}{0.5\ \text{mmol of benzyl alcohol}} \text{ x } \frac{4\text{H}_e\ \text{of biphenyl}}{1} \text{ x } \frac{0.80}{2\ \text{H}_a} \text{ x } 100 = 15.6\%$$

$$\%\ \mathbf{1b} = \frac{0.0487\ \text{mmol of biphenyl}}{0.5\ \text{mmol of benzyl alcohol}} \text{ x } \frac{4\text{H}_e\ \text{of biphenyl}}{1} \text{ x } \frac{1.20}{2\ \text{H}_b} \text{ x } 100 = 23.4\%$$

$$\%\ \mathbf{1c} = \frac{0.0487\ \text{mmol of biphenyl}}{0.5\ \text{mmol of benzyl alcohol}} \text{ x } \frac{4\text{H}_e\ \text{of biphenyl}}{1} \text{ x } \frac{2.80}{4\ \text{H}_c} \text{ x } 100 = 27.3\%$$

Mass balance = 29.2 + 15.6 + 23.4 + 27.3 = 95.5%

From the calculatios, the percentage of benzyl alcohol was 29.2%, **1a** was 15.6%, **1b** was 23.4% and benzyl ether (**1c**) was 27.3%. The mass balance was calculated by the total percentage of recovery substrate and products.

Previous researches studied the efficiency of different metal chloride impregnated on aluminium pillared montmorillonite. $InCl_3$/Al-PLM and $NdCl_3$/Al-PLM were synthesized and used for alkylation of phenol. $InCl_3$/Al-PLM was selective to produce *O*-alkylation whereas *C*-alkylation was predominat when $NdCl_3$/Al-PLM was employed [5, 47].

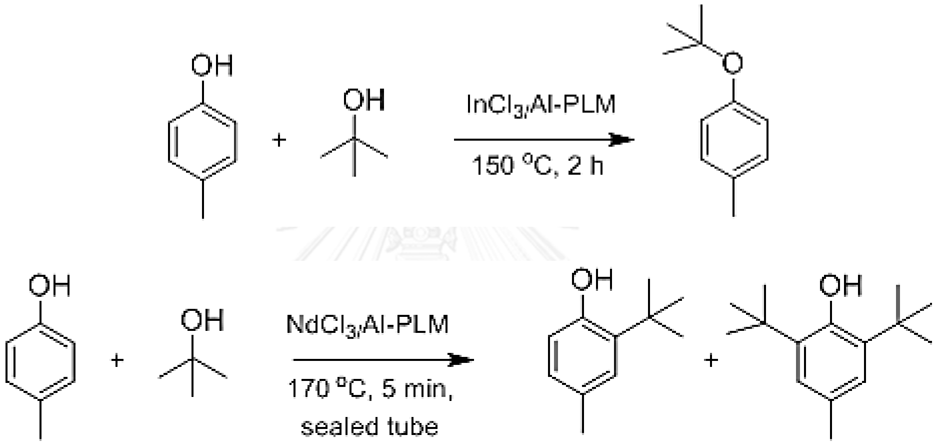

From those available information, the purpose of this research was to promote *C*-benzylation of aromatics by using $NdCl_3$/Al-PLM as a catalyst. Since Friedel-Crafts benzylation of aromatics is an important process for wide variety benzylated products. They are key intermediates for the production in pharmaceutical and industry [21-26].Various factors were studied for the optimum conditions.

3.2.1 The effect of 2%$NdCl_3$/Al-PLM on benzylation of toluene

The effect of 2%$NdCl_3$/Al-PLM was studied in benzylation of toluene with benzyl alcohol. The results are shown in Table 3.2.

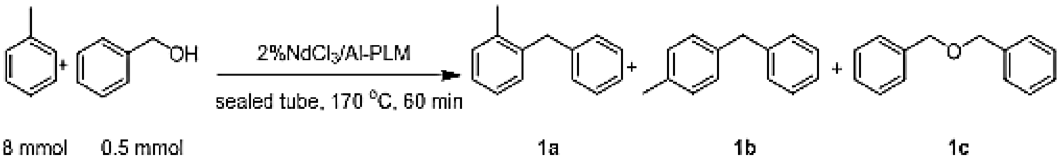

Table 3.2 The effect of 2%$NdCl_3$/Al-PLM amount on benzylation of toluene

Entry	Amount of catalyst (mg)	*%recovery	*%products			MB	ratio of 1b/1a	ratio of (1a+1b)/1c
			%*ortho*-1a	%*para*-1b	% 1c			
1	0	96.9	0	0	0	96.9	-	-
2	10	29.2	15.6	23.4	27.3	95.5	1.50	1.43
3	20	0	39.0	59.3	0	98.3	1.52	-
4	50	0	42.3	62.9	0	105.2	1.49	-

*quantified by ^{1}H NMR

The products (**1a**, **1b** and **1c**) were not observed in the absence of clay catalyst (entry 1), while 10 mg of 2%$NdCl_3$/Al-PLM (entry 2) yielded 39.0% of *C*-benzylation products (The mixtures of **1a** and **1b**) and 27.3% *O*-benyzylation product (**1c**). Although benzyl ether was formed by self-condensation from a partial benzyl alcohol but benzyl toluene (**1a** and **1b**) was occurred by benzylation of toluene (entry 2). A little amount of 2%$NdCl_3$/Al-PLM produced *C*- and *O*- benzylation products with ratio *C*- to *O*- benzylation products at 1.43 (entry 2). However, the acidity of catalyst 10 mg was not enough to generate benzyl toluene successfully (**1a** and **1b**). Then, the increasing amount of 2%$NdCl_3$/Al-PLM to 20 and 50 mg (entries 3 and 4, respectively) affected quantitative of benzyl toluene (**1a** and **1b**) 98.3-105.2% with ratio *p*- **(1b)**: *o***- (1a)** 1.5. High selectivity of *p*-benzyl toluene **(1b)** was detected possibly because of the presence of small pores in 2% $NdCl_3$/Al-PLM [22]. Hence, 20 mg of 2% $NdCl_3$/Al-PLM was the appropriate amount owing to its acidity sufficed for *C*-benzylation (entry 3).

3.2.2 The effect of reaction temperature

The effect of the reaction temperature on benzylation of toluene catalyzed by 2%$NdCl_3$/Al-PLM was carried out and the results are presented in Table 3.3.

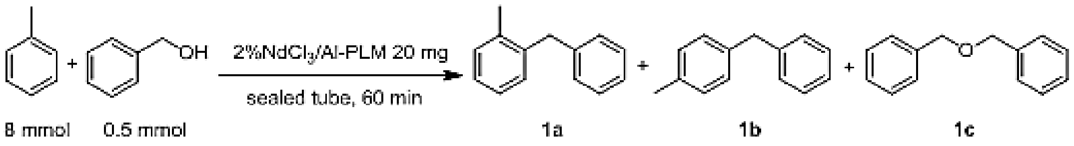

Table 3.3 The effect of reaction temperature on benzylation of toluene

Entry	**Temperature (°C)**	***%recovery**	***%products**			**MB**	**ratio of 1b/1a**	**ratio of (1a+1b)/1c**
			%*ortho*-1a	**%*para*-1b**	**% 1c**			
1	RT (30)	92.6	0	0	0	92.6	-	-
2	70	92.2	0	0	0	92.2	-	-
3	120	92.2	0.7	1.0	1.2	94.4	1.43	1.42
4	170	0	39.0	59.3	0	98.3	1.52	-

*quantified by ^{1}H NMR

The range of temperature at 30-170°C were selected for benzylation of toluene with benzyl alcohol. The results were tabulated in Table 3.3 and found that the reaction temperature at 170 °C gave 98.3% yield of benzyl toluenes (**1a** and **1b**) by *C*-benzylation of toluene (entry 4). However, at 120°C, only trace products of benzyl toluenes (**1a** and **1b**) and benzyl ether were occurred with the ratio benzyl toluene to benzyl ether of 1.42 (entry 2). Obviously, the production of *C*- and *O*-benzylations could not proceed at reaction temperature 70°C and RT (entries 1-2). Hence, the appropriate temperature was 170°C.

3.2.3 Comparison the reaction system on benzylation of toluene

From the previous research, *C*-alkylation of phenol was accomplished by using a sealed tube as a reaction system at 170°C [47]. It was interesting that, if the pressure could give a favor to the production of *C*-benzylation. The sealed tube was a representative for pressured system whereas reflux condition was a representative for the reaction performing at atmospheric pressure. The results are demonstrated in Table 3.4.

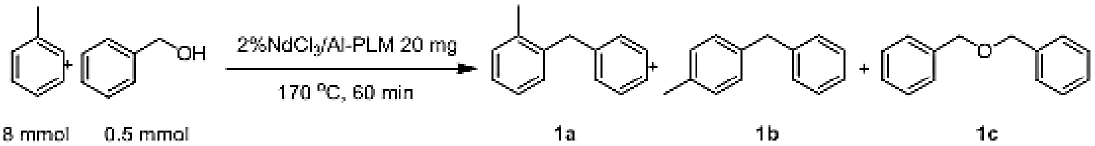

Table 3.4 Comparison the reaction system on benzylation of toluene

Entry	reaction system	*%recovery	*%products			MB	ratio of 1b/1a	ratio of (1a+1b)/1c
			%*ortho*-1a	%*para* - 1b	% 1c			
1	sealed tube	0	39.0	59.3	0	98.3	1.52	-
2	reflux	80.3	0.9	1.5	7.0	89.7	1.71	0.34

*quantified by ^{1}H NMR

Under the same conditions, the reaction in a sealed tube gave 98.3% yield (entry 1) whereas under reflux conditions gave 3.1% yield of benzyl toluenes (**1a** and **1b**), respectively. Sealed tube was a chemical reaction vessel which can conduct a reaction under pressure at high temperature. In the reaction mixture, the pressure rendered to the number of collisions between benzyl alcohol and toluene. Hence, a sealed tube was a method which proper for this reaction.

3.2.4 The effect of reaction time

The effect of the reaction time on benzylation catalyzed by 2%$NdCl_3$/Al-PLM was carried out and the results are presented in Table 3.5.

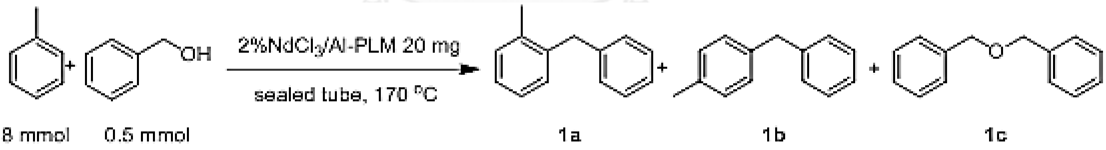

Table 3.5 The effect of reaction time on benzylation of toluene

Entry	Time (min)	*%recovery	*%products			MB	ratio of 1b/1a	ratio of (1a+1b)/1c
			%*ortho*-1a	%*para*-1b	%1c			
1	15	75.3	4.6	7.0	6.4	93.3	1.52	1.81
2	30	0	41.4	60.7	5.5	107.6	1.47	18.56
3	60	0	39.0	59.3	-	98.3	1.52	-

*quantified by ^{1}H NMR

The reaction time was varied (Table 3.5). The yield of products was increased when the reaction time increased (entries 1-3). The high amount of recovered benzyl alcohol 75.3 and 18% yield of benzyl toluenes (**1a** and **1b**) and benzyl ether (**1c**) were observed for 15 min (entry 1). When the reaction time was extended to 30 min, benzyl toluenes (**1a** and **1b**) were 102.1% yield but little yield of benzyl ether (**1c**) 5.5% was occurred *via* self-condensation of benzyl alcohol (entry 2). When the reaction time was extended to 60 min (entry 3), benzyl toluenes (**1a** and **1b**) were completely occurred in the reaction (98.3%), whereas benzyl ether (**1c**) was not observed. Benzyl alcohol was easier to adsorb on catalyst surface *via* H-bond so it simply contacted to active sites on catalyst surface [53]. Moreover, the OH^- group made benzyl alcohol more reactive benzylating agent [19]. After the production of *C*- and *O*-benzylation (benzyl ether) were entirely occurred from benzyl alcohol within 30 min (entry 2). There were vacant sites for a small amount of benzyl ether (5.5%, entry 2) to adsorb on clay surface and react with toluene (entry 3) [53].

3.2.5 The effect of molar ratio

In order to avoid the production of benzyl ether in benzylation of toluene, molar ratios of toluene to benzyl alcohol were studied.

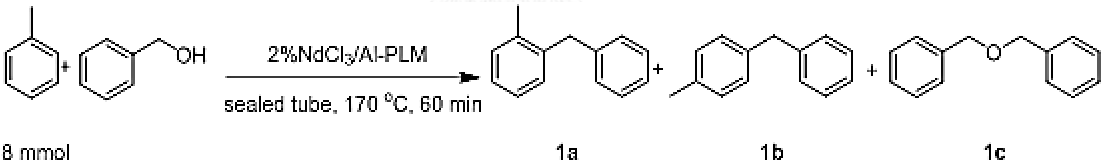

Table 3.6 The effect of molar ratio on benzylation of toluene

Entry	Ratio toluene to benzyl alcohol	*%recovery	*%products			MB	ratio of 1b/1a	ratio of (1a+1b)/1c
			%*ortho*-1a	%*para*-1b	%1c			
1	8:1	15.8	22.5	33.5	32.7	104.5	1.49	3.54
2	8:0.5	0	39.0	59.3	-	98.3	1.52	-
3	8:0.25	0	37.2	62.8	-	99.9	1.69	-
4	8:0.125	0	43.7	67.1	-	110.8	1.53	-

*quantified by ^1H NMR

Benzylation of toluene with benzyl alcohol was carried out by varying the molar ratio of toluene to benzyl alcohol as follows: 8:1, 8:0.5, 8:0.25 and 8:0.125, respectively. None of benzyl alcohol and benzyl ether was formed when benzyl alcohol was used less than or equal to 0.5 mmol (entries 2-4). The amount of toluene was high enough to prevent self-condensation of benzyl alcohol. Increasing of benzyl alcohol to 1 mmol affected to the incomplete conversion of substrate and rising of benzyl ether formation, respectively (entry 1) because toluene was not enough to react with benzyl alcohol. Therefore, the molar ratio of toluene to benzyl alcohol 8:0.5 was the best ratio under optimal conditions (entry 2).

It could be summarized that the standard conditions for benzylation of toluene with benzyl alcohol catalyzed by 2%$NdCl_3$/Al-PLM as follows. *C*-benzylation (**1a** and **1b**) were occurred efficiently under this optimum conditions.

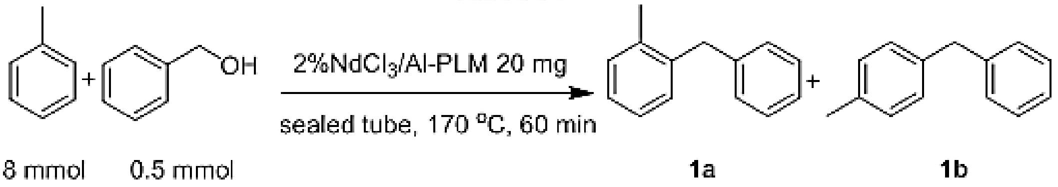

3.2.6 The mechanism of benzylation of toluene with benzyl alcohol

The proposed mechanism of benzylation of toluene with benzyl alcohol using 2%$NdCl_3$/Al-PLM as a catalyst can be illustrated in Figure 3.8.

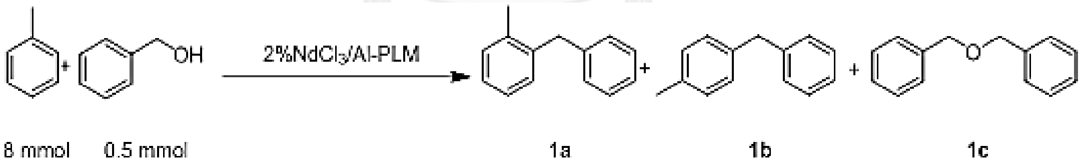

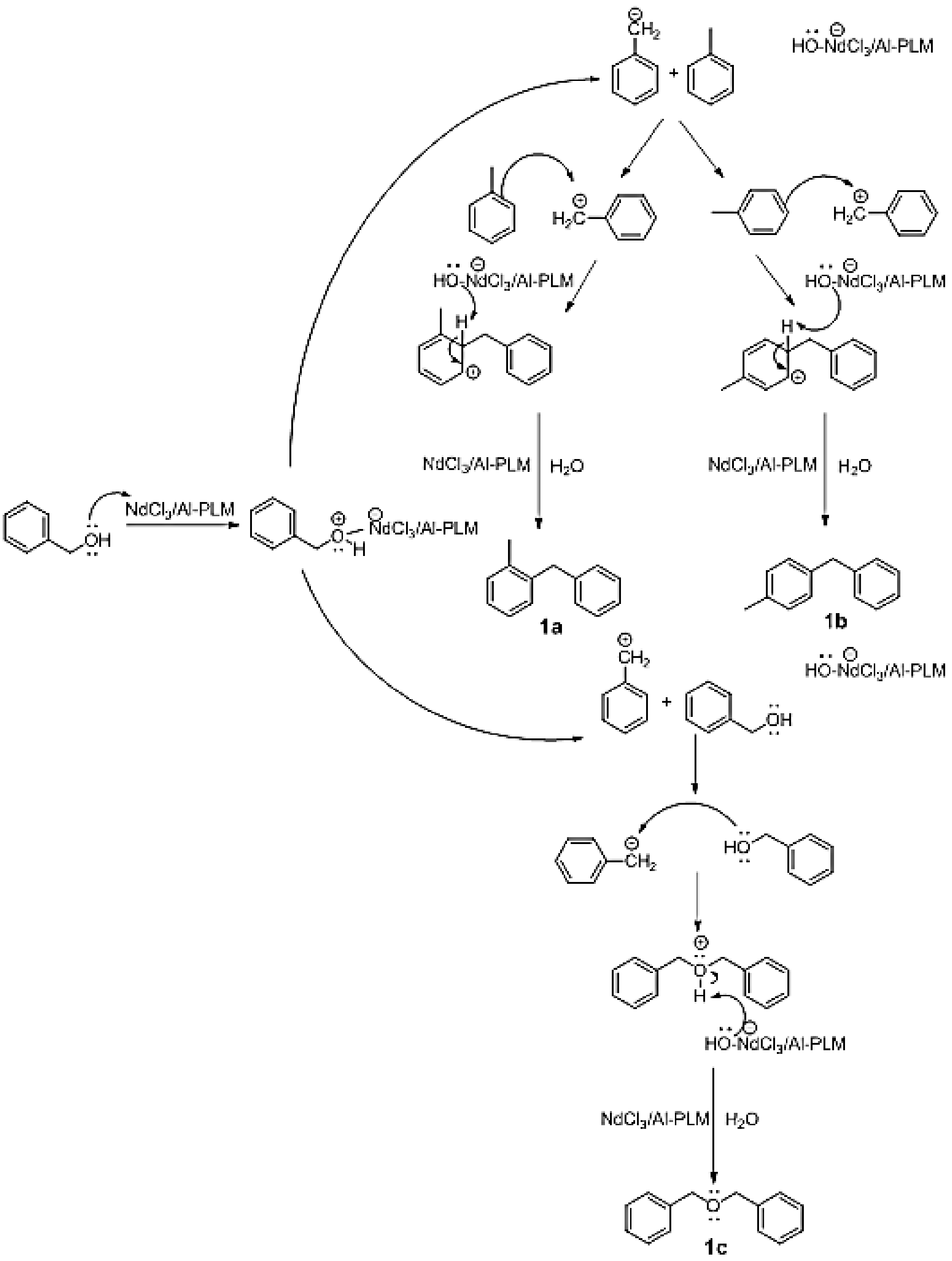

Figure 3.8 Proposed mechanism of benzylation of toluene with benzyl alcohol

Friedel-Crafts benzylation of toluene was preceded by electrophilic aromatic substitution. 2%$NdCl_3$/Al-PLM as Lewis acid could accept a lone pair of electrons from benzyl alcohol resulting in the formation of a benzyl carbocation. Then benzyl carbocation would lead to the formation of benzyl toluene and benzyl ether in different pathways.

For benzyl toluene production, pi electrons of toluene attacked benzyl carbocation and gave resonance stabilized benzyl toluene carbocations, then, re-aromatized those intermediates, forming *o*- and *p*-benzyl toluenes. The other pathway, benzyl carbocation was coupled with benzyl alcohol resulting in benzyl ether formation.

3.3 Scope of benzylation of toluene with benzyl alcohol catalyzed by 2%NdCl$_3$/Al-PLM

The relative reactivity of several benzylating agents including benzyl alcohol, benzyl chloride and benzyl ether were studied for benzylation of toluene.

3.3.1 The effect of benzylating agent

In order to study the suitable benzylating agent for benzylation of toluene, benzyl chloride, benzyl alcohol and benzyl ether were chosen to investigate.

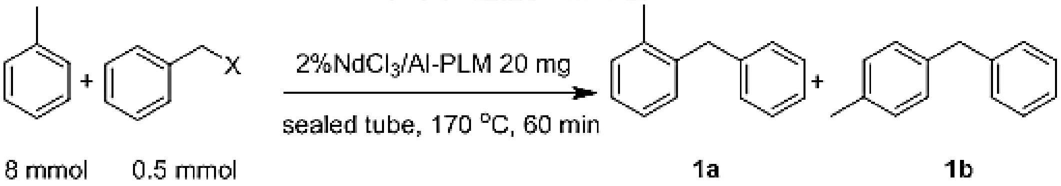

X= OH$^-$ (benzyl alcohol), Cl$^-$ (benzyl chloride) and O-C_6H_5 (benzyl ether)

Table 3.7 The effect of benzylating agent on benzylation of toluene

Entry	Benzylating agents	*%recovery	*%products		MB	ratio of 1b/1a
			%*ortho*- 1a	%*para*- 1b		
1	benzyl alcohol	0	59.3	39.0	98.3	1.52
2	benzyl chloride	0	58.8	42.2	101	1.39
3	benzyl ether	104.3	0.6	0.3	105.2	1.81

*quantified by ^{1}H NMR

The *C*-benzylation products (**1a** and **1b**) were occurred entirely from benzyl alcohol and benzyl choride within 1 h in entries 1 and 2. Both of benzyl alcohol and benzyl chloride gave desirable yield products under the optimized conditions. Benzyl chloride was classified in a good leaving group [19]. In case of benzyl alcohol, the catalyst 2%$NdCl_3$/Al-PLM accepted lone pair electrons from oxygen, resulting in rapid leaving of $^{\ominus}$OH-$NdCl_3$/Al-PLM and forming benzyl carbocation, respectively. However, only trace products of **1a** and **1b** were observed when benzyl ether was a benzylating agent (entry 3). The higher concentration of benzyl ether leaded to a higher adsorption of benzyl ether molecules onto the catalyst surface, and less availability toluene molecules reacted with benzyl ether in benzylation reaction [54]. Thus, the capability of benzylating agent in this reaction is as follows:

benzyl alcohol ≈ benzyl chloride > benzyl ether

Although both benzyl alcohol and benzyl chloride gave appreciable yields (entries 1 and 2) within 1 h, benzyl alcohol released H_2O from the reaction, whereas benzyl chloride was corrosive and released HCl. In addition, the formation of HCl in benzylation could cause the structural damage of the clay catalyst [19].

3.3.2 Variation of aromatics

Selected aromatics namely toluene, ethylbenzene, *tert*-butylbenzene, anisole, *p*-cresol, *p*-xylene, benzene, biphenyl, 2-naphthol and nitrobenzene were employed to study the reactivity of this reaction under these conditions.

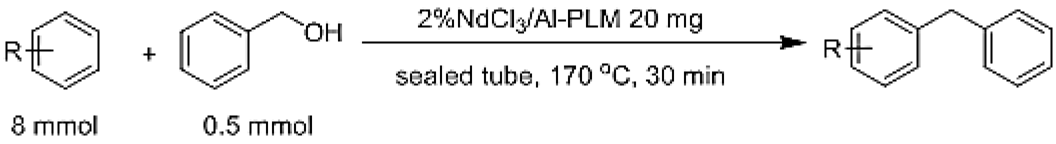

3.3.2.1 Benzylation of ethylbenzene

Ethylbenzene was chosen as a representative bearing activating substituents. The alkyl group could be readily introduced on an aromatic ring in **2a** and **2b** positions with ratio *p*-:*o*- 1.51. The narrow porous catalyst was favored to produce *p*- more than *o*-benzyl ethylbenzene because the latter was steric [22]. The benzylation of ethylbenzene could be accomplished under the optimized conditions in good yield (100%).

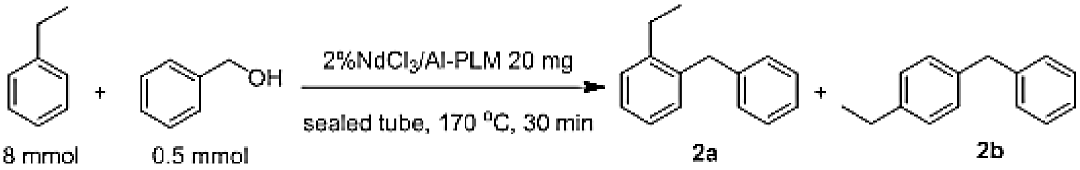

Table 3.8 Benzylation of ethylbenzene with benzyl alcohol using 2%$NdCl_3$/Al-PLM as catalyst

*%recovery	*%products		MB	ratio of 2b/2a
	%*ortho*-2a	%*para*-2b		
0	39.9	60.1	100	1.51

*quantified by ^{1}H NMR

In the reaction mixture, %yield of products (**2a** and **2b**) were quantified by ^{1}H NMR by using biphenyl as an internal standard. The authentic samples were synthesized from benzylation of ethylbenzene with benzyl chloride using anhydrous $FeCl_3$ as a homogeneous catalyst. The authentic mixtures of **2a** and **2b** were confirmed by ^{1}H NMR in Figure 3.9.

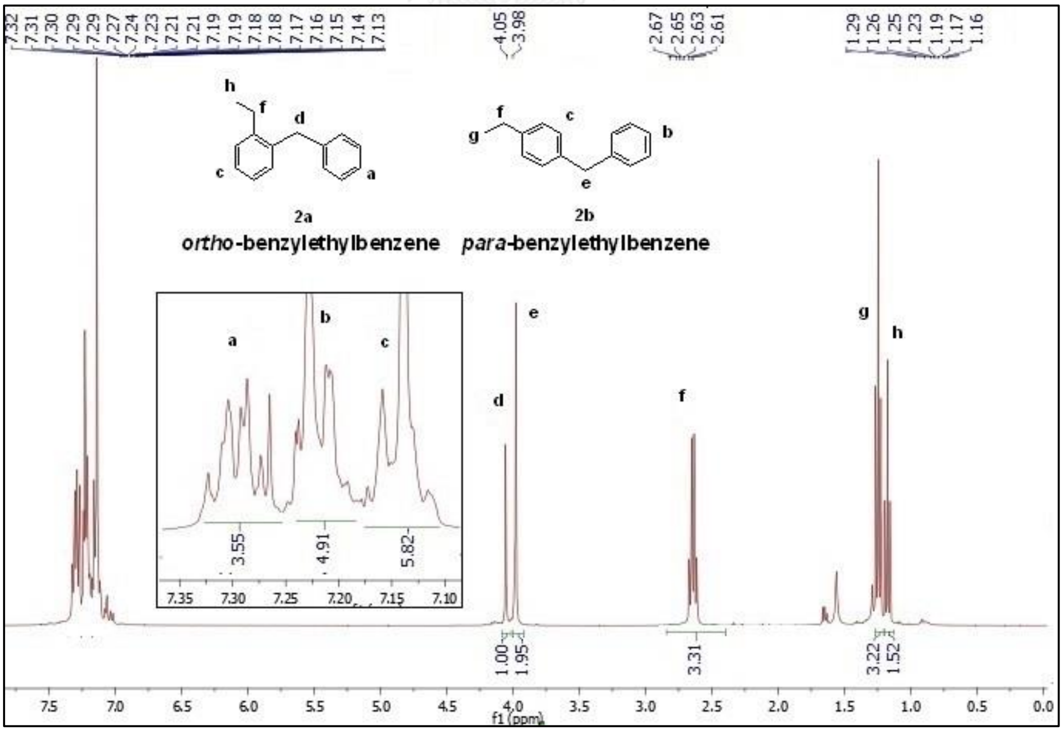

Figure 3.9 The ^{1}H NMR of authentic mixtures *o*- and *p*-benzylethylbenzene (**2a** and **2b**)

The benzyl aromatic protons of **2a** and **2b** revealed multiplet peaks at δ_H 7.32–7.27 (m, 5H$_a$) and 7.24–7.19 (m, 5H$_b$, Ar**H**), respectively. Both ethylbenzene aromatic protons of **2a** and **2b** showed multiplet peaks at δ_H 7.17-7.08 (m, 4H$_c$, **2a** and **2b,** Ar**H**). The characteristic methylene protons of **2a** and **2b** revealed singlet peaks at δ_H 4.06 (s, 2H$_d$, C**H$_2$**) and 3.98 (s, 2H$_e$, C**H$_2$**), respectively. Another methylene protons of **2a** and **2b** displayed quartet peaks at δ_H 2.67-2.61 (q, J = 7.7 Hz, 2H$_f$, **2a** and **2b**, C**H$_2$**). The methyl protons of **2a** and **2b** revealed triplet peaks at δ_H 1.19-1.16 (t, J = 7.5 Hz, 3H$_h$, C**H$_3$**) and δ_H = 1.27-1.23 (t, J = 7.5 Hz, 3H$_g$, C**H$_3$**), respectively. These ^{1}H NMR of **2a** and **2b** were in good correlated with the literature [16].

3.3.2.2 Benzylation of *tert*-butylbenzene

The bulky effect of electron donating group in case of *tert*-butylbenzene was studied under the optimized conditions with reaction time of 30 min. From the results, a quantitative yield of *C*-benzylation, benzyl-*tert*-butylbenzenes (**3a** and **3b**) was observed. The high selectivity toward *p*-benzyl-*tert*-butylbenzenes with ratio *p*- (**3b**) to *o*- (**3a**) was 1.96. This ratio *p*-:*o*- (1.96) was higher than other substrates in case of toluene (1.52) and ethylbenzene (1.51). This indicated that *tert*-butylbenzene was steric and bulky than toluene and ethylbenzene. The substitution of benzyl carbocation at *p*- position was more convenient because the structure inside the pore of clay catalyst could limit the bulky formation of **3a** [55].

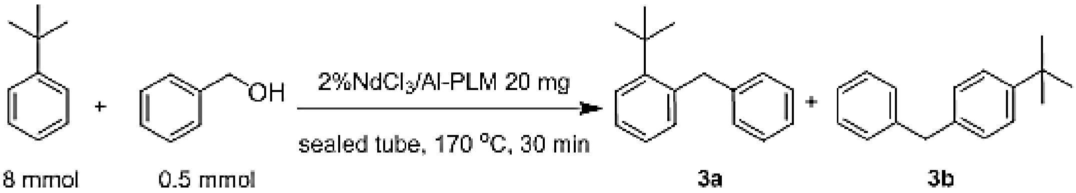

Table 3.9 Benzylation of *tert*-butylbenzene with benzyl alcohol using 2%NdCl$_3$/Al-PLM as catalyst

***%recovery**	***%products**		**MB**	**ratio of 3b/3a**
	%*ortho*- 3a	**%*para*- 3b**		
0	33.8	66.4	100.2	1.96

*quantified by ^{1}H NMR

In reaction mixture, the %yield of products (**3a** and **3b**) were quantified by ^{1}H NMR using biphenyl as an internal standard. The ^{1}H NMR spectrum of **3a** and **3b** in the crude mixture were compared with that of authentic samples as described in chapter II [56, 57]. The authentic mixtures of **3a** and **3b** are presented by ^{1}H NMR in Figure 3.10.

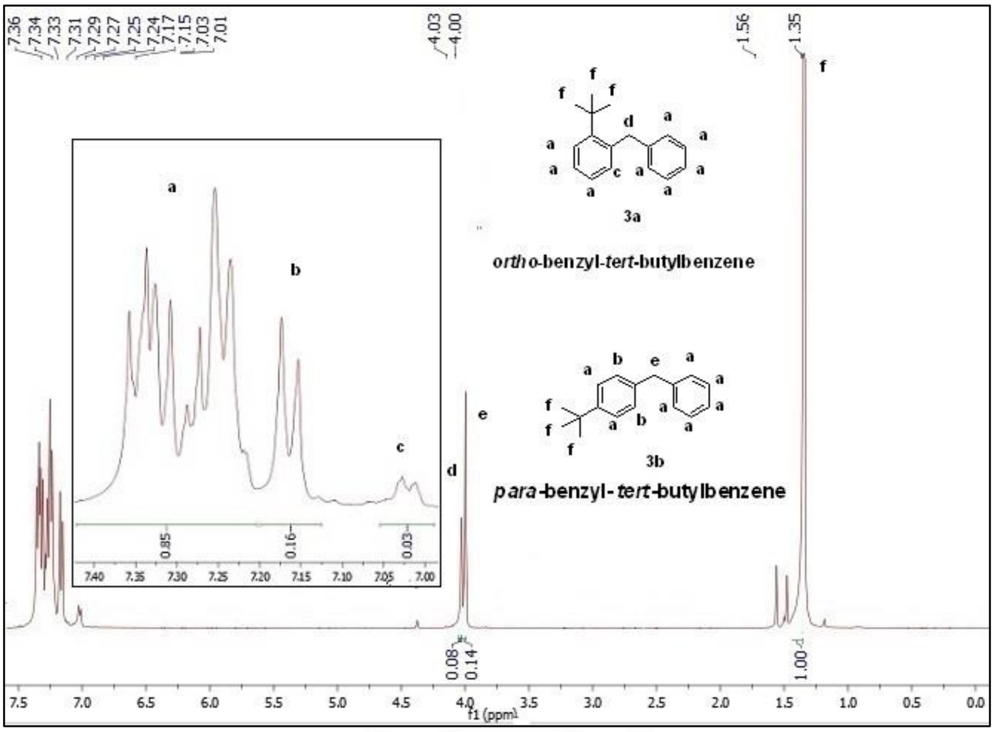

Figure 3.10 The ^{1}H NMR of authentic mixtures of *o*- and *p*-benzyl-*tert*-butylbenzene (**3a** and **3b**)

The benzyl aromatic protons of **3a** and **3b** revealed multiplet peaks at δ_H 7.36–7.01 (m, 8H_a-**3a** and 7H_a-**3b**). The aromatic protons of **3a** and **3b** displayed doublet peaks at δ_H 7.03-7.01 (d, 1H_b, **3a,** Ar**H**) and 7.17-7.15 (d, 2H_b, **3b,** Ar**H**), respectively. The characteristic methylene protons of **3a** and **3b** revealed a singlet peak at δ_H 4.03 (s, 2H_d, C**H$_2$**) and 4.00 (s, 2H_e, C**H$_2$**), respectively. The methyl protons of **4a** and **4b** revealed singlet peak at δ_H 1.35 (s, 9H_f**, 3a** and **3b,** C**H**$_3$).

3.3.2.3 Benzylation of anisole

C-benzylations (**4a** and **4b**) were generated from the reaction between anisole and benzyl alcohol as the major products, while benzyl ether (**4c**) was by-product due to the dehydration of benzyl alcohol. The summation of %yield of products (**4a**, **4b**, **4c**) were quantitative. The ratio of **4b**/**4a** *C*-benzylations with ratio *p*-:*o*- was 0.87. This ratio displayed low regioselective to produce *p*- (**4b**). It could be described that, a strong electron donating group (-OCH_3) enhanced the production of *o*- than *p*- in the porous of catalyst [58].

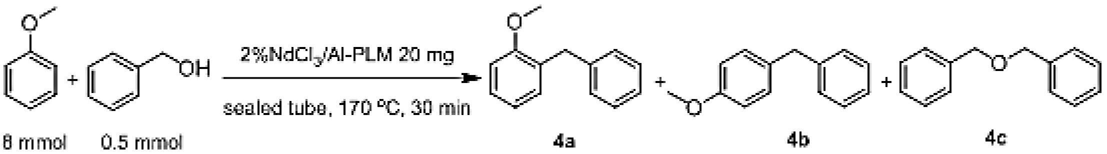

Table 3.10 Benzylation of anisole with benzyl alcohol using 2%$NdCl_3$/Al-PLM as catalyst

***%recovery**	***%products**			**MB**	**ratio of 4b/4a**	**ratio of (4a+4b)/4c**
	%*ortho*- 4a	**%*para*- 4b**	**%4c**			
0	52.5	45.6	2.0	100.1	0.87	49.05

*quantified by ^{1}H NMR

In reaction mixture, the %yield of products (**4a**, **4b** and **4c**) were quantified by ^{1}H NMR using biphenyl as an internal standard. The ^{1}H NMR spectrum of **4a** and **4b** in the crude mixture was compared with that of authentic samples as described in chapter II. These ^{1}H NMR spectra of authentic **4a** and **4b** were in good correlated with the literature [18]. The authentic samples of **4a** and **4b** were presented by ^{1}H NMR in Figures 3.11 and 3.12, respectively.

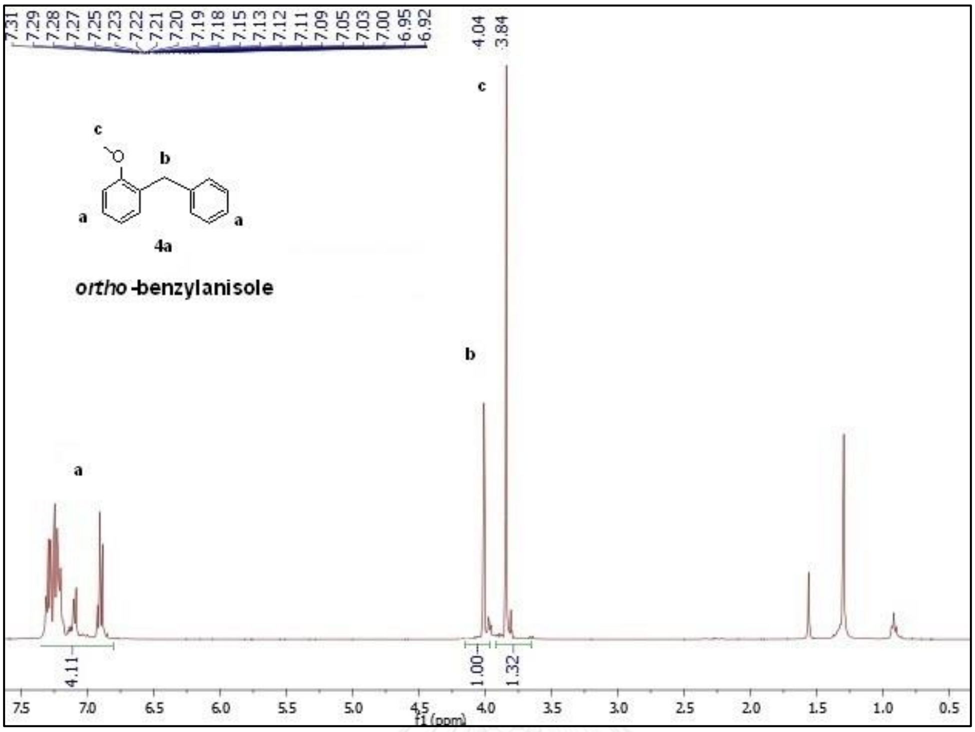

Figure 3.11 The ^{1}H NMR spectrum of authentic *o*-benzylanisole (**4a**)

The aromatic protons of **4a** revealed multiplet peaks at δ_H 7.31–6.92 (m, 9H$_a$, Ar**H**). The methylene and methyl protons revealed singlet peak at δ_H 4.04 (s, 2H$_b$, C$\mathbf{H_2}$) and δ_H 3.84 (s, 3H$_c$, C$\mathbf{H_3}$), respectively.

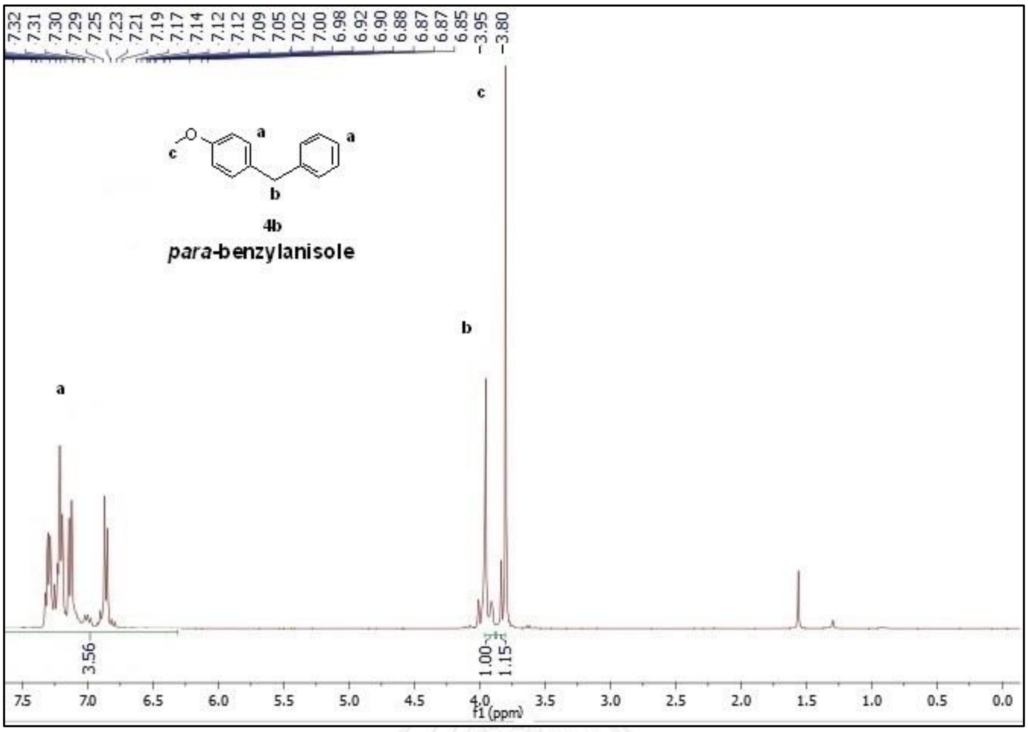

Figure3.12 The ^{1}H NMR spectrum of authentic *p*-benzylanisole (**4b**)

The aromatic protons of **4b** displayed multiplet peaks at δ_H 7.32–6.85 (m, 9H_a, Ar**H**). The methylene and methyl protons showed singlet peak at δ_H 3.95 (s, 2H_b, C$\mathbf{H_2}$) and δ_H 3.80 (s, 3H_c, C$\mathbf{H_3}$), respectively.

3.3.2.4 Benzylation of *p*-cresol

Further exploration, benzyl alcohol was reacted with *p*-cresol. It was a reactive aromatic substrate because it had two electron donating groups OH and CH_3 groups. When *p*-cresol was used as a substrate, a high amount of *C*-benzylation of *p*-cresol was generated (2-benzyl-4-methylphenol, **5**) 91.5% yield. None of benzyl ether and dialkylated products was occurred in the reaction.

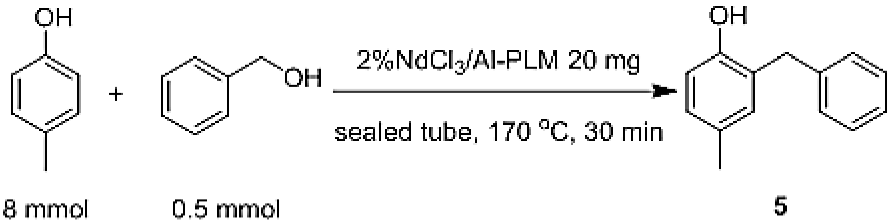

Table 3.11 Benzylation of *p*-cresol with benzyl alcohol using 2%$NdCl_3$/Al-PLM as catalyst

*%recovery	*%product (5)	MB
0	91.5	91.5

*quantified by ^1H NMR

The %yield of 2-benzyl-4-methylphenol (**5**) was quantified by ^1H NMR using biphenyl as an internal standard. The ^1H NMR spectrum of **5** in the crude mixtures was compared with authentic sample. The ^1H NMR spectrum of authentic sample of 2-benzyl-4-methylphenol (**5**) was illustrated in Figure 3.13.

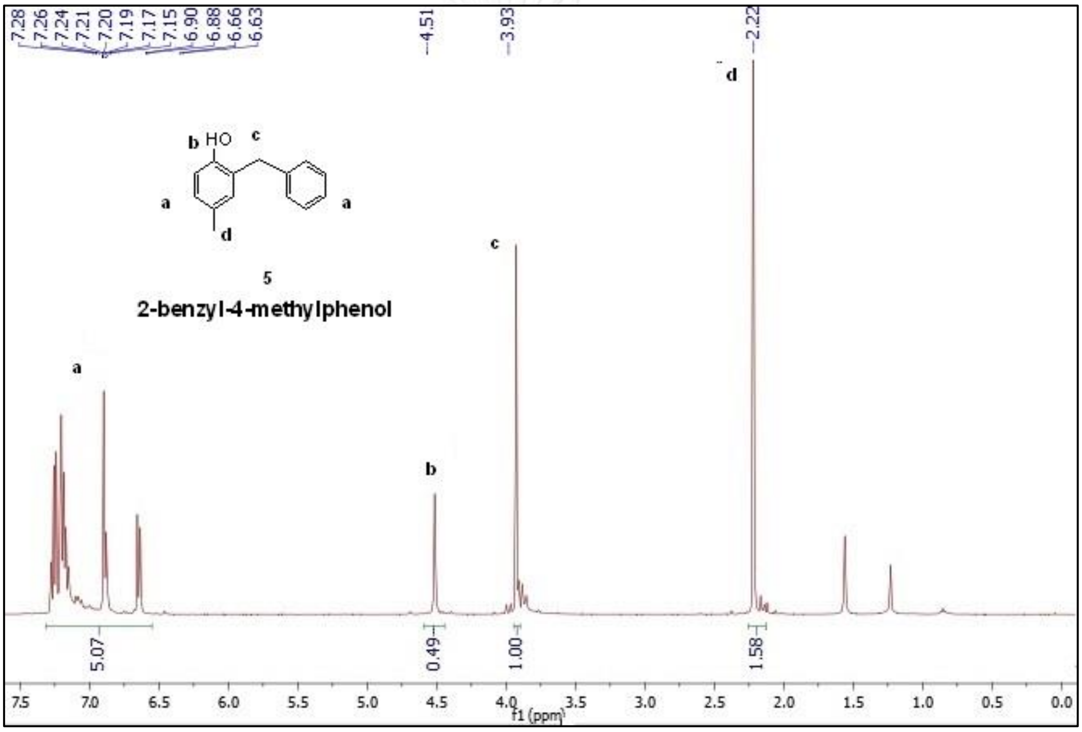

Figure 3.13 The ^1H NMR spectrum of authentic 2-benzyl-4-methylphenol (**5**)

The ^1H NMR spectrum of 2-benzyl-4-methylphenol (**5**) was presented in Figure 3.13. The multiplet peaks of aromatic protons were illustrated at δ 7.30-6.60 (m, $8H_a$, Ar**H**). The singlet peak of hydroxyl proton was demonstrated at δ 4.51 (s, $1H_b$, O**H**). The broad singlet peak of methylene protons was visualized at δ 3.93 (broad s, $2H_c$, C$\mathbf{H_2}$). The methyl protons showed a singlet peak at δ 2.22 (s, 3H, C$\mathbf{H_3}$). This ^1H NMR spectrum was in good correlation with literature [18].

3.3.2.5 Benzylation of *p*-xylene

p-xylene was another reactive aromatic substrate because it had two electron donating groups (CH_3 groups) at *p*-position. Only 2-benzyl-1,4-dimethylbenzene **(6)** occurred in the reaction with the appreciable yield (100%). None of benzyl ether and dialkylated products was occurred in the reaction.

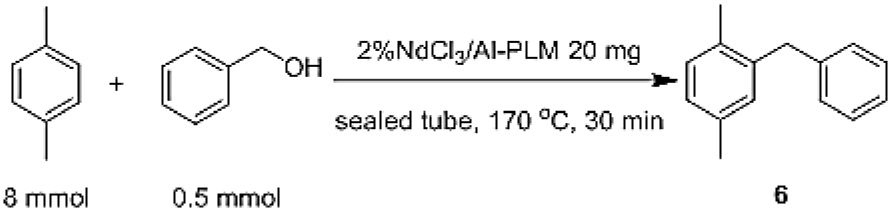

Table 3.12 Benzylation of *p*-xylene with benzyl alcohol using 2%$NdCl_3$/Al-PLM as catalyst

*%recovery	*%product (6)	MB
0	100	100

*quantified by ^1H NMR

The %yield of 2-benzyl-1,4-dimethylbenzene **(6)** was quantified by ^1H NMR using biphenyl as an internal standard. The ^1H NMR spectrum of **6** in the crude mixture was compared with authentic sample. The authentic sample of 2-benzyl-1,4-dimethylbenzene **(6)** was illustrated in Figure 3.14.

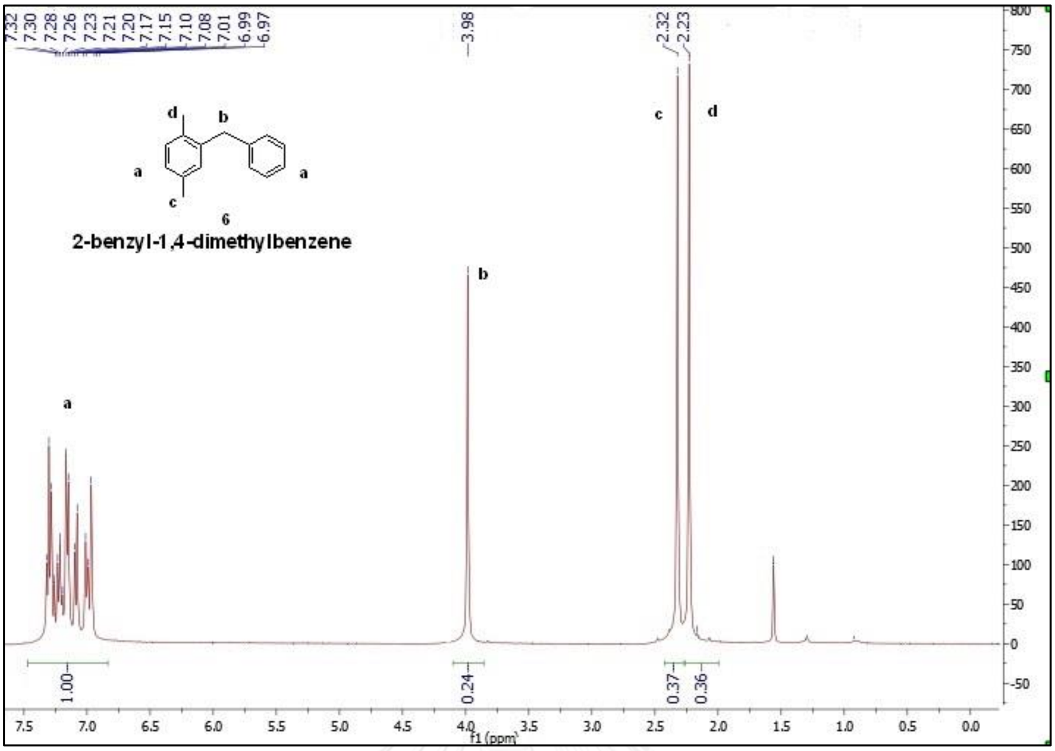

Figure 3.14 The ^{1}H NMR spectrum of authentic 2-benzyl-1,4-dimethylbenzene (**6**)

The ^{1}H NMR spectrum of 2-benzyl-1,4-dimethylbenzene (**6**) was shown in Figure 3.14. The multiplet peaks of aromatic protons were illustrated at δ 7.32-6.97 (m, $8H_a$, Ar**H**). The singlet peak of methylene protons was demonstrated at δ 3.98 (s, $2H_b$, C$\mathbf{H}_2$). The methyl protons showed a singlet peak at δ 2.32 (s, $3H_{\mathbf{c}}$, -C$\mathbf{H}_3$) and 2.23 (s, $3H_{\mathbf{d}}$, C$\mathbf{H}_3$), respectively. This ^{1}H NMR spectrum was in good correlation with literature [18].

3.3.2.6 Benzylation of benzene

Benzylation of benzene with benzyl alcohol produced a major product as diphenylmethane **(7a)** in good yield (81.8%) whereas polybenzylation benzenes (**7b** and **7c)** were obtained in 7.6 and 14.4 % yield, respectively. The selectivity ratio of *C*-monobenzylation (**7a**) to *C*-dibenzylation (**7b** and **7c**) was 3.71. Diphenylmethane (**7a**) had electron density more than benzene. The latter thus revealed higher reactivity to form **7b** and **7c** [59]. The results suggested that dibenzylbenzene (**7b** and **7c)** occurred in the reaction as side products because **7a** reacted with benzyl alcohol to produce **7b** and **7c** [54].

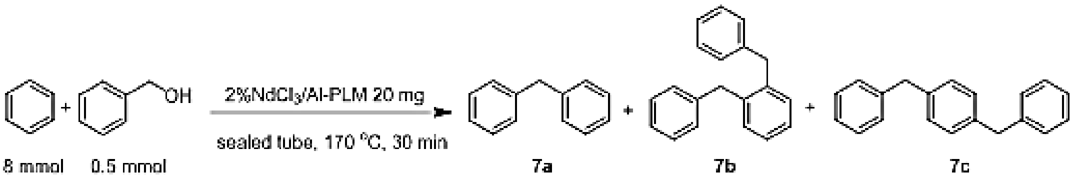

Table 3.13 Benzylation of benzene with benzyl alcohol using 2%NdCl$_3$/Al-PLM as catalyst

*%recovery	*%products			%yield	MB	7a/(7b+7c)
	7a	7b	7c			
0	81.8	7.6	14.4	103.8	103.8	3.71

*quantified by ^{1}H NMR

These benzylations of benzene products (**7a**, **7b** and **7c**) were observed by ^{1}H NMR. Their ^{1}H NMR spectra were compared with authentic samples. Biphenyl was added as an internal standard. The ^{1}H NMR of authentic samples **7a**, **7b** and **7c** were illustrated in Figures 3.15, 3.16 and 3.17, respectively. These ^{1}H NMR spectra were in good correlated with literature [16].

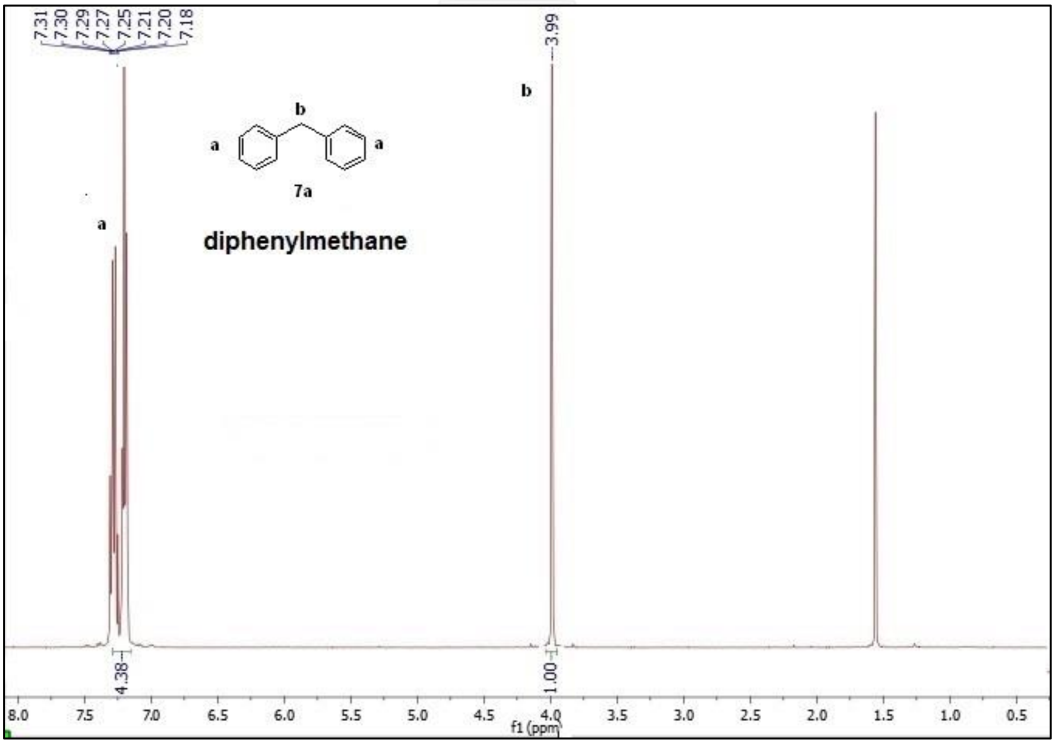

Figure 3.15 The ^{1}H NMR spectrum of authentic diphenylmethane (**7a**)

The multiplet peaks of aromatic protons were illustrated at δ 7.31-7.18 (m, 10H$_a$, Ar**H**). The singlet peak of methylene protons was demonstrated at δ 3.99 (s, 2H$_b$, CH$_2$).

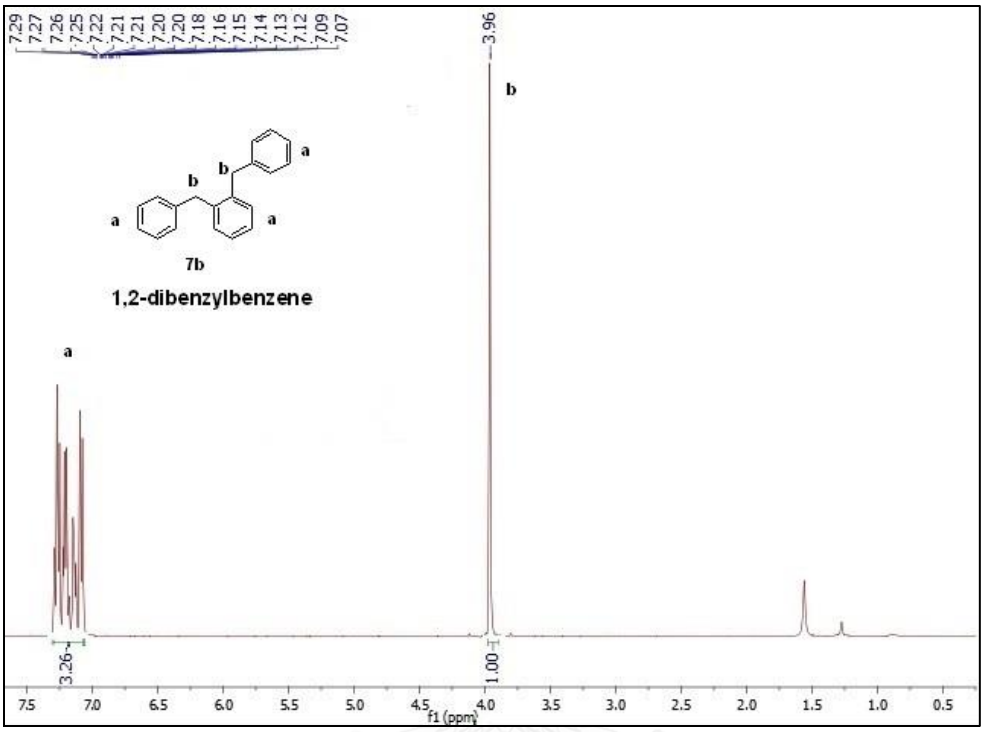

Figure 3.16 The ^{1}H NMR spectrum of authentic 1,2-dibenzylbenzene (**7b**)

The multiplet peaks of aromatic protons were illustrated at δ 7.29-7.07 (m, 14H$_a$, Ar**H**). The singlet peak of methylene protons was demonstrated at δ 3.96 (s, 4H$_b$, CH$_2$).

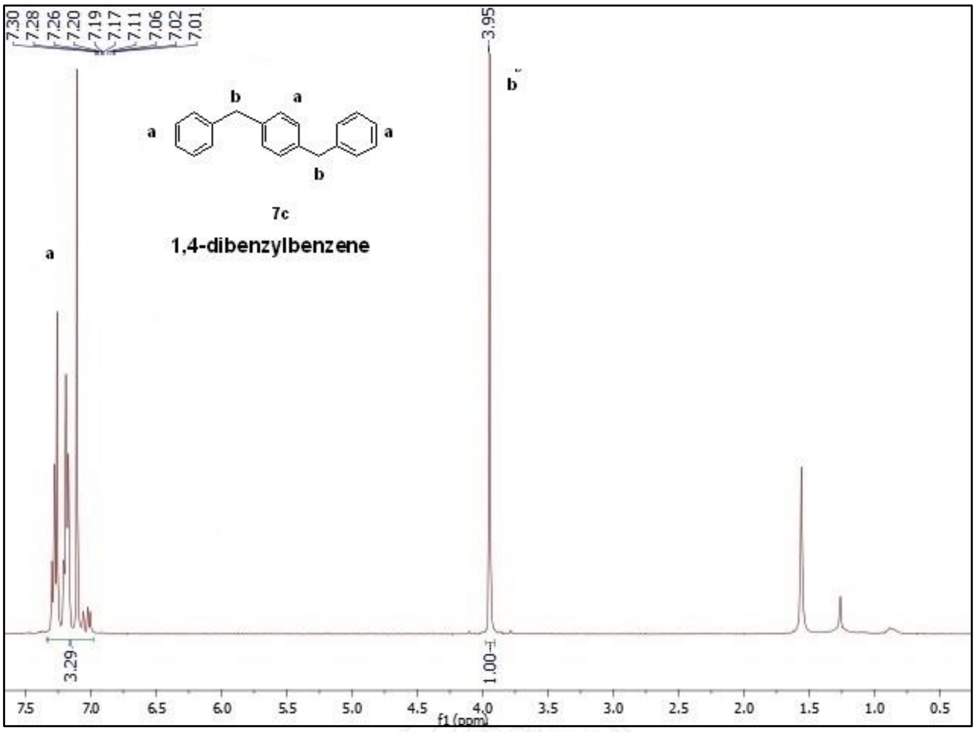

Figure 3.17 The ^{1}H NMR spectrum of authentic 1,4-dibenzylbenzene (**7c**)

The multiplet peaks of aromatic protons were illustrated at δ 7.30-7.01 (m, 14H$_a$, Ar**H**). The singlet peak of methylene protons was demonstrated at δ 3.95 (s, 4H$_b$, CH$_2$).

3.3.2.7 Benzylation of biphenyl

Two products: *o*-benzylbiphenyl **(8a)** and *p*-benzylbiphenyl **(8b)** were produced *via* benzylation of biphenyl with benzyl alcohol in good yield (97.2%) with *p*-**8b** and *o*-**8a** in the equal amount (ratio **8b**/**8a** 1.0). Biphenyl was a condense ring structure which had electron rich [60]. Hence, high yields of target products **(8a** and **8b)** were observed. However, a trace recovery of benzyl alcohol (2.8%) was left in the reaction. Since biphenyl was bulky and steric, so its diffusion was inconvenient to perform the reaction in clay porous [61].

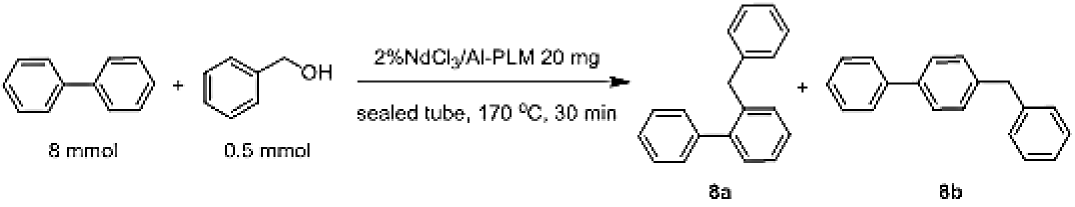

Table 3.14 Benzylation of biphenyl with benzyl alcohol using 2%$NdCl_3$/Al-PLM as catalyst

*%recovery	*%products		MB	8b/8a
	ortho-8a	*para*-8b		
2.8	48.6	48.6	100	1.0

*quantified by ^{1}H NMR

The %recovery of benzyl alcohol and yields of benzyl biphenyl products (**8a** and **8b**) could be quantified by ^{1}H NMR. The ^{1}H NMR spectra was compared with authentic samples. Cyclododecane was added as an internal standard. The ^{1}H NMR of authentic samples **8a** and **8b** were illustrated in Figures 3.18 and 3.19, respectively. These ^{1}H NMR spectra showed good correlation chemical shift in comparison with literature [18].

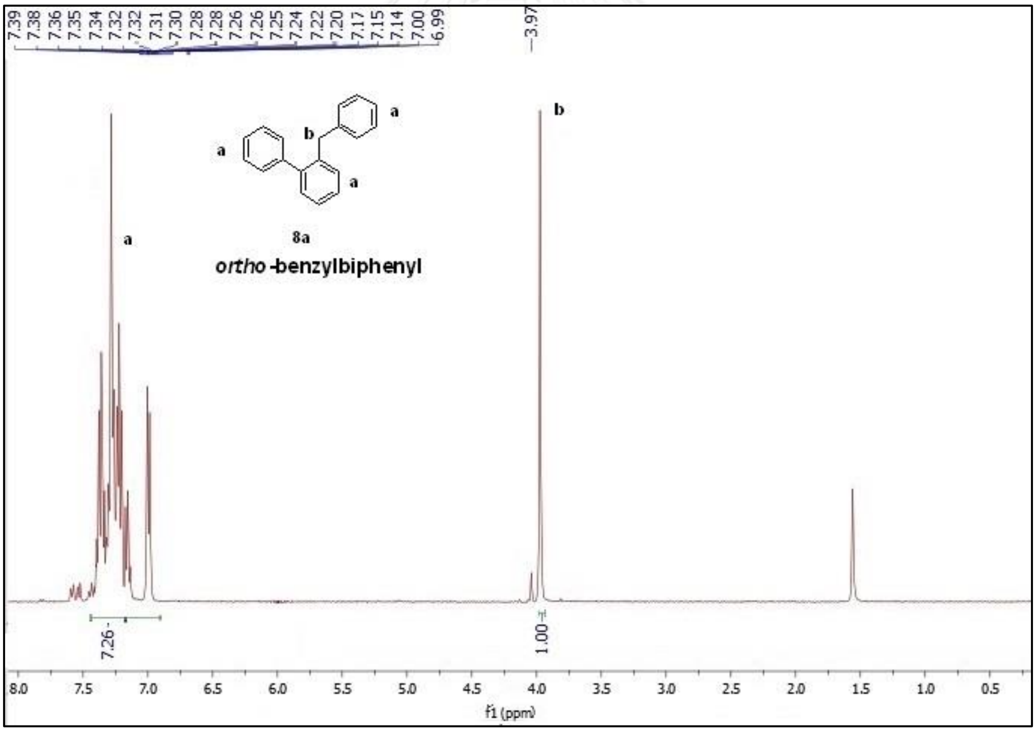

Figure 3.18 The ^{1}H NMR spectrum of authentic *o*-benzylbiphenyl (**8a**)

The multiplet peaks of aromatic protons were detected at δ 7.39-6.99 (m, $14H_a$, Ar**H**), whereas the singlet peak of methylene proton was illustrated at δ 3.97 (s, $2H_b$, C$\mathbf{H}_2$).

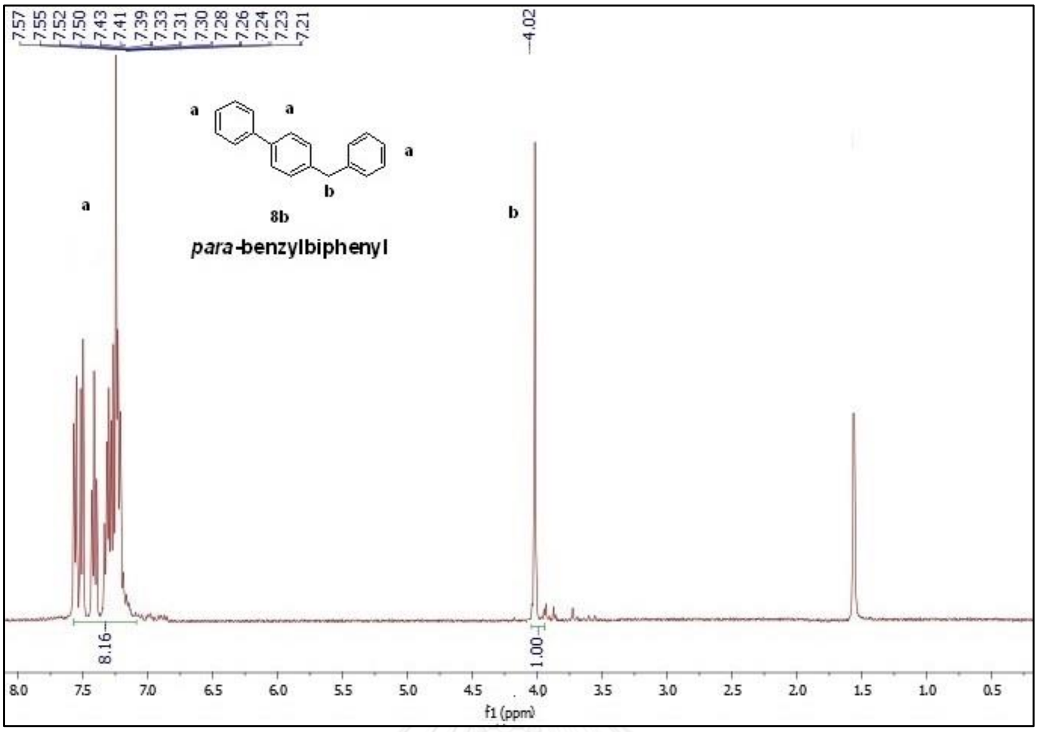

Figure 3.19 The ^{1}H NMR spectrum of authentic *p*-benzylbiphenyl (**8b**)

The multiplet peaks of aromatic protons were visualized at δ 7.57-7.21 (m, 14H$_a$, Ar**H**), whereas the singlet peak of methylene protons was illustrated at δ 4.02 (s, 2H$_b$, C**H**$_2$).

3.3.2.8 Benzylation of 2-naphthol

Further exploration, 2-naphthol was reacted with benzyl alcohol under optimized conditions with reaction time of 30 min. 2-Naphthol was classified as an electron donating group. *C*-benzylation product, 1-benzyl-2-naphthol (**9**) was obtained in 60.4% yield. An insignificant amount of benzyl alcohol (2%) was remained due to the bulky of substrate (2-naphthol). However, the mass balance was only 62.4% because dialkylted products occurred in the reaction which could not identify their structures [62]. Dialkylated products were formed from the reaction between monoalkylated (1-benzyl-2-naphthol) and benzyl alcohol [54]. Indicating that, the porous clay catalyst of 2%NdCl$_3$/Al-PLM could not restrict the production of dialkylated products due to the high reactivity of 1-benzyl-2-naphthol.

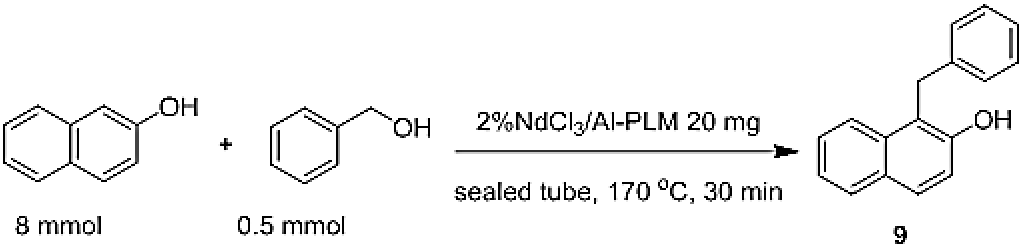

Table 3.15 Benzylation of 2-naphthol with benzyl alcohol using 2%$NdCl_3$/Al-PLM as catalyst

*%recovery	*%Products (8)	MB
2	60.4	62.4

*quantified by ^{1}H NMR

In the reaction mixture, the %recovery of benzyl alcohol and yield of 1-benzyl-2-naphthol (**9**) were quantified by ^{1}H NMR. The ^{1}H NMR spectrum of the latter was compared with that of authentic sample **9**. The ^{1}H NMR spectrum of authentic samples **9** was illustrated in Figure 3.20 which was in good correlated with literature [63].

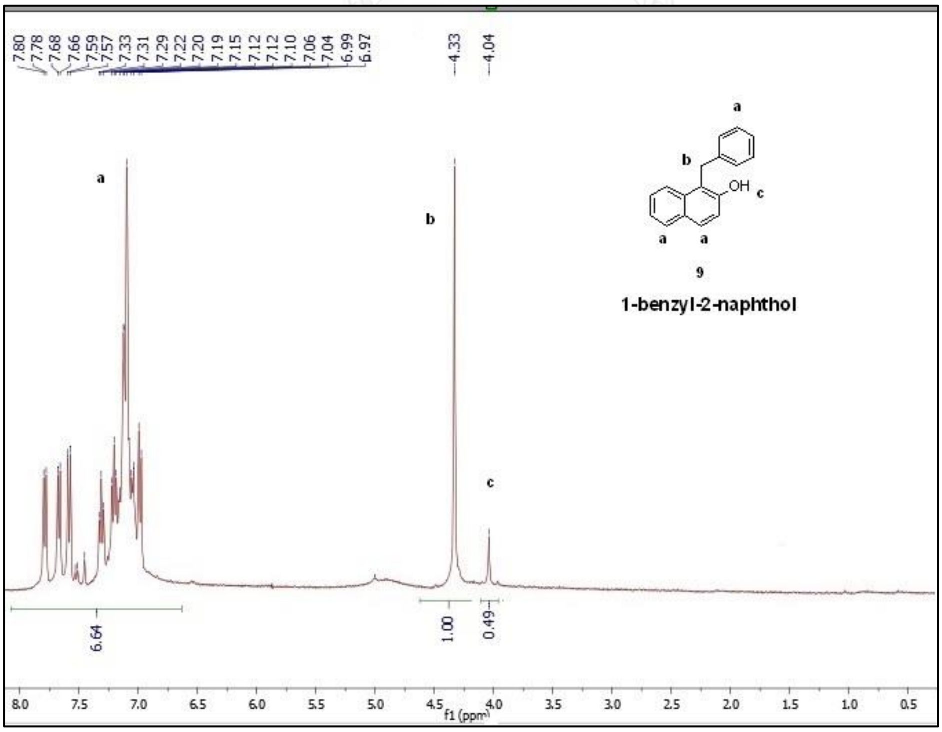

Figure 3.20 The ^{1}H NMR spectrum of authentic 1-benzyl-2-naphthol (**9**)

The ^{1}H NMR spectrum of 1-benzyl-2-naphthol (**9**) was presented in Figure 3.20. The multiplet peaks of aromatic protons were illustrated at δ 7.80-6.97 (m, 11H$_a$, Ar**H**). The singlet peak of methylene protons was shown at δ 4.33 (s, 2H$_b$, C**H**$_2$). The singlet peak of hydroxyl proton was demonstrated at δ 4.04 (s, 1H$_c$, O**H**).

3.3.2.9 Benzylation of nitrobenzene

Under the optimized conditions, the benzylation of nitrobenzene was not successful. The starting material (benzyl alcohol) was recovered in 44.4% whereas benzyl ether was occurred in 66.6% *via* dehydration of benzyl alcohol. Thus, the benzylation of nitrobenzene with benzyl alcohol was slow and *m*-benzylnitrobenzene was not generated under these conditions.

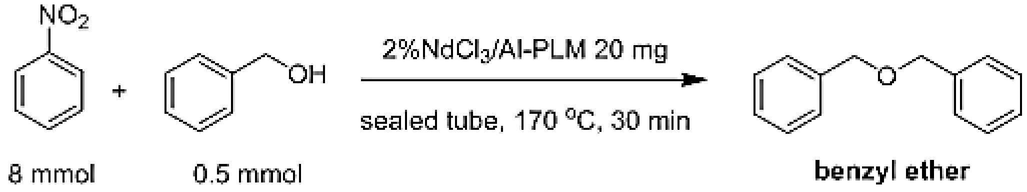

Table 3.16 Benzylation of nitrobenzene with benzyl alcohol using 2%NdCl$_3$/Al-PLM as catalyst

*%recovery	%benzyl ether	*yield	MB
44.4	55.6	55.6	100

*quantified by ^{1}H NMR

In the reaction mixture, the yields of benzyl alcohol and benzyl ether were calculated from the ^{1}H NMR spectrum using biphenyl as an internal standard. The ^{1}H NMR spectra of benzyl alcohol and benzyl ether were compared with commercially available chemicals.

In short, either increasing or decreasing in yield products depended entirely on the nucleophilicity of the type of substituent on benzene rings. The benzylation of benzene gave 82% yield of *C*-monobenzylation (**7a**) and 22% yield of *C*-dibenzylation (**7b** and **7C**) products, respectively. For electron-donating substituents on benzene (toluene, ethylbenzene, *tert*-butylbenzene, anisole, *p*-cresol, *p*-xylene, biphenyl and 2-naphthol) gave 60 to 100% yield of *C*-monobenzylated products under these optimized conditions with reaction time 30 min using 2%$NdCl_3$/Al-PLM as a catalyst. The porous of clay catalyst could limit the production of dibenzylated products with high yield of *C*-monobenzylated products (82-100%) in case of those aromatics except for 2-naphthol. However, under these optimized conditions, the benzylation of unactivated benzene could not achieve.

3.4 Regeneration of 2%$NdCl_3$/Al-PLM in benzylation of toluene with benzyl alcohol

3.4.1 The characterization of regenerated 2%$NdCl_3$/Al-PLM

After benzylation of toluene and benzyl alcohol was completed, 2%$NdCl_3$/Al-PLM was filtered, washed and re-calcination at 450 °C for 4 h to eliminate coke in clay catalyst before use in next run. The characterization of regenerated 2%$NdCl_3$/Al-PLM by XRD and nitrogen adsorption-desorption comparing with 2%$NdCl_3$/Al-PLM were examined. In addition, FT-IR spectra acidity test for regenerated 2%$NdCl_3$/Al-PLM was also investigated.

3.4.1.1 XRD pattern of fresh 2%$NdCl_3$/Al-PLM and regenerated 2%$NdCl_3$/Al-PLM

The XRD patterns of the naïve 2%$NdCl_3$/Al-PLM and the regenerated one are compared as showed in Figure 3.21.

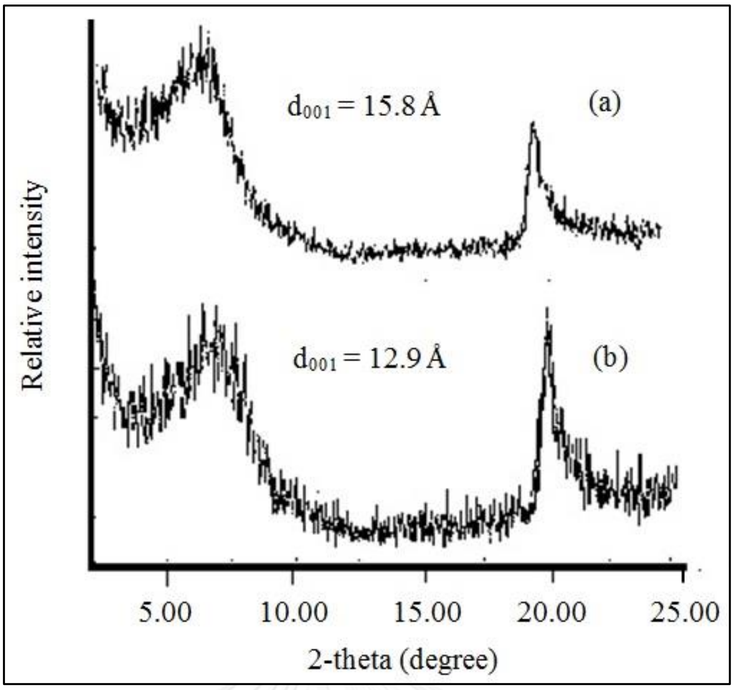

Figure 3.21 XRD patterns of: (a) 2%NdCl3/Al-PLM (b) regenerated 2%$NdCl_3$/Al-PLM

The XRD pattern of regenerated 2%$NdCl_3$/Al-PLM **(b)** was similar to that of 2%$NdCl_3$/Al-PLM **(a)** suggesting that, almost crystallinity phase in regenerated 2%$NdCl_3$/Al-PLM was exhibited which could confirmed the stability of clay catalyst. However, its d-basal spacing value (12.9 Å) was lower than 2%$NdCl_3$/Al-PLM (15.8 Å) because the attrition in reaction process caused partial crystallinity phase collapsed [33].

3.4.1.2 BET specific surface area and BJH pore size diameter

The nitrogen adsorption-desorption isotherms of 2%$NdCl_3$/Al-PLM and regenerated 2%$NdCl_3$/Al-PLM are shown in Table 3.17. The 0.04 g of clay samples were pretreated at 150°C for 2 h. Then, their surface area and pore size diameter were analyzed by BET and BJH methods, respectively.

Table 3.17 The BET specific surface area and BJH pore size diameter of clay catalysts

Entry	Type of clay catalyst	BET specific surface area (m^2/g)	Pore size diameter (Å)
1	$NdCl_3$/Al-PLM	66.37	32.8

2	Regenerated $NdCl_3$/Al-PLM	20.20	24.4

From the results in Table 3.17, the BET specific surface area and BJH pore size diameter of regenerated 2%$NdCl_3$/Al-PLM were decreased comparing with the original 2%$NdCl_3$/Al-PLM. It could be described that the partial pillared structure was collapsed during the reaction process and high calcination temperature for regenerated clay catalyst caused the reduction of BET specific surface area and BJH pore size diameter of regenerated 2%$NdCl_3$/Al-PLM.

3.4.1.3 Determination of acidity of regenerated 2%$NdCl_3$/Al-PLM

Attenuated total reflectance Fourier transform infrared (ATR-FTIR) spectroscopy has been used to determine the nature of acid site of regenerated 2%$NdCl_3$/Al-PLM using the diagnostic base, pyridine. This catalyst was dried in hot air for 1 h at 100°C prior to pyridine treatment. Regenerated 2%$NdCl_3$/Al-PLM 50 mg and pyridine 0.1 mL were poured into a sample cup. Then, the sample cup was kept in a hot air oven at 120°C for 1 h to remove physisorbed pyridine. After cooling this catalyst, IR spectra was recorded in transmittance as a function of wave number ranging from 1400 to 1700 cm^{-1}.

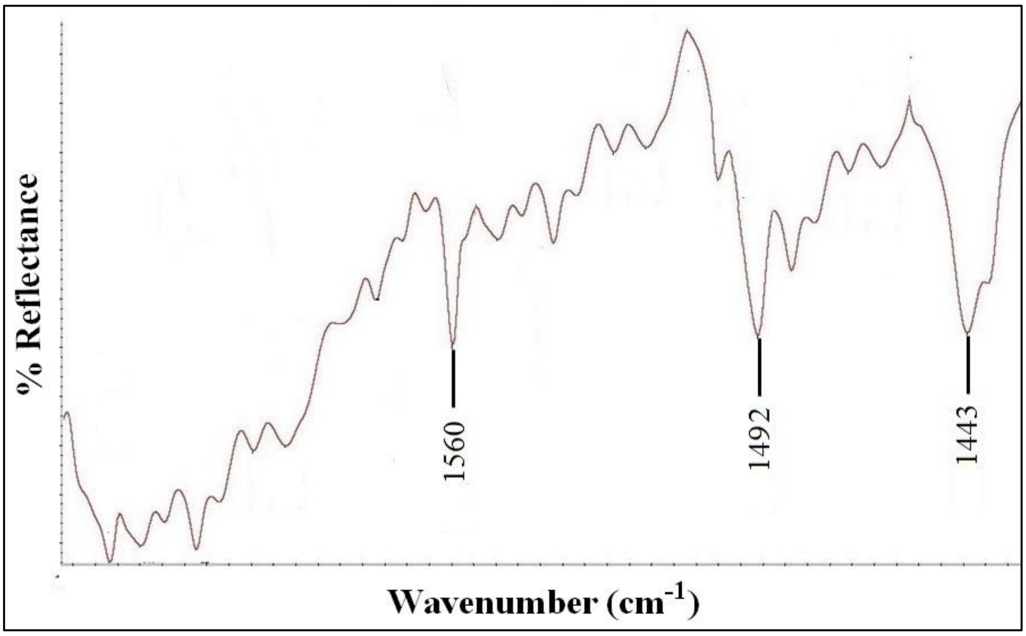

Figure 3.22 FT-IR spectrum of regenerated 2%$NdCl_3$/Al-PLM

The FT-IR spectrum of regenerated 2%$NdCl_3$/Al-PLM was presented in Figure 3.22. Two major transmittance bands at 1443 and 1492 cm^{-1} corresponded to Lewis acidity. The assignment of moisture subtraction artefact was illustrated at 1560 cm^{-1} indicating that regenerated 2%$NdCl_3$/Al-PLM still had Lewis acid after first run.

3.4.2 The activity of regenerated 2%$NdCl_3$/Al-PLM

2%$NdCl_3$/Al-PLM could be easily recovered by filtration and re-calcination which is useful for industrial economy. After washing with acetone, drying at 80°C in oven and calcination at 450°C at the rate of 5°C/min for 4 h, the recovered 2%$NdCl_3$/Al-PLM was used in the next run. The results are shown in Table 3.18.

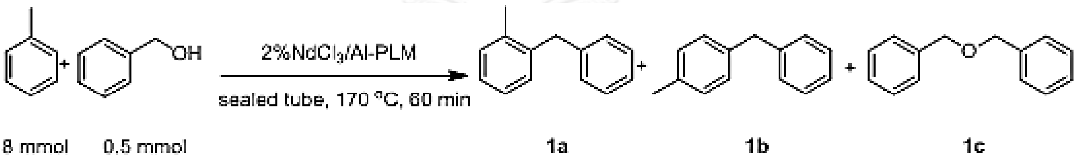

Table 3.18 Activity of regenerated 2%NdCl3/Al-PLM on benzylation of toluene

Entry	Time Cycles	Amount of catalyst (mg)	*% recovery	*%products			MB	ratio of 1b/1a	ratio of (1a+1b)/1c
				%*ortho*-1a	%*para*-1b	%1c			
1	1	20	0	39.6	60.9	0	100.5	1.54	-
2		50	0	44.1	67.1	0	111.1	1.52	-
3		100	0	41.1	63.8	0	104.9	1.55	-
4	2	20	0	37.8	58.1	5.9	101.8	1.54	16.19
5		50	0	40.2	63.7	1.9	105.9	1.58	53.69
6		100	0	42.1	64.2	0	106.3	1.53	-
7	3	20	95.1	0.4	0.6	0.5	96.7	1.49	1.92
8		50	5.6	27.8	42.6	29.8	105.8	1.53	2.36
9		100	0	38.8	60.8	0	99.6	1.57	-
10	4	100	0	40.5	61.8	0.9	103.2	1.53	113.83
11	5	100	0	40.8	63.6	0.9	105.3	1.56	110.71
12	6	100	0	36.9	56.5	6.5	99.9	1.53	14.33
13	7	100	0	35.8	56.1	12.5	104.4	1.57	7.38

14	8	100	8.8	27.4	43.1	20.9	100.2	1.57	3.37

*quantified by ^{1}H NMR

The first and second reuses of the catalyst 20 mg (entries 1 and 4, respectively) under the same optimized conditions showed approximate 100% yield of products (**1a**, **1b** and **1c**). Although the second reuse of catalyst 20 mg caused a small amount of benzyl ether 5.6% (entry 4). Nonetheless, the efficiency for the third run was not good and showed 95% recovery of benzyl alcohol (entry 7). According to the results, the efficiency of catalysts was reduced when the reusability cycle numbers were increased. This could be described that 2%$NdCl_3$/Al-PLM could not display the same activity because of the structural deterioration in reaction process and consequently lowered its activity.

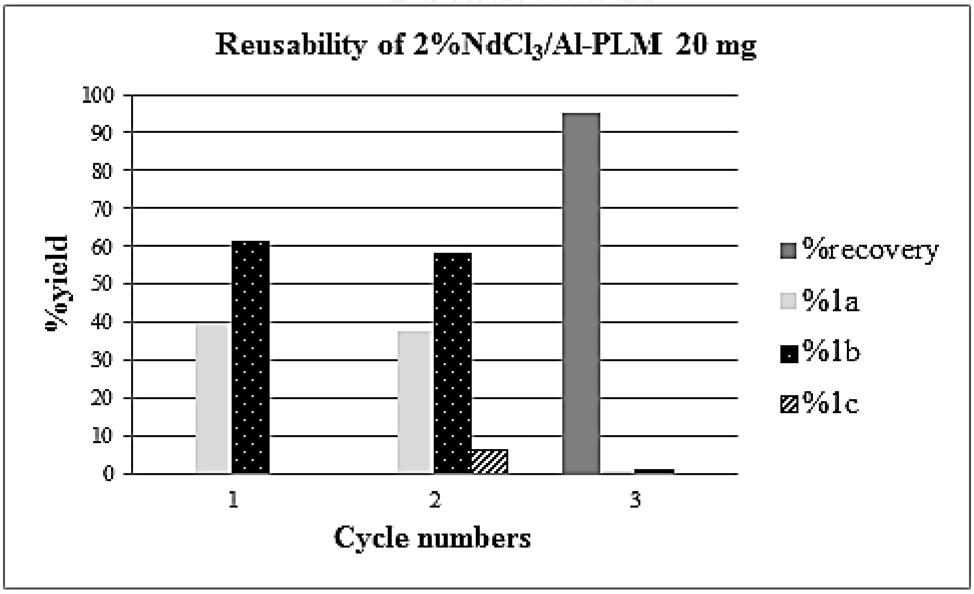

Figure 3.23 Cycle number of 2%$NdCl_3$/Al-PLM 20 mg on benzylation of toluene

50 mg of first, second and third cycles of regenerated 2%$NdCl_3$/Al-PLM were explored for the catalyst efficiency. The first and second reuse catalyst 50 mg showed high selectivity to *C*-benzylation (**1a** and **1b**) with good yields in entries 2 and 5, respectively. An insignificant of by-product (**1c**) occurred in the reaction in entry 5. However, benzyl alcohol could not completely consume for *C*-benzylation (**1a** and **1b**) in the third reused catalyst 50 mg (entry 8).

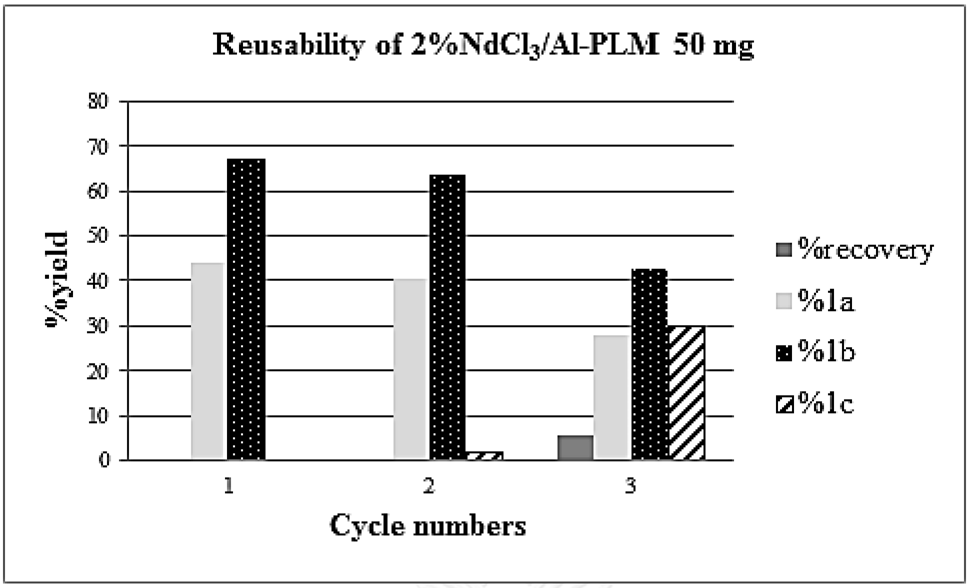

Figure 3.24 Cycle number of 2%NdCl$_3$/Al-PLM 50 mg on benzylation of toluene

Hence, it was reasonable to use higher amount of catalyst to 100 mg in the next run (Figure 3.25). On the other hand, the forth and fifth reused catalysts could give high yield of *C*-benzylation (**1a** and **1b**) in entries 10 and 11. The sixth and seventh reused catalyst still exhibited 100% conversion, but higher amount of benzyl ether was detected as a result of insufficient Lewis acid in the catalytic process (entries 12 and 13, respectively). The eighth reused catalyst was inefficient for benzylation of toluene with benzyl alcohol since there was 8.8% recovery of substrate benzyl alcohol (entry 14). This indicated that the catalyst could be reused at least five times by adding 100 mg of catalyst without appreciable loss of activity.

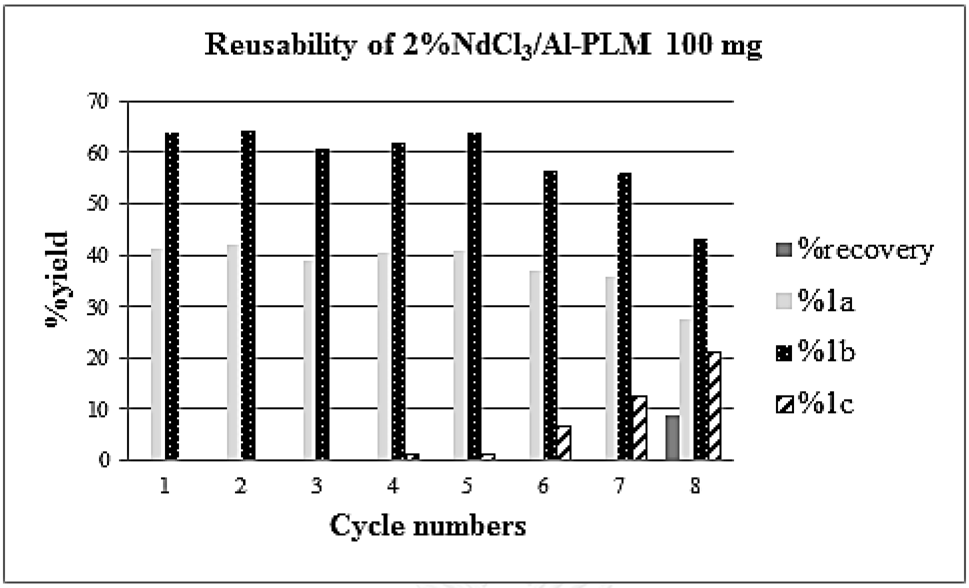

Figure 3.25 Cycle number of 2%$NdCl_3$/Al-PLM 100 mg on benzylation of toluene

3.5 Summary of benzylation of aromatics

2%$NdCl_3$/Al-PLM was synthesized by intercalation, impregnation and calcination to perform the efficient catalyst in benzylation of aromatics which are key synthetic intermediates in pharmaceutical and fine chemical industries. The synthetic clay was characterized with XRD, N_2 adsorption-desorption and FT-IR technique. The optimal conditions were disclosed in terms of appropriate amount of catalyst, temperature, time, molar ratio, type of benzylating agent. To illustrate this, toluene (8 mmol), benzyl alcohol (0.5 mmol), sealed tube, 170°C, 60 min and 2%$NdCl_3$/Al-PLM (20 mg). In addition, the reusability of catalyst was studied. For catalytic reaction, 2%$NdCl_3$/Al-PLM exhibited highly reactive in *C*-benzylation of activated aromatics and could be recovered at least five times by adding 100 mg of 2%$NdCl_3$/Al-PLM in the next run.

3.6 Optimum conditions study on tetrahydropyranylation of benzyl alcohol

3,4-Dihydro-*2H*-pyran (DHP) is a versatile reagent for the protection of hydroxyl group yielding tetrahydropyranyl ethers, which are useful intermediates to further functional transformation in organic reactions. Benzyl alcohol was chosen as a chemical model in this study. The efficiency of 2%$NdCl_3$/Al-PLM affecting on tetrahydropyranylation of benzyl alcohol was explored. The effect of solvent, temperature, amount of catalyst, reaction time and the ratio of DHP with benzyl alcohol were investigated.

Tetrahydropyranylation of benzyl alcohol produced 2-(benzyloxy)tetrahydro-2*H*-pyran (**10**) with none of by-product.

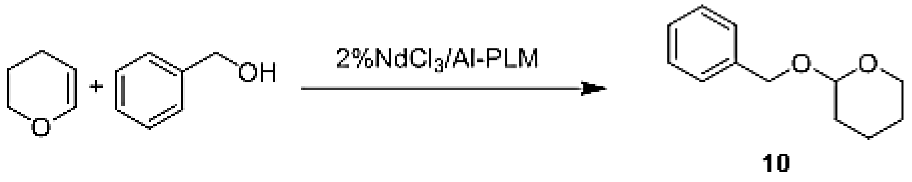

%Recovery of benzyl alcohol and %yield of product **10** were quantified by ^{1}H NMR with biphenyl as an internal standard. The ^{1}H NMR spectrum of benzyl alcohol in the crude mixture was compared with commercially available chemical. The ^{1}H NMR spectrum of **10** in the reaction mixture was compared with the authentic sample in Figure 3.26. The authentic sample (**10**) was synthesized from tetrahydropyranylation of benzyl alcohol catalyzed by $AlCl_3 \cdot 6H_2O$.

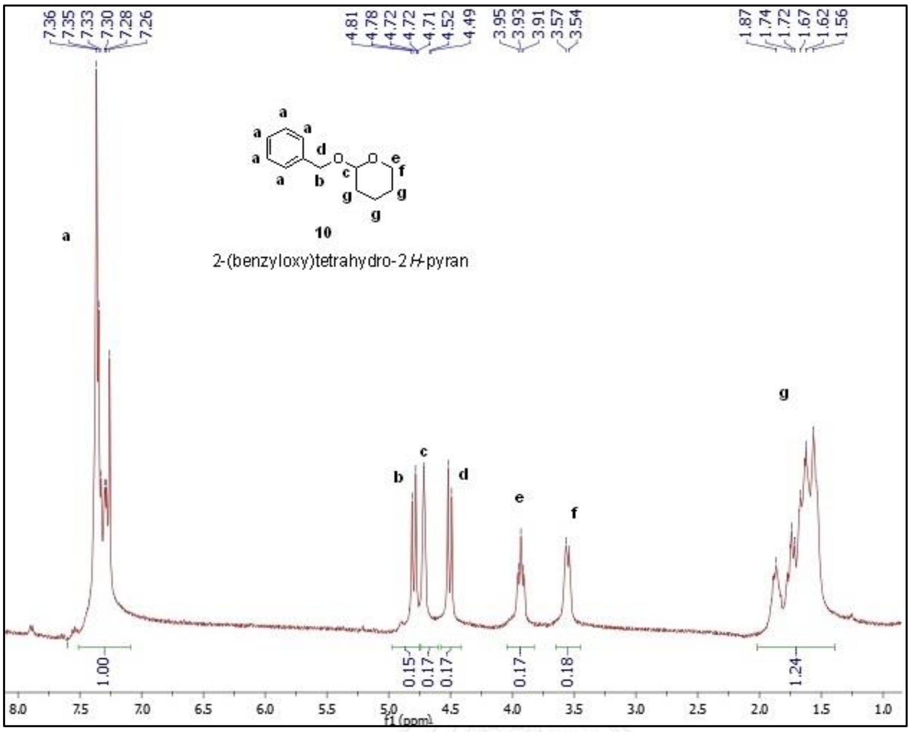

Figure 3.26 The ^1H NMR spectrum of authentic 2-(benzyloxy)tetrahydro-2H-pyran (**10**)

The benzyl protons of **10** revealed multiplet peaks at δ_H 7.36–7.28 (m, $5H_a$, Ar**H**). The methyl protons exhibited doublet peaks at δ_H 4.81–4.78 and 4.52-4.49 with J = 12.0 Hz of H_b and H_d (d, J = 12.0 Hz, $1H_{\mathbf{b,d}}$, OC**H**$_2$), respectively. Another methyl proton exhibited triplet peaks at δ_H 4.72–4.71 of $1H_c$ (t, J = 3.4 Hz, $1H_{\mathbf{c}}$, OC**H**O). The methyl protons displayed multiplet peaks of $H_{\mathbf{e}}$ and $H_{\mathbf{f}}$ at δ_H 3.95–3.91 and 3.57-3.54, respectively. The methylene protons of H_g showed multiplet peaks at δ_H 1.87–1.56 (m, $6H_{\mathbf{g}}$, C**H**$_2$). The ^1H NMR spectrum of authentic sample **10** was in good correlation with literature [33].

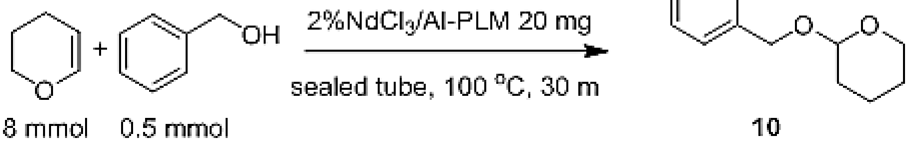

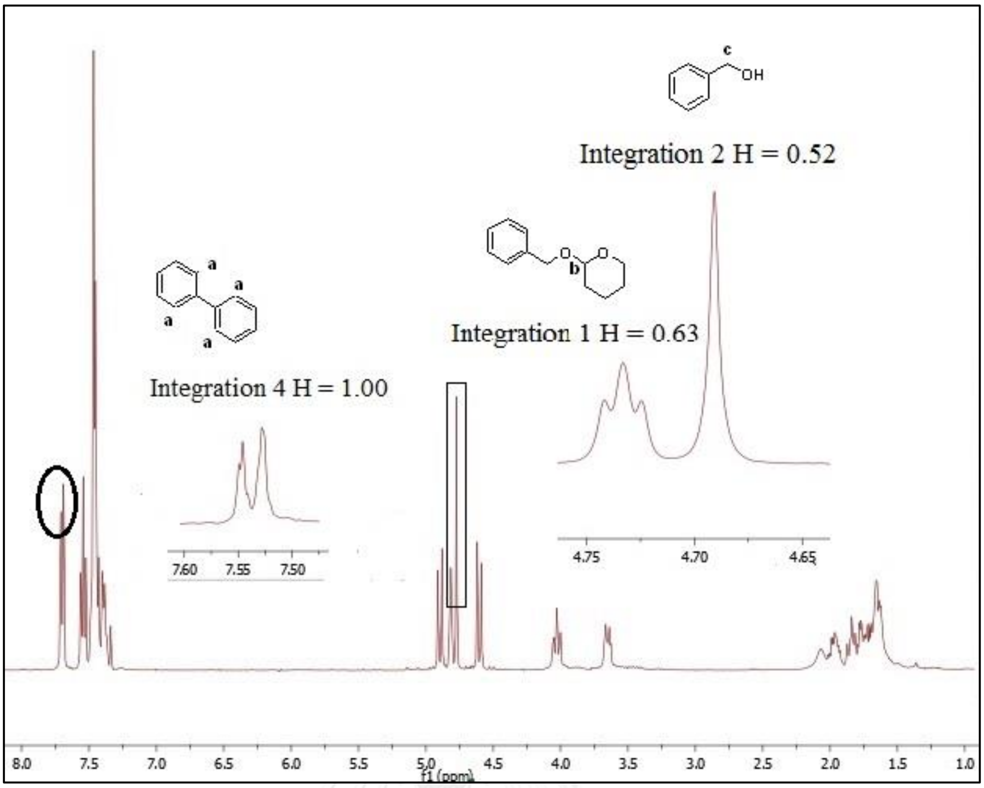

Figure 3.27 The ^{1}H NMR spectrum of tetrahydropyranylation of benzyl alcohol in the crude reaction mixture by using biphenyl as an internal standard

The ^{1}H NMR spectrum presented in Figure 3.27 was obtained from the crude reaction mixture of benzyl alcohol 0.5 mmol reacted with DHP 1 mmol in the presence of 2%$NdCl_3$/Al-PLM 20 mg at 100°C and reaction time of 30 min. After the reaction was finished, biphenyl 0.139 mmol was added as an internal standard for calculation of %recovery and yields based on benzyl alcohol.

From Figure 3.27, the peak area of H_b was taken to calculate for the percentage yield of product (**10**) whereas H_c was taken to calculate for %recovery, respectively. Those interested peaks were calculated in comparison with H_a of internal standard (biphenyl).

$$\%\ \text{recovery} = \frac{0.139\ \text{mmol of biphenyl}}{0.545\ \text{mmol of benzyl alcohol}} \text{ X } \frac{4\ H_a\ \text{of biphenyl}}{1} \text{ X } \frac{0.52}{2\ H_c} \text{ X } 100 = 27.1\%$$

$$\%\ \mathbf{10} = \frac{0.139\ \text{mmol of biphenyl}}{0.545\ \text{mmol of benzyl alcohol}} \text{ X } \frac{4H_a\ \text{of biphenyl}}{1} \text{ X } \frac{0.63}{1\ H_b} \text{ X } 100 = 65.6\%$$

Mass balance = 27.1% + 65.6% = 92.7%

From the calculations, %recovered benzyl alcohol was 27.1%, and 2-(benzyloxy)tetrahydro-*2H*-pyran (**10**) was 65.6%. The mass balance was calculated by the total percentage of recovery substrate and product. Then, this pattern was applied to every part of percentage recovery and yield calculation.

3.6.1 The effect of solvents on tetrahydropyranylation of benzyl alcohol at room temperature

From the literature reviews [33-37], the reactions were performed under RT in various solvents for 1 h. The first part was attempted to use 2%$NdCl_3$/Al-PLM as a catalyst in tetrahydropyranylation of benzyl alcohol at RT in various solvents such as CH_2Cl_2, diethylether, THF, MeCN, MeOH and none of solvent. The results are collected in Table 3.19.

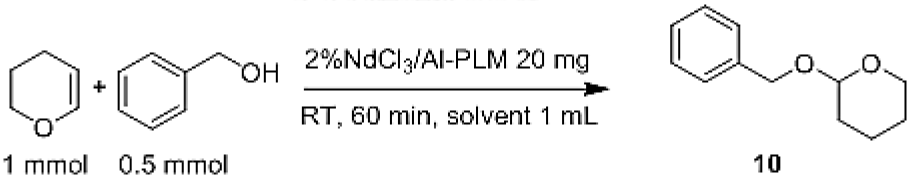

Table 3.19 The effect of solvents on tetrahydrppyranylation of benzyl alcohol at RT

Entry	Type of solvents	*%recovery	*%yield	MB
1	None of solvent	73.0	27.4	100.4
2	Diethylether	98.5	0	98.5
3	CH_2Cl_2	84.8	14.6	99.4
4	THF	79.9	17.7	97.6
5	MeCN	97.6	0	97.6
6	MeOH	98.0	0	98

*quantified by ^1H NMR

The observation of various solvents at RT for 1 h was presented in Table 3.19. The yield of product 10 was less than 20% in the presence of solvents (entries 2-6) whereas without solvent gave 27.4% of product 10 (entry 1). However, under these conditions in the absence of solvent, the reaction did not proceed to give the appreciable yield of 10. Therefore, the optimum conditions for benzylation of toluene were applied to tetrahydropyranylation of benzyl alcohol as shown below.

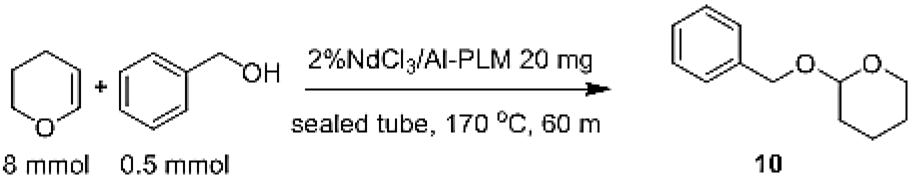

3.6.2 The effect of temperature on tetrahydropyranylation of benzyl alcohol

Since the reaction was not succeed when performing at RT in the absence of solvent within 1 h. The temperature was considered as a main factor to synthesize 10 in a quantitative yield. Hence, the temperature at 100 and 170°C were applied for the reaction.

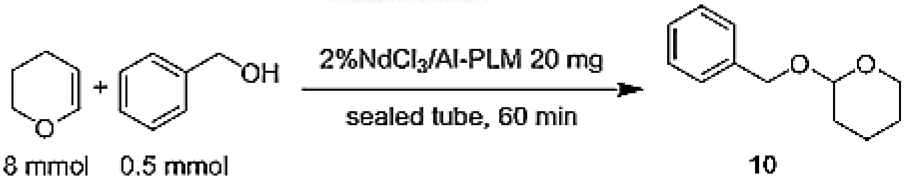

Table 3.20 The effect of temperature on tetrahydropyranylation of benzyl alcohol in the absence of solvent

Entry	Temperature	*%recovery	*%yield	MB
1	170	16.0	51.7	67.7
2	100	0	96.5	96.5

*quantified by ^{1}H NMR

At 170°C (entry 1), 51.7% yield of product 10 and 16% recovered benzyl alcohol with unacceptable mass balance 67.7 (less than 95). The results indicated that reaction temperature of 170 °C may cause the evaporation of DHP (bp 86 °C), resulted in incomplete benzyl alcohol conversion and not satisfied mass balance (entry 1). Then, the temperature was reduced to 100°C (entry 2). Surprisingly, these conditions were suitable for the production of 10 in an excellent yield (96.5%) and none of recovered benzyl alcohol was left. Thus, the general procedure for tetrahydropyranylation was benzyl alcohol 0.5 mmol, DHP 8 mmol, 2%$NdCl_3$/Al-PLM 20 mg, sealed tube, reaction temperature 100 °C and reaction time 1 h. It was noted that heat was advocated to activate this catalyst for tetrahydropyranylation reaction.

3.6.3 The effect of 2%$NdCl_3$/Al-PLM amount on tetrahydropyranylation of benzyl alcohol

The exploration of the amount of 2%$NdCl_3$/Al-PLM on tetrahydropyranylation of benzyl alcohol was observed. The addition of the catalyst at 10 and 20 mg as well as without the catalyst in the reaction was studied in comparison. The results are presented in Table 3.21.

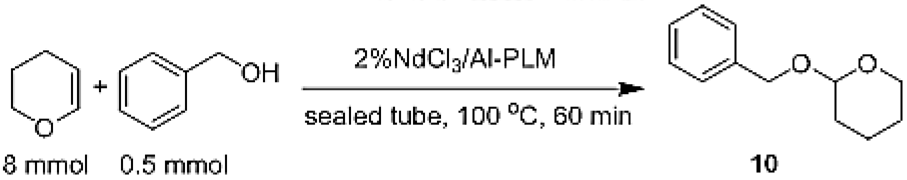

Table 3.21 The effect of 2%$NdCl_3$/Al-PLM amount on tetrahydropyranylation of benzyl alcohol

Entry	Amount of 2%$NdCl_3$/Al-PLM	*%recovery	*%yield	MB
1	0	82.9	17.3	100.2
2	10	53.3	45.0	98.4
3	20	0	96.5	96.5

*quantified by ^{1}H NMR

The product **10** was produced in low yield (17.3%, entry 1) in the absence of catalyst whereas in the presence of catalyst 10 and 20 mg provided 45.0 and 96.5% yield, respectively (entries 2-3). Hence, 20 mg of 2% $NdCl_3$/Al-PLM was the appropriate amount (entry 3).

3.6.4 The observation of the effect of reaction time on tetrahydropyranylation of benzyl alcohol

The effect of the reaction time on tetrahydropyranylation of benzyl alcohol was carried out and the results are tabulated in Table 3.22.

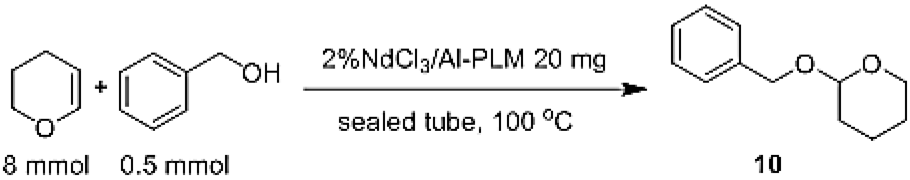

Table 3.22 The effect of reaction time on tetrahydropyranylation of benzyl alcohol

Entry	reaction time (min)	*%recovery	*%yield	MB
1	15	66.8	27.8	94.6
2	30	27.1	65.6	92.7
3	60	0	96.5	96.5

*quantified by ^{1}H NMR

The reaction time was varied to study %recovery of substrate and %yield (Table 3.22). The yield of product was increased when the reaction time increased (entries 1-3). The high amount of the recovered benzyl alcohol 66.8 and 27.8% yield of product (**10**) were observed for 15 min (entry 1). When the reaction time was extended to 30 min, product (**10**) was increased to 65.6% yield, but benzyl alcohol was left in the reaction (27.1%). When the reaction time was prolonged to 60 min (entry 3), product (**10**) was completely occurred in the reaction (96.5%). Therefore, the appropriate reaction time to furnish the successful tetrahydropyranylation of benzyl alcohol was 60 min.

3.6.5 The effect of molar ratio on tetrahydropyranylation of benzyl alcohol

The effect of molar ratio of DHP was carried out and the results were presented in Table 3.23.

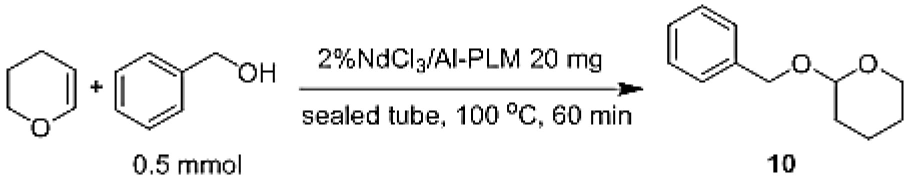

Table 3.23 The effect of molar ratio on tetrahydropyranylation of benzyl alcohol

Entry	ratio DHP to benzyl alcohol	*%recovery	*%yield	MB
1	8:0.5	0	96.5	96.5
2	4:0.5	0	104.8	104.8
3	2:0.5	0	104.0	104.0
4	1:0.5	0	106.6	106.6

*quantified by ^{1}H NMR

Tetrahydropyranylation of benzyl alcohol was carried out with various molar ratios of DHP to benzyl alcohol as follows: 8:0.5, 4:0.5, 2:0.5, and 1:0.5, respectively (entries 1-4). There was none of benzyl alcohol left in the studied ratios (entries 1-4) as shown in Table 3.23. Hence, the proper ratio of DHP to benzyl alcohol was 1:0.5. Only 1 mmol of DHP was reacted with 0.5 mmol of benzyl alcohol to produce 2-(benzyloxy)tetrahydro-2*H*-pyran (**10**) in quantitative yield (entry 4).

To summarize, the standard conditions for tetrahydropyranylation of benzyl alcohol catalyzed by 2%NdCl$_3$/Al-PLM as follows. The product 2-(benzyloxy)tetrahydro-2*H*-pyran (**10**) was occurred efficiently under this optimum conditions.

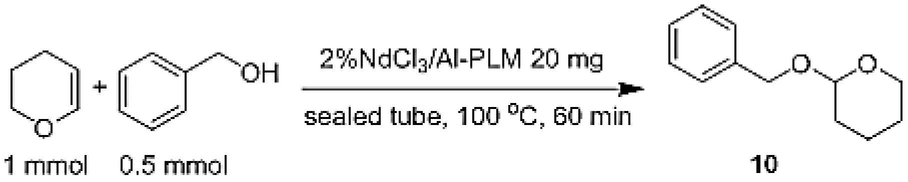

3.6.6 The mechanism of tetrahydropyranylation of benzyl alcohol

The proposed mechanism of tetrahydropyranylation of benzyl alcohol using 2%NdCl$_3$/Al-PLM as a catalyst could be illustrated in Figure 3.28.

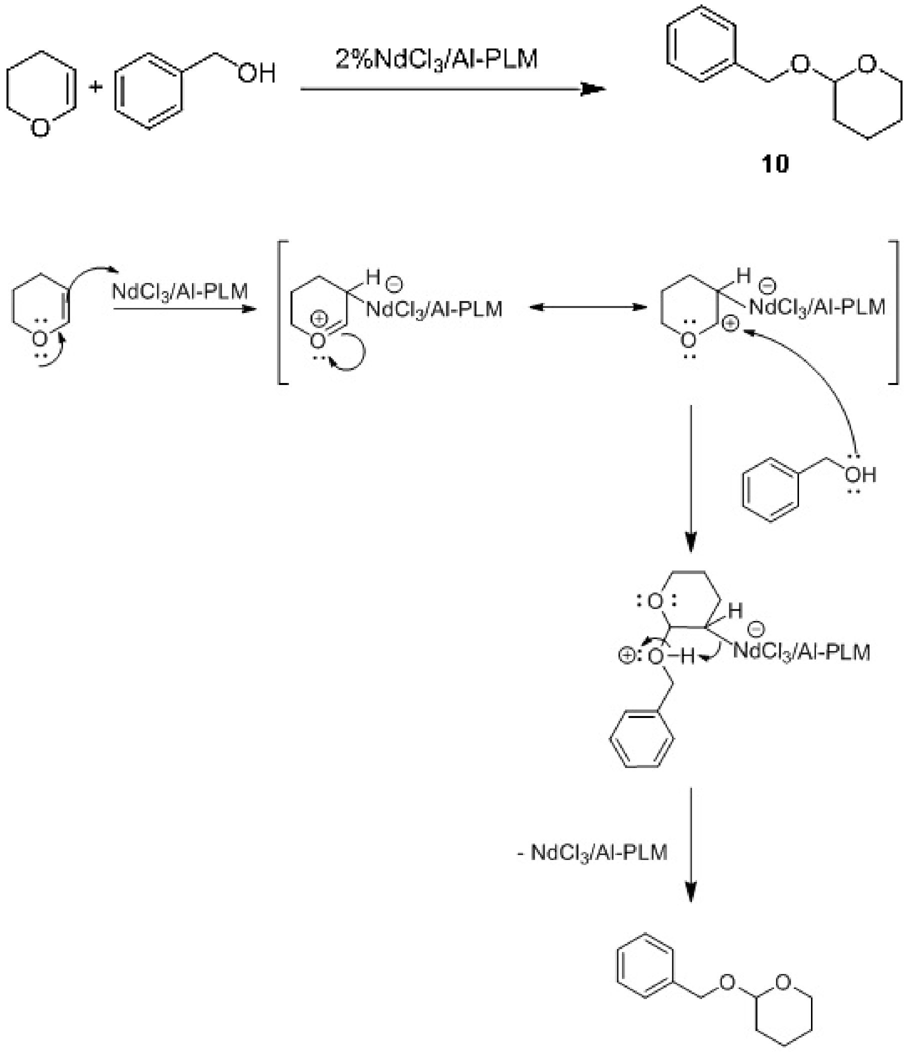

Figure 3.28 The proposed mechanism of tetrahydropyranylation of benzyl alcohol using 2%$NdCl_3$/Al-PLM as a catalyst

Tetrahydropyranylation of benzyl alcohol was preceded by nucleophilic addition. Lewis acid catalyst $NdCl_3$/Al-PLM reacted with 3,4-dihydro-2*H*-pyran (DHP). Then, benzyl alcohol further attacked DHP to form 2-(benzyloxy)tetrahydro-2*H*-pyran (**10**). This mechanism was well related to the literature on other Lewis acid catalysts [37].

3.7 Regenerated 2%$NdCl_3$/Al-PLM in tetrahydropyranyltion of benzyl alcohol

3.7.1 The characterization of regenerated 2%$NdCl_3$/Al-PLM

After tetrahydropyranylation of benzyl alcohol was completed, the used catalyst 2%$NdCl_3$/Al-PLM was filtered, washed, and dried, respectively. Then, the spent catalysts were regenerated by two different modes, re-calcination (**A**) and not re-calcination (**B**) as shown in Figure 3.29 in order to compare the efficiency of the catalysts under different methods.

Treatment type A

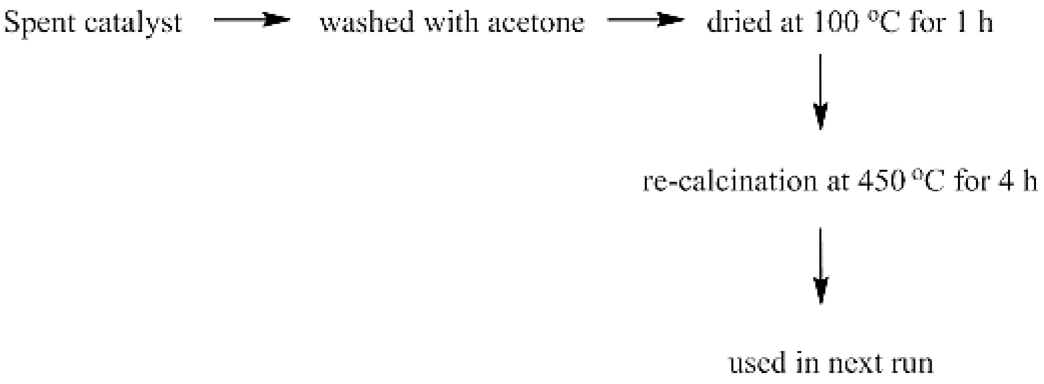

Treatment type B

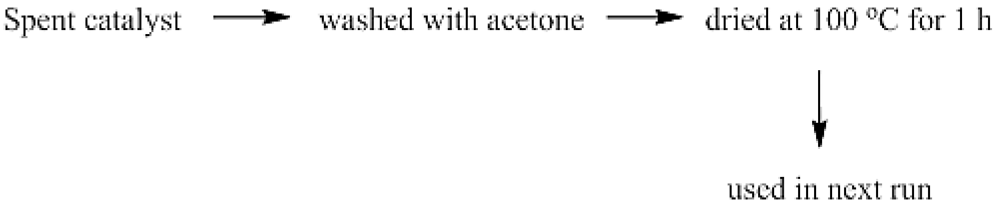

Figure 3.29 Two different methods for regenerated catalysts

These experiments were attempted to compare the efficiency of the regenerated catalysts between severe-temperature calcination (**A**) and not re-calcination (**B**) treatments before using in the next run. The changes of their structures were characterized by XRD and nitrogen adsorption-desorption in comparison with

$2\%NdCl_3$/Al-PLM. In addition, FT-IR spectra was used for acidity determination for the regenerated $2\%NdCl_3$/Al-PLM **A** and **B**.

3.7.1.1 XRD pattern of fresh $2\%NdCl_3$/Al-PLM, regenerated $2\%NdCl_3$/Al-PLM A and B

The XRD pattern of $2\%NdCl_3$/Al-PLM and regenerated $2\%NdCl_3$/Al-PLM **A** and **B** are shown in Figure 3.30.

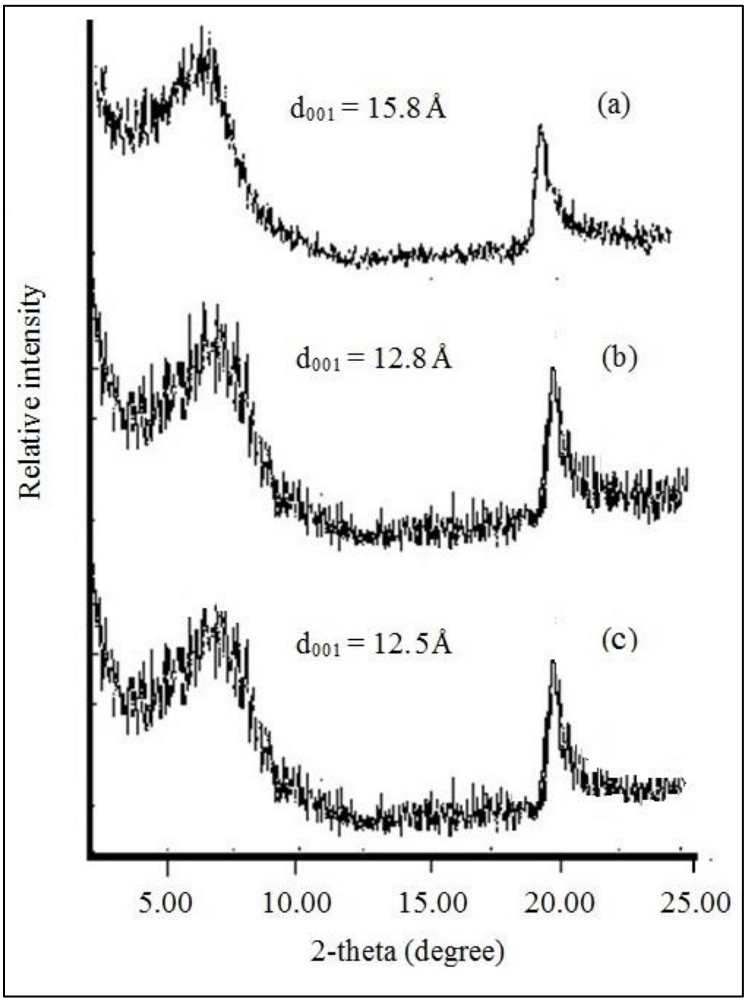

Figure 3.30 XRD patterns of: $2\%NdCl_3$/Al-PLM (a) regenerated $2\%NdCl_3$/AlPLM type A and (b) regenerated $2\%NdCl_3$/Al-PLM type B (c)

The regenerated catalysts **A** (Figure 3.30**, b**) and **B** (Figure 3.30, **c**) were similar to the fresh catalyst (Figure 3.30, **a**) suggesting that almost crystallinity phase exhibited the stability of clay catalysts. Both of them revealed d-basal spacing around

12 Å, lower than fresh 2%$NdCl_3$/Al-PLM (15.8 Å), indicating that the layers were collapsed slightly during the reaction process [33].

3.7.1.2 BET specific surface area and BJH pore size diameter

The nitrogen adsorption-desorption isotherms of 2%$NdCl_3$/Al-PLM and regenerated 2%$NdCl_3$/Al-PLM **A** and **B** are shown in Table 3.24. The 0.04 g of clay samples were pretreated at 150°C for 2 h. Then, their surface area and pore size diameter were analyzed by BET and BJH methods, respectively.

Table 3.24 The BET specific surface area and BJH pore size diameter of catalysts

Entry	Type of clay catalyst	BET specific surface area (m^2/g)	Pore size diameter (Å)
1	$NdCl_3$/Al-PLM	66.4	32.8
2	Regenerated **A**	58.4	24.4
3	Regenerated **B**	73.3	24.4

From the results in Table 3.24, the BET surface area of those clay catalysts (entries 1-3) had specific surface area in the same range 58.4-73.3 m^2/g. The pore size diameters of the regenerated catalysts (entry 2-3) were decreased due to the attrition during reaction process.

3.7.1.3 Determination of acidity of regenerated 2%$NdCl_3$/Al-PLM

Attenuated total reflectance Fourier transform infrared (ATR-FTIR) spectroscopy was used to determine the nature of acid site of the regenerated 2%$NdCl_3$/Al-PLM type **A** and **B** with pyridine. These regenerated catalysts were dried in hot air for 1 h at 100 °C, prior to pyridine treatment. Fifty milligrams of the regenerated catalysts and 1 mL of pyridine were poured into sample cups. Then, the sample cups were kept in a hot air oven at 120°C for 1 h to remove physisorbed pyridine. After cooling, IR spectra were recorded in transmittance as function of wave number ranging from 1400 to 1700 cm^{-1}.

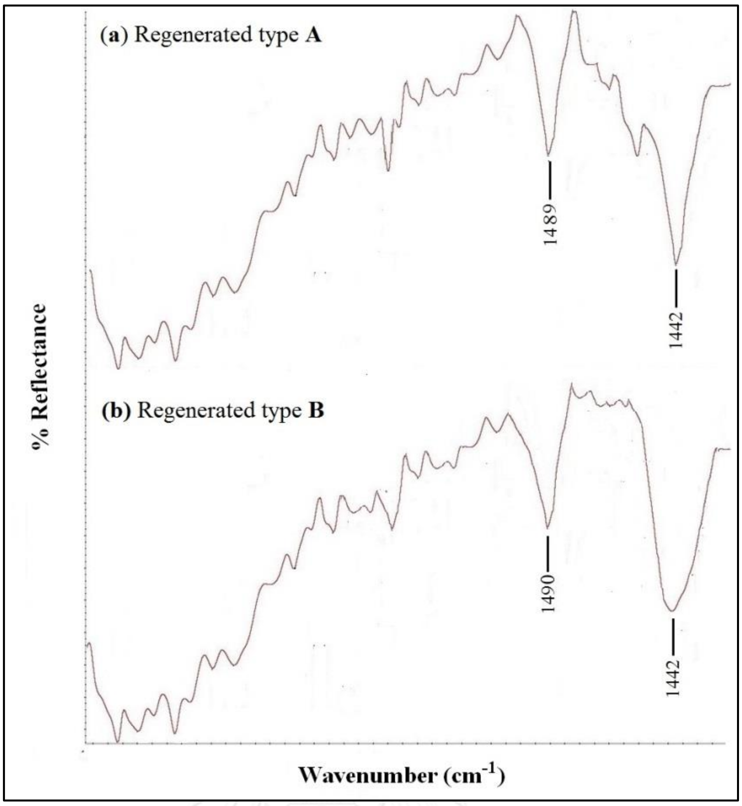

Figure 3.31 The FT-IR spectra of regenerated 2%$NdCl_3$/Al-PLM type A (**a**) type B (**b**)

The FT-IR spectra of regenerated 2%$NdCl_3$/Al-PLM type **A** and **B** were presented in Figure 3.31. Two major transmittance bands at 1442 and 1489-1490 cm^{-1} in both regenerated catalysts type **A** and **B** corresponded to Lewis acid. They still revealed Lewis acid characteristics after the first run although they were treated with different methods before use in the next runs.

3.7.2 The activity of regenerated 2%$NdCl_3$/Al-PLM

After tetrahydropyranylation of benzyl alcohol was completed, the used catalyst 2%$NdCl_3$/Al-PLM was filtered, washed and dried, respectively. Then, the catalysts were regenerated by following two modes: dry and re-calcination at 450°C (**A**) and dry without re-calcination (**B**). These regenerated catalytic activities were carried out for tetrahydropyranylation of benzyl alcohol under the optimum conditions for the five cycle runs. The results are presented in Table 3.25.

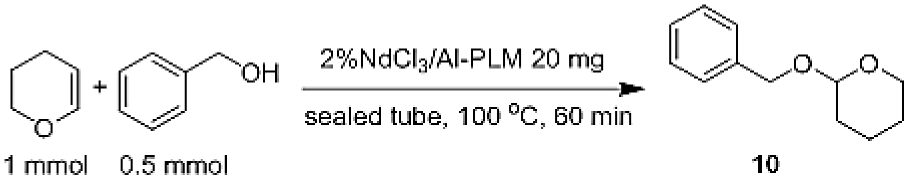

Table 3.25 Activity of regenerated 2%NdCl$_3$/Al-PLM on tetrahydropyranylation of benzyl alcohol

Entry	**Time cycles**	**Regenerated type A**			**Regenerated type B**		
		***recovery**	***%yield**	**MB**	***recovery**	***%yield**	**MB**
1	1	0	100.5	100.5	0	99.1	99.1
2	2	0	99.2	99.2	11.5	87.5	99
3	3	0	100.4	100.4	12.9	86.3	99.1
4	4	11.8	90.6	102.4	18.1	85.6	103.7
5	5	13.9	88.2	102.1	49.2	46.3	95.5

*quantified by ^{1}H NMR

Both regenerated catalysts type **A** and **B** gave the excellent yields of **10** in 86-100% yield (entries 1-4) in the forth cycle runs. The difference was observed in the fifth run (entry 5), type A gave 88.2% yield while type B gave 46.2% yield, respectively. Type **A** showed higher performance than **B**. After the reaction was finished, coke deposited in porous clay catalyst. The presence of coke reduced the catalytic activity because it fouled in porous and blocked the active site [64]. Dry at 100 °C for 1 h (**B**) was not enough to get rid of coke accumulation so the catalytic activity of the regenerated type **B** was dropped. The regenerated catalyst which was activated by high calcination temperature (**A**) was a necessary process to activate the spent catalyst in order to removing coke as CO and CO$_2$ *via* heat treatment [65]. In conclusion, the regenerated catalyst type **A** was more predominant performance than **B** because it showed catalytic activity for five cycle runs with an appreciable yield (88.2-100.5%).

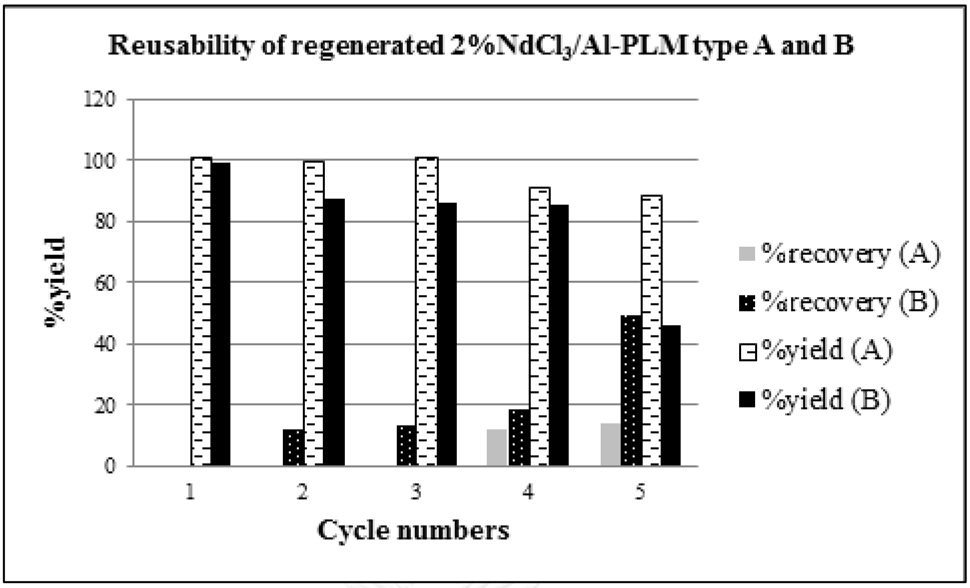

Figure 3.32 Cycle number of regenerated 2%NdCl$_3$/Al-PLM type A and B on tetrahydropyranylation of benzyl alcohol

3.8 Summary of tetrahydropyranylation of benzyl alcohol

2%NdCl$_3$/Al-PLM was a beneficial catalyst which could be used either benzylation or tetrahydropyranylation reactions. The tetrahydropyranyl group is a versatile protecting group for alcohols and phenols because hydroxyl group is a derivative lacking active hydrogen in some organic reactions. The optimal conditions which demonstrated appropriate amount of the catalyst, temperature, time, molar ratio, and reusability as the cycling number were studied. The optimum reaction conditions were DHP (1 mmol), benzyl alcohol (0.5 mmol), sealed tube, 100°C, 60 min and 2%NdCl$_3$/Al-PLM (20 mg). For catalytic reaction, 2%NdCl$_3$/Al-PLM exhibited highly reactive in tetrahydropyranylation of benzyl alcohol and could be recovered at least five times by regenerated catalyst *via* calcination process at 450°C.

CHAPTER IV
CONCLUSION

In this study, the main focus was to synthesize 2%neodymium chloride impregnated on aluminium oxdide pillared montmorillonite (2%$NdCl_3$/Al-PLM) and search for the optimum conditions for benzylation of aromatics and tetrahydropyranylation of benzyl alcohol.

Aluminium oxide pillared montmorillonite (Al-PLM) was synthesized by intercalation of aluminium polyoxocation into clay layers and calcined at 500˚C for 1 h with the rate 5˚C/min. Furthermore, the impregnation method of neodymium chloride ($NdCl_3$) was impregnated on aluminium oxide pillared montmorillonite (Al-PLM) by using temperature at 450˚C for 4 h in calcination method. The attestation synthesis step of clay was characterized by XRD, nitrogen adsorption-desorption, and FT-IR technique. The XRD patterns were carried out to investigate the difference d_{001} basal spacing increasing. It was increased when pillared by aluminium species and impregnated by neodymium chloride, respectively. Nitrogen adsorption-desorption was used to measure BET surface area and BJH pore size diameter, respectively. The BET surface area of 2%$NdCl_3$/Al-PLM was decreased whereas the BJH pore size diameter was increased after impregnation method. For classified acidity, 2%$NdCl_3$/Al-PLM was presented Lewis acid which confirmed by FT-IR.

The 2%$NdCl_3$/Al-PLM clay was then used for benzylation of aromatics with benzyl alcohol. Toluene was a model substrate. The optimum conditions for benzylation of toluene were toluene 8 mmol, benzyl alcohol 0.5 mmol, 2%$NdCl_3$/Al-PLM 20 mg, reaction temperature 170 °C and reaction time 1 h. The reaction was conducted in a sealed tube. At the optimized conditions, 2%$NdCl_3$/Al-PLM provided high yield and selectivity with *C*-monobenzylation of toluene. Then, the reactivity of electron-donating and electron-withdrawing substituents on benzene was observed within 30 min of the reaction time by using 2%$NdCl_3$/Al-PLM as a catalyst. The type of electron-donating substituents on benzene gave the good yields of *C*-monobenzylated whereas electron withdrawing group could not provide *C*-

monobenzylated products. The spent catalyst was regenerated by filtered, washed, dried, and calcined at 450 °C. The reusability of 2%$NdCl_3$/Al-PLM 100 mg in benzylation of toluene with benzyl alcohol presented for five cycle runs with an appreciable yield.

Then, this catalyst was used in tetrahydropyranylation of benzyl alcohol. The optimum conditions for this reaction were 3,4-dihydro-2*H*-pyran 1 mmol, benzyl alcohol 0.5 mmol, 2%$NdCl_3$/Al-PLM 20 mg, reaction temperature 100 °C, and reaction time 1 h. The reaction was conducted in a sealed tube. At the optimized conditions, 2%$NdCl_3$/Al-PLM gave an excellent yield of 2-(benzyloxy)tetrahydro-2*H*-pyran. The reusability of this catalyst was studied by following the optimized conditions. The spent catalysts were regenerated by two different modes, re-calcination at 450 °C for 4 h and not re-calcination in order to compare their efficiency. The first type could be recovered at least five times whereas the latter could be recovered for the fourth time, respectively to produce a good yield of the product.

Propose for the future work

This research concerns with the development of the activity and selectivity in catalytic system. *C*-benzylation of aromatics with 2%$NdCl_3$/Al-PLM as a catalyst was studied. Hence, other metal such as $FeCl_3$, $CuCl_2$, and $ZnCl_2$ may be used to impregnate on alumimium oxide pillared instead of $NdCl_3$ because they are cheap. The efficiency of them will be studied on activity and selectivity in organic reactions furthermore.

REFERENCES

[1] Varma, R.S. Clay and clay-supported reagents in organic synthesis. Tetrahedron 58(7) (2002): 1235-1255.

[2] Brigatti, M., Galan, E., and Theng, B. Structure and mineralogy of clay minerals. in Handbook of Clay Science, pp. 21-81: Elsevier Amsterdam, 2013.

[3] Odom, I. Smectite clay minerals: properties and uses. Philosophical Transactions of the Royal Society of London A: Mathematical, Physical and Engineering Sciences 311(1517) (1984): 391-409.

[4] Figueras, F. Pillared clays as catalysts. Catalysis Reviews Science and Engineering 30(3) (1988): 457-499.

[5] Kaewbuarom, P. Regioselectivity of phenol alkylation using metal impregnated aluminium pillared bentonite. M. Sc., Petrochemistry and polymer science Chulalongkorn university, 2011.

[6] Hassan, S.A., Yehia, F.Z., Hassan, H.A., Sadek, S.A., and Darwish, A.S. Various characteristics and catalytic performance of iron (II) phthalocyanine immobilized onto titania-and vanadia-pillared bentonite clay in in situ polymerization of methyl methacrylate: An attempt to synthesize novel polymer/iron phthalocyanine/pillared clay nanocomposites. Journal of Molecular Catalysis A: Chemical 332(1) (2010): 93-105.

[7] Tomul, F. Effect of ultrasound on the structural and textural properties of copper-impregnated cerium-modified zirconium-pillared bentonite. Applied Surface Science 258(5) (2011): 1836-1848.

[8] Barrett, E.P., Joyner, L.G., and Halenda, P.P. The determination of pore volume and area distributions in porous substances. I. Computations from nitrogen isotherms. Journal of the American Chemical society 73(1) (1951): 373-380.

[9] Reddy, C.R., Bhat, Y., Nagendrappa, G., and Prakash, B.J. Brønsted and Lewis acidity of modified montmorillonite clay catalysts determined by FT-IR spectroscopy. Catalysis Today 141(1) (2009): 157-160.

[10] Kumar, C.R., Rao, K.V., Prasad, P.S., and Lingaiah, N. Tin exchanged heteropoly tungstate: An efficient catalyst for benzylation of arenes with

benzyl alcohol. Journal of Molecular Catalysis A: Chemical 337(1) (2011): 17-24.

[11] Cuong, N.D., et al. Nanoporous hematite nanoparticles: Synthesis and applications for benzylation of benzene and aromatic compounds. Journal of Alloys and Compounds 582 (2014): 83-87.

[12] Preethi, M.E.L., Revathi, S., and Sivakumar, T. Green synthesis of benzylated aromatics using iron loaded mesoporous materials. Journal of Chemistry 5(3) (2008): 467-472.

[13] Hattori, H., Yamamoto, S., Iwata, M., Takashima, E., Yamada, T., and Suzuki, O. Determination of diphenylmethane antihistaminic drugs and their analogues in body fluids by gas chromatography with surface ionization detection. Journal of Chromatography B: Biomedical Sciences and Applications 581(2) (1992): 213-218.

[14] Hu, X., Chuah, G., and Jaenicke, S. Liquid-phase regioselective benzylation of bromobenzene and other aromatics over microporous zeolites. Microporous and mesoporous materials 53(1) (2002): 153-161.

[15] Khadilkar, B.M. and Borkar, S.D. Environmentally clean synthesis of diphenylmethanes using silica gel-supported ZnCl2 and FeCl3. Journal of Chemical Technology and Biotechnology 71(3) (1998): 209-212.

[16] Yi, W.-B. and Cai, C. Rare earth (III) perfluorooctanesulfonates catalyzed Friedel–Crafts alkylation in fluorous biphase system. Journal of fluorine chemistry 126(5) (2005): 831-833.

[17] Wang, B.-Q., et al. Benzylation of arenes through FeCl 3-catalyzed Friedel–Crafts reaction via C–O activation of benzyl ether. Tetrahedron Letters 49(27) (2008): 4310-4312.

[18] Sakai, N., Kawana, K., Ikeda, R., Nakaike, Y., and Konakahara, T. InBr3-Catalyzed Deoxygenation of Carboxylic Acids with a Hydrosilane: Reductive Conversion of Aliphatic or Aromatic Carboxylic Acids to Primary Alcohols or Diphenylmethanes. European Journal of Organic Chemistry 2011(17) (2011): 3178-3183.

[19] Smutek, B., Kunz, W., and Goettmann, F. Hydrothermal alkylation of phenols with alcohols in diluted acids. Comptes Rendus Chimie 15(1) (2012): 96-101.

[20] Huang, R., et al. Benzylation of arenes with benzyl halides synergistically promoted by in situ generated superacid boron trifluoride monohydrate and tetrahaloboric acid. Tetrahedron 71(10) (2015): 1540-1546.

[21] Losfeld, G., Escande, V., de La Blache, P.V., L'Huillier, L., and Grison, C. Design and performance of supported Lewis acid catalysts derived from metal contaminated biomass for Friedel–Crafts alkylation and acylation. Catalysis Today 189(1) (2012): 111-116.

[22] Narayanan, S. and Deshpande, K. Alumina pillared montmorillonite: characterization and catalysis of toluene benzylation and aniline ethylation. Applied Catalysis A: General 193(1) (2000): 17-27.

[23] Shrigadi, N.B., Shinde, A.B., and Samant, S.D. Study of catalytic activity of free and K10-supported iron oxyhydroxides and oxides in the Friedel–Crafts benzylation reaction using benzyl chloride/alcohol to understand their role in the catalysis by the Fe-exchanged/impregnated K10 catalysts. Applied Catalysis A: General 252(1) (2003): 23-35.

[24] Bachari, K. and Cherifi, O. Benzylation of aromatics on tin-containing mesoporous materials. Applied Catalysis A: General 319 (2007): 259-266.

[25] Li, J., et al. Synthesis, characterization and catalytic properties of Fe-containing HMCM-68 for the benzylation of toluene. Catalysis Communications 38 (2013): 59-62.

[26] Choudhary, V.R., Jha, R., and Narkhede, V.S. In-Mg-hydrotalcite anionic clay as catalyst or catalyst precursor for Friedel–Crafts type benzylation reactions. Journal of Molecular Catalysis A: Chemical 239(1) (2005): 76-81.

[27] Hajipour, A.R. and Azizi, G. Mild and efficient solvent-free tetrahydropyranylation (THP) of alcohols catalyzed by reusable acidic ionic liquid [Et3N (CH2) 4SO3H][OTs]. Iranian Journal of Catalysis 4(3) (2014): 213-218.

[28] Wang, Y.-G., Wu, X.-X., and Jiang, Z.-Y. A mild and efficient selective tetrahydropyranylation of primary alcohols and deprotection of THP ethers of phenols and alcohols using PdCl 2 (CH 3 CN) 2 as catalyst. Tetrahedron letters 45(14) (2004): 2973-2976.

[29] Heravi, M.M., Taheri, S., Bakhtiari, K., and Oskooie, H.A. Cupric sulfate pentahydrate: a mild and efficient catalyst for the chemoselective synthesis of 1, 1-diacetates from aldehydes in a solvent-free system. Monatshefte für Chemie/Chemical Monthly 137(8) (2006): 1075-1078.

[30] Wang, M., Song, Z.G., Gong, H., and Jiang, H. Copper methanesulfonate–acetic acid as a novel catalytic system for tetrahydropyranylation of alcohols and phenols. Chinese Chemical Letters 18(7) (2007): 799-802.

[31] Bodipati, N., Palla, S.R., and Peddinti, R.K. Trifluoroacetic acid catalyzed tetrahydropyranylation of alcohols and phenols and direct conversion of THP ethers into acetates. INDIAN JOURNAL OF CHEMISTRY SECTION B-ORGANIC CHEMISTRY INCLUDING MEDICINAL CHEMISTRY 51(2) (2012): 356-361.

[32] Bodipati, N., Palla, S.R., Komera, V., and Peddinti, R.K. 3, 5-Dinitrobenzoic acid catalyzed synthesis of 2, 3-unsaturated O-and S-glycosides and tetrahydropyranylation of alcohols and phenols. Tetrahedron Letters 55(50) (2014): 6878-6881.

[33] Ballini, R., Bigi, F., Carloni, S., Maggi, R., and Sartori, G. Solvent free tetrahydropyranylation of phenols and alcohols over zeolites HSZ as reusable catalysts. Tetrahedron letters 38(23) (1997): 4169-4172.

[34] Yang, J.H., Zhang, X., and Liu, W.Y. Efficient and green tetrahydropyranylation and deprotection of alcohols and phenols by using activated carbon supported sulfuric acid. Chinese Chemical Letters 19(8) (2008): 893-896.

[35] Narender, N., Reddy, K.S.K., Kumar, M.A., Rohitha, C., and Kulkarni, S. Tetrahydropyranylation of alcohols over modified zeolites. Catalysis letters 134(1-2) (2010): 175-178.

[36] Moghadam, M., Tangestaninejad, S., Mirkhani, V., Mohammadpoor-Baltork, I., and Gharaati, S. Tetrahydropyranylation of alcohols and phenols catalyzed by a new polystyrene-bound tin (IV) porphyrin. Journal of Molecular Catalysis A: Chemical 337(1) (2011): 95-101.

[37] Taghavi, S.A., Moghadam, M., Mohammadpoor-Baltork, I., Tangestaninejad, S., Mirkhani, V., and Khosropour, A.R. Highly efficient

tetrahydropyranylation of alcohols and phenols catalyzed by a new and reusable high-valent vanadium (IV) porphyrin. Comptes Rendus Chimie 14(12) (2011): 1095-1102.

[38] Yurdakoç, M., Akçay, M., Tonbul, Y., Ok, F., and Yurdakoç, K. Preparation and characterization of Cr-and Fe-pillared bentonites by using CrCl 3, FeCl 3, Cr (acac) 3 and Fe (acac) 3 as precursors. Microporous and mesoporous materials 111(1) (2008): 211-218.

[39] Yadav, J., Reddy, B., Balanarsaiah, E., and Raghavendra, S. Montmorillonite clay catalyzed cleavage of aziridines with alcohols. Tetrahedron letters 43(29) (2002): 5105-5107.

[40] Yadav, J., Reddy, B.S., Eeshwaraiah, B., and Srinivas, M. Montmorillonite KSF clay catalyzed one-pot synthesis of α-aminonitriles. Tetrahedron 60(8) (2004): 1767-1771.

[41] De Paolis, O., Teixeira, L., and Toeroek, B. Synthesis of quinolines by a solid acid-catalyzed microwave-assisted domino cyclization–aromatization approach. Tetrahedron Letters 50(24) (2009): 2939-2942.

[42] Choudary, B.M., Sateesh, M., Kantam, M.L., and Prasad, K.V.R. Acylation of aromatic ethers with acid anhydrides in the presence of cation-exchanged clays. Applied Catalysis A: General 171(1) (1998): 155-160.

[43] Jiang, J., Ma, K., Zheng, Y., Cai, S., Li, R., and Ma, J. Cobalt salophen complex immobilized into montmorillonite as catalyst for the epoxidation of cyclohexene by air. Applied Clay Science 45(3) (2009): 117-122.

[44] Singh, D.U., Singh, P.R., and Samant, S.D. Fe-exchanged montmorillonite K10—the first heterogeneous catalyst for acylation of sulfonamides with carboxylic acid anhydrides. Tetrahedron letters 45(24) (2004): 4805-4807.

[45] Bineesh, K.V., Kim, M.-i., Lee, G.-H., Selvaraj, M., and Park, D.-W. Catalytic performance of vanadia-doped alumina-pillared clay for selective oxidation of H 2 S. Applied Clay Science 74 (2013): 127-134.

[46] Ren, S., et al. Promotion of Ni/clay catalytic activity for hydrogenation of naphthalene by organic modification of clay. Chinese Journal of Catalysis 35(4) (2014): 546-552.

[47] Bunchoo, N. Selective C-alkylation of phenols using neodymium impregnated on pillared bentonite. M.Sc., petrochemistry and polymer science program chulalongkorn university, 2014.

[48] Trikittiwong, P., Sukpirom, N., and Chavasiri, W. Regioselective epoxide ring opening mediated by iron oxide-pillared clay. Journal of Molecular Catalysis A: Chemical 378 (2013): 76-81.

[49] Penkova, A., Bobadilla, L.F., Romero-Sarria, F., Centeno, M.A., and Odriozola, J.A. Pyridine adsorption on NiSn/MgO–Al 2 O 3: An FTIR spectroscopic study of surface acidity. Applied Surface Science 317 (2014): 241-251.

[50] Ferri, D., Frauchiger, S., Bürgi, T., and Baiker, A. Interactions of a vinyl ether with acid-modified silica-based catalyst studied by ATR-IR spectroscopy. Journal of Catalysis 219(2) (2003): 425-433.

[51] Billingham, J., Breen, C., and Yarwood, J. In situ determination of Brønsted/Lewis acidity on cation-exchanged clay mineral surfaces by ATR-IR. Clay minerals 31(4) (1996): 513-522.

[52] Kumar, C.R., Rambabu, N., Maheria, K., Dalai, A., and Lingaiah, N. Iron exchanged tungstophosphoric acid supported on activated carbon derived from pinecone biomass: Evaluation of catalysts efficiency for liquid phase benzylation of anisole with benzyl alcohol. Applied Catalysis A: General 485 (2014): 74-83.

[53] Ali, T.T., Narasimharao, K., Ahmed, N.S., Basahel, S., Al-Thabaiti, S., and Mokhtar, M. Nanosized iron and nickel oxide zirconia supported catalysts for benzylation of benzene: Role of metal oxide support interaction. Applied Catalysis A: General 486 (2014): 19-31.

[54] Kumar, C.R., Rambabu, N., Lingaiah, N., Prasad, P.S., and Dalai, A. Hafnium salts of dodeca-tungstophosphoric acid catalysts for liquid phase benzylation of anisole with dibenzylether. Applied Catalysis A: General 471 (2014): 1-11.

[55] Shinde, A.B., Shrigadi, N.B., and Samant, S.D. Development of Fe-, Sb-, Bi- and Al-impregnated silica catalysts using rice husk silica as a support for Friedel–Crafts benzylation of arenes. Journal of Chemical Technology and Biotechnology 78(12) (2003): 1234-1238.

[56] Desroches, J., Champagne, P.A., Benhassine, Y., and Paquin, J.-F. In situ activation of benzyl alcohols with XtalFluor-E: formation of 1, 1-diarylmethanes and 1, 1, 1-triarylmethanes through Friedel–Crafts benzylation. Organic & biomolecular chemistry 13(8) (2015): 2243-2246.

[57] ElDouhaibi, A.S., Lozanov, M., and Montgomery, J. A multicomponent approach to substituted benzenes involving sequential nickel-catalyzed reactions. Tetrahedron 62(49) (2006): 11460-11469.

[58] Choudhary, V.R. and Jana, S.K. Benzylation of benzene and substituted benzenes by benzyl chloride over InCl 3, GaCl 3, FeCl 3 and ZnCl 2 supported on clays and Si-MCM-41. Journal of Molecular Catalysis A: Chemical 180(1) (2002): 267-276.

[59] Choudhary, V.R. and Jana, S.K. Benzoylation of benzene and substituted benzenes by benzoyl chloride over In 2 O 3/Si-MCM-41 catalyst. Journal of Molecular Catalysis A: Chemical 184(1) (2002): 247-255.

[60] Pushpaletha, P., Rugmini, S., and Lalithambika, M. Correlation between surface properties and catalytic activity of clay catalysts. Applied Clay Science 30(3) (2005): 141-153.

[61] da Silva, M.S.M., da Costa, C.L., de Magdala Pinto, M., and Lachter, E.R. Benzylation of benzene, toluene and anisole with benzyl alcohol catalyzed by cation-exchange resins. Reactive Polymers 25(1) (1995): 55-61.

[62] Balint, E., Kovacs, O., Drahos, L., and Keglevich, G. Microwave-assisted solid-liquid phase alkylation of naphthols. Letters in Organic Chemistry 10(5) (2013): 330-336.

[63] Paul, N.K., Dietrich, L., and Jha, A. A New Procedure for the Synthesis of 1-Arylmethyi-2-Naphthols.

[64] Forzatti, P. and Lietti, L. Catalyst deactivation. Catalysis today 52(2) (1999): 165-181.

[65] Gallastegi-Villa, M., Aranzabal, A., Romero-Sáez, M., González-Marcos, J., and González-Velasco, J. Catalytic activity of regenerated catalyst after the oxidation of 1, 2-dichloroethane and trichloroethylene. Chemical Engineering Journal 241 (2014): 200-206.

APPENDIX

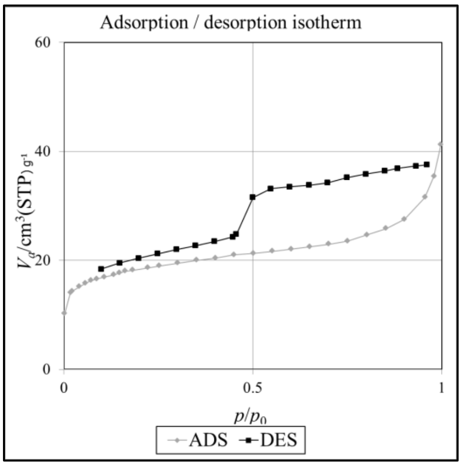

Figure A-1 N_2-adsorption desorption isotherm of montmorillonite

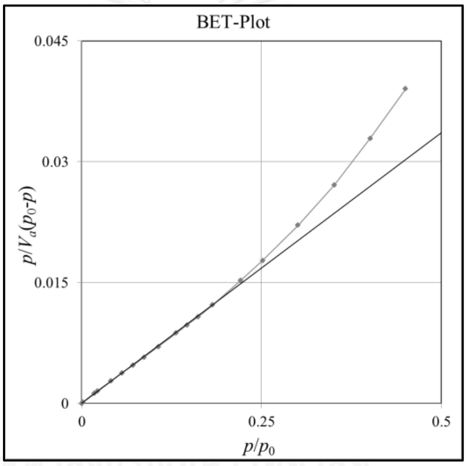

Figure A-2 BET plot of montmorillonite

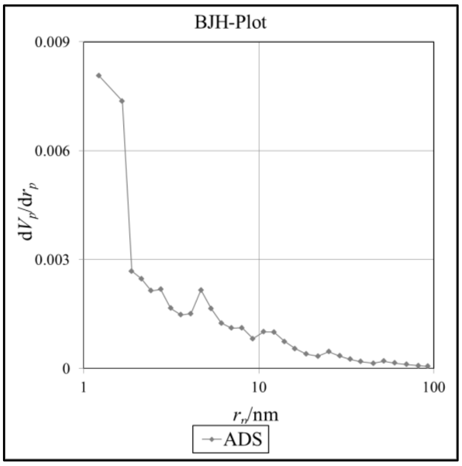

Figure A-3 BJH plot of montmorillonite

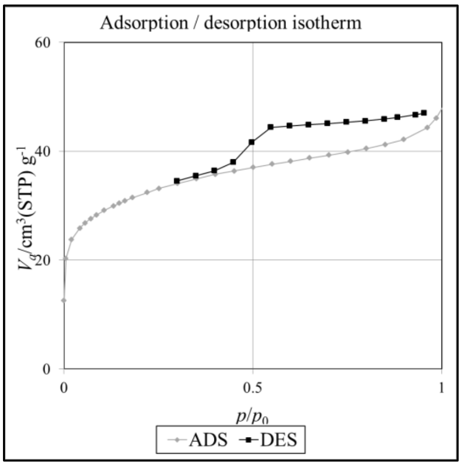

Figure A-4 N_2-adsorption desorption isotherm of Na-montmorillonite

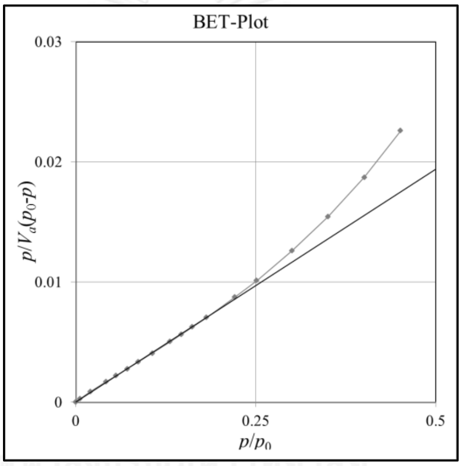

Figure A-5 BET plot of Na-montmorillonite

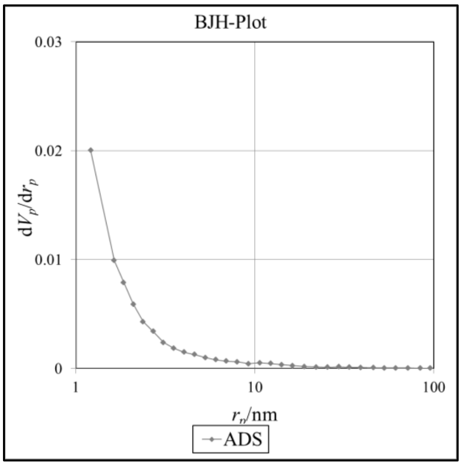

Figure A-6 BJH plot of Na-montmorillonite

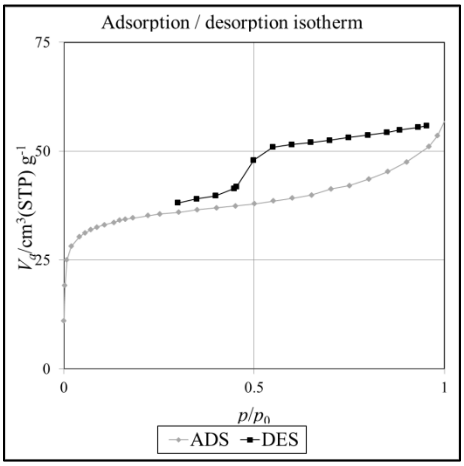

Figure A-7 N_2-adsorption desorption isotherm of Al-PLM

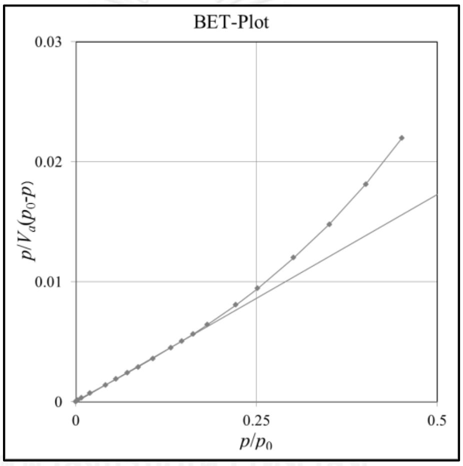

Figure A-8 BET plot of Al-PLM

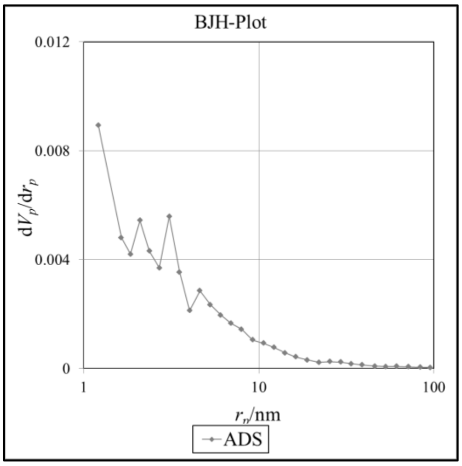

Figure A-9 BJH plot of Al-PLM

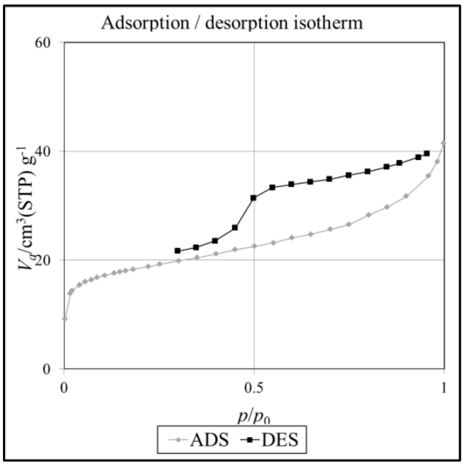

Figure A-10 N_2-adsorption desorption isotherm of 2%$NdCl_3$/Al-PLM

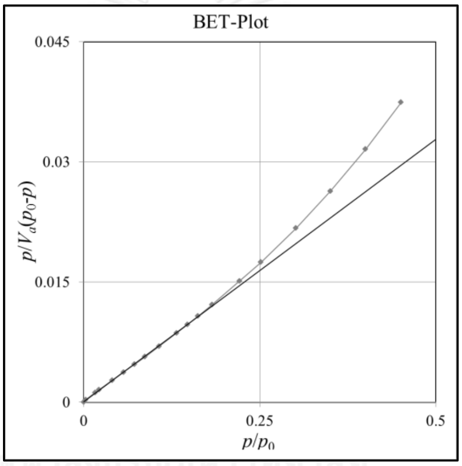

Figure A-11 BET plot of 2%$NdCl_3$/Al-PLM

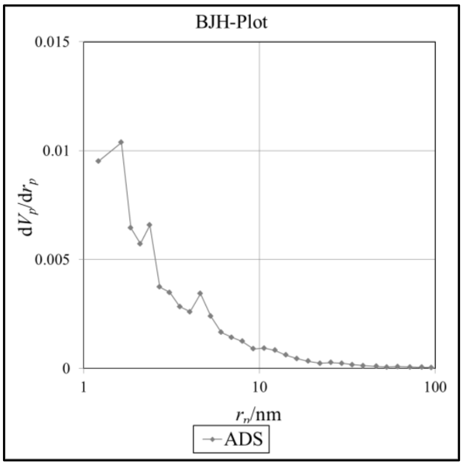

Figure A-12 BJH plot of 2%$NdCl_3$/Al-PLM

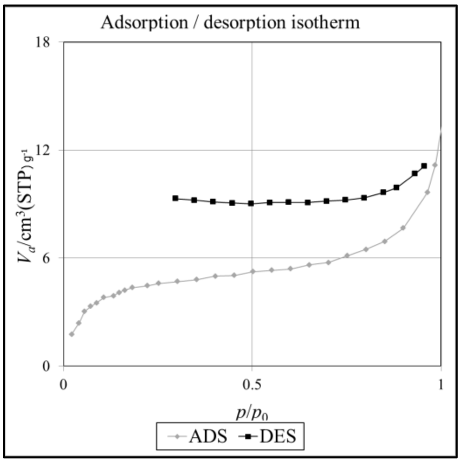

Figure A-13 N_2-adsorption desorption isotherm of regenerated 2%$NdCl_3$/Al-PLM in benzylation reaction

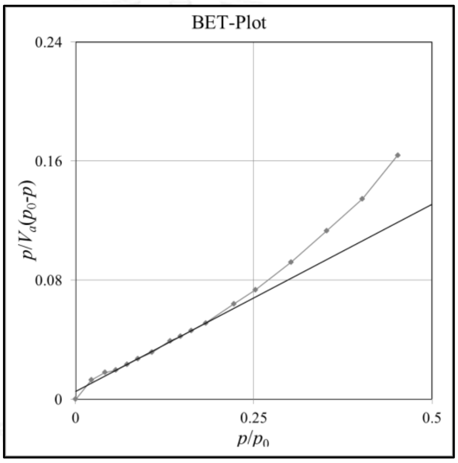

Figure A-14 BET plot of regenerated 2%$NdCl_3$/Al-PLM in benzylation reaction

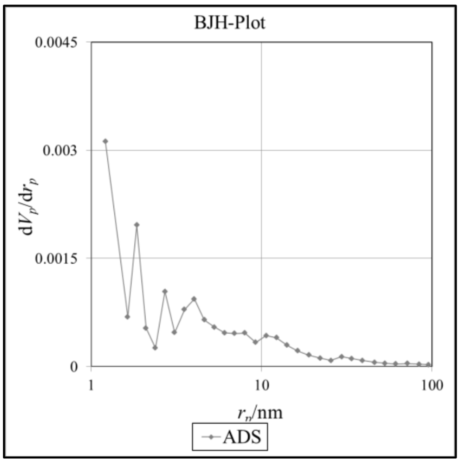

Figure A-15 BJH plot of regenerated 2%$NdCl_3$/Al-PLM in benzylation reaction

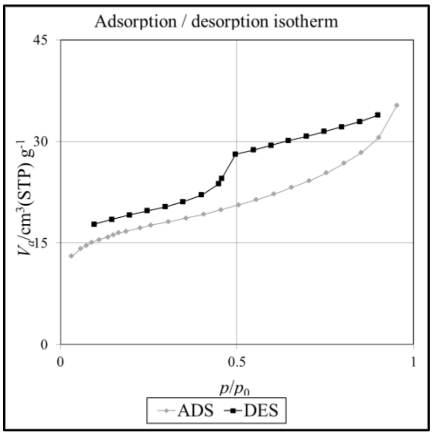

Figure A-16 N$_2$-adsorption desorption isotherm of regenerated 2%NdCl$_3$/Al-PLM type **A** in tetrahydropyranylation reaction

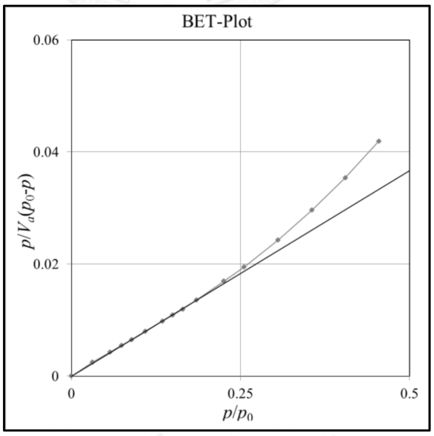

Figure A-17 BET plot of regenerated 2%NdCl$_3$/Al-PLM type **A** in tetrahydropyranylation reaction

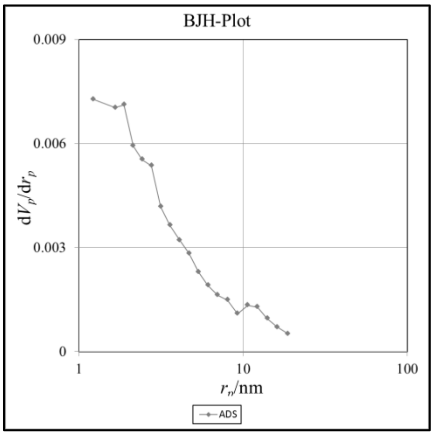

Figure A-18 BJH plot of regenerated 2%NdCl$_3$/Al-PLM type **A** in tetrahydropyranylation reaction

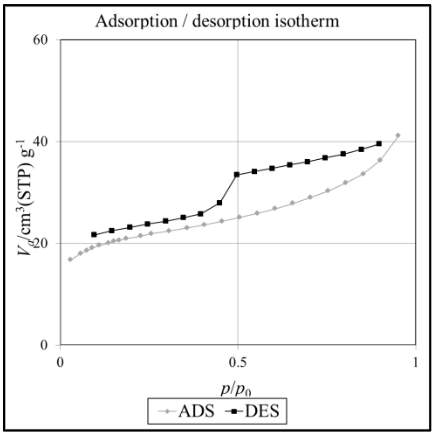

Figure A-19 N_2-adsorption desorption isotherm of regenerated 2%$NdCl_3$/Al-PLM type **B** in tetrahydropyranylation reaction

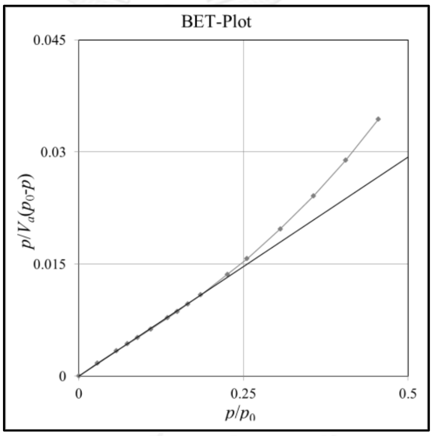

Figure A-20 BET plot of regenerated 2%$NdCl_3$/Al-PLM type **B** in tetrahydropyranylation reaction

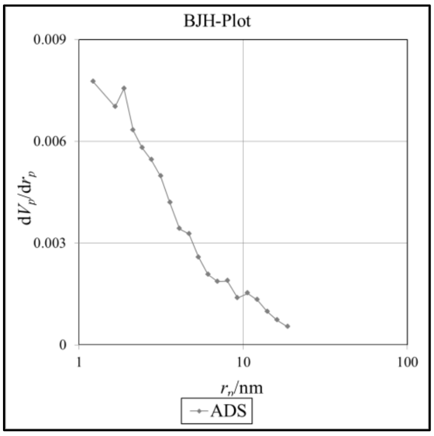

Figure A-21 BJH plot of regenerated 2%$NdCl_3$/Al-PLM type **B** in tetrahydropyranylation reaction

Table A-1 Benzylation of aromatics using 2%NdCl$_3$/Al-PLM as a catalyst

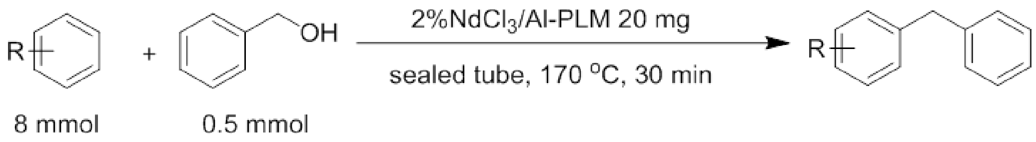

Entry	Aromatics	*%recovery	*%yield	MB	ratio b/a (*p*-/*o*-)
1	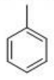 toluene	0	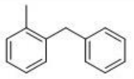 (**1a**) 60.7 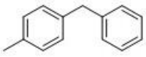 (**1b**) 41.1 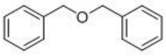 (**1c**) 5.5	107.6	1.52
2	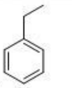 ethylbenzene	0	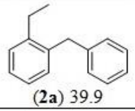 (**2a**) 39.9 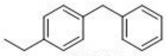 (**2b**) 60.1	100.0	1.51
3	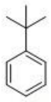 *tert*-butylbenzene	0	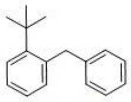 (**3a**) 33.8 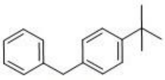 (**3b**) 66.4	100.2	1.96
4	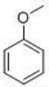 anisole	0	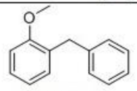 (**4a**) 52.5 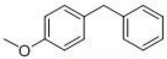 (**4b**) 45.6 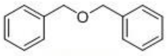 (**4c**) 2.0	100.1	0.87
5	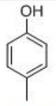 *p*-cresol	0	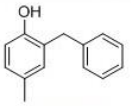 (**5**) 91.5	91.5	-
6	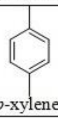 *p*-xylene	0	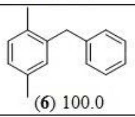 (**6**) 100.0	100.0	-
7	 benzene	0	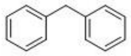 (**7a**) 81.8 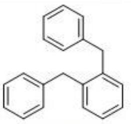 (**7b**) 7.6 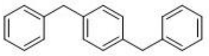 (**7c**) 14.4	103.8	-
8	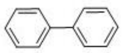 biphenyl	2.8	 (**8a**) 48.6 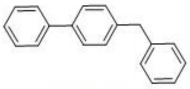 (**8b**) 48.6	100.0	1.0
9	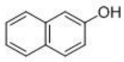 2-naphthol	2	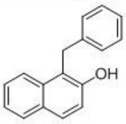 (**9**) 60.4	62.4	-
10	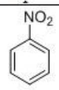 nitrobenzene	44.4	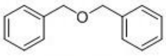 (**10**) 55.6	100.0	-

*quantified by ^{1}H NMR

VITA

Miss Natthida Maneechandra was born on August 16, 1989 in Lampang, Thailand. She graduated with Bachelor degree of Science in Chemistry from Chulalongkorn University in 2011. Since then, she has been a graduate student studying Petrochemistry and Polymer Science at Chulalongkorn University.

Her present address is 124/1, R. Nagoum, T. Sobtue, A. Muang, Lampang, 52100, Thailand.